

공학박사 학위논문

**Quorum Sensing based Biofouling
Control in Membrane Bioreactor for
Advanced Water Treatment**

세균의 정족수 감지 기작을 활용한 고도 수처리용
막결합형 생물반응기에서의 막오염 제어 연구

2009년 8월

서울대학교 대학원

화학생물공학부

연 경 민

Abstract

Quorum Sensing based Biofouling Control in Membrane Bioreactor for Advanced Water Treatment

Kyung-Min Yeon

School of chemical and biological engineering

The Graduate School

Seoul National University

Bacteria perceive their population density using small signal molecules called autoinducer and regulate specific group behaviors such as biofilm formation on the surface in cell density dependent way (Quorum sensing, QS). In this study, the concept of bacterial QS was applied to membrane bioreactor (MBR) for advanced wastewater treatment as a new biofouling control paradigm. The overall research was conducted in the following phases:

- (1) Evidence of autoinducer signal in MBR
- (2) Correlation between QS and membrane biofouling
- (3) Control of membrane biofouling by quorum quenching
- (4) Preparation of magnetic enzyme carrier (MEC)
- (5) Application of MEC to the MBR in continuous operation

A bioassay with *Agrobacterium tumefaciens* A136 reporter strain proved that *N*-acyl homoserine lactone (AHL) autoinducers of gram-negative bacteria were produced in the MBR. Furthermore, thin-layer chromatographic analysis

identified at least three different AHLs in the biocake, of which *N*-octanoyl-homoserine lactone was the most abundant.

During continuous MBR operation, the membrane-biocake showed strong AHL activity simultaneously with the abrupt increase in the transmembrane pressure (TMP). Furthermore, both autoinducer level per unit biomass and filtration resistance in the biocake increased under very similar tendency, which implies that QS was closely associated with the membrane biofouling.

Porcine kidney acylase I (EC-number 3.5.1.14), which can inactivate the AHL molecule by amide bond cleavage, was confirmed to prevent membrane biofouling by quenching AHL autoinducers, which suggested that quorum quenching, enzymatic destruction of QS autoinducer, could be a novel biofouling control approach in MBR.

Despite of its high potential as a novel biofouling control approach, the short catalytic lifetime and difficulty in recovering free enzyme hamper the successful application of the quorum quenching technique in the MBR under a long-term continuous operation. A magnetic enzyme carrier (MEC) was prepared by immobilizing the quorum quenching enzyme (acylase) on magnetic particles to overcome the technical limitations of free enzyme. The MEC showed no activity decrease under both continuous shaking for 14 days and 29 iterative cycles of reuse. Furthermore, the comparison of the MEC with free enzyme in a batch-type MBR showed that the MEC efficiently alleviated the membrane biofouling and showed a great advantage over free enzyme in terms of recycled use and stability in mixed liquor. When the MEC was applied to the lab scale MBR in a continuous operation, it also enhanced the membrane permeability to a large extent compared with a conventional MBR with no enzyme.

Keywords: Membrane bioreactor, Biofouling control, Quorum sensing, Magnetic enzyme carrier

Student Number: 2003-30957

Table of Contents

Abstract.....	i
Table of Contents.....	iii
List of Figures.....	vi
List of Tables.....	x ii
1. Introduction: Background and Objectives	1
1.1. Background.....	2
1.2. Objectives.....	5
2. Literature Review on Membrane Bioreactor, Quorum Sensing, and Enzyme Immobilization	7
2.1. MBR for Advanced Wastewater Treatment	8
2.1.1. Concept and Process	8
2.1.2. Trends in MBR: Market and Research.....	16
2.2. Fouling Control in MBR.....	19
2.2.1. Engineering Approach	19
2.2.2. Material Approach	21
2.2.3. Chemical Approach	22
2.2.4. New Perspective: Biofilm on the Membrane Surface.....	24
2.3. Quorum Sensing.....	34
2.3.1. Definition and Mechanism.....	34
2.3.2. Role of QS in Biofilm	74
2.4. QS Control Strategy	81
2.4.1. Blockage of Signal Synthesis.....	81

2.4.2.	Interference with Signal Molecules	84
2.4.3.	Inactivation of Signal Molecules	105
2.4.4.	Patent Analysis	111
2.5.	Enzyme immobilization	116
2.5.1.	Conventional Methods	119
2.5.2.	Nanobiocatalysis: New Trends in Enzyme Technology....	135
3.	Quorum Sensing as a New Biofouling Control Paradigm in Membrane Bioreactor	153
3.1.	Introduction.....	154
3.2.	Experimental Section	155
3.2.1.	Reporter Strain for the Autoinducer Detection	155
3.2.2.	Bioassay for the <i>in situ</i> AHL Detection	156
3.2.3.	TLC for the AHL Identification	156
3.2.4.	DNA Extraction and PCR-DGGE Analysis.....	162
3.2.5.	Reactor Operation	164
3.2.6.	Analytical Methods	167
3.3.	Results and Discussion	168
3.3.1.	Evidence of the Autoinducer Signal in the MBR.....	168
3.3.2.	Correlation between QS Activity and Biofouling in MBR	172
3.3.3.	Control of Membrane Biofouling based on QS	179
3.4.	Conclusions.....	185
4.	Magnetic Enzyme Carrier for the Biofouling Control in Membrane Bioreactor based on the Enzymatic Quorum Quenching.....	186
4.1.	Introduction.....	187
4.2.	Experimental Section	191
4.2.1.	Preparation of MEC	191

4.2.2.	Confocal Laser Scanning Microscopy (CLSM).....	194
4.2.3.	Measurement of Enzyme Activity and Stability	198
4.2.4.	Reactor Operation	200
4.2.5.	Analytical Methods	204
4.3.	Results and Discussion	205
4.3.1.	Preparation of the MEC	205
4.3.2.	Stabilities of the free enzyme, adsorbed enzyme and the MEC.....	211
4.3.3.	Comparison of the MEC with Free Enzyme in Batch Type MBR.....	215
4.3.4.	Application of the MEC to the MBR in Continuous Operation.....	219
4.4.	Conclusions.....	225
	Abstract in Korean	226
	References	228

List of Figures

Figure 1.1.	Concept of QS-based biofouling control in MBR.....	4
Figure 2.1.	Schematics of the (a) side stream MBR and (b) submerged MBR	10
Figure 2.2.	Estimation of market value of MBR by (a) configuration (submerged side stream) and (b) type of biological process (aerobic vs anaerobic).	14
Figure 2.3.	Trends in MBR: (a) global market value and (b) number of sresearch articles published since 1995.	18
Figure 2.4.	The biofilm life cycle in three steps: attachment, growth of micro-colonies, swarming phenomena and detachment in clump	27
Figure 2.5.	Conceptual illustration of the heterogeneity of biofilm structure with bacterial clusters, streamers, and water channels.....	28
Figure 2.6.	Three qualitatively distinct patterns of chemical heterogeneity arise in biofilms. (a) metabolic substrate, (b) metabolic product and (c) metabolic intermediate.....	29
Figure 2.7.	Physiological heterogeneity in a single-species biofilm.	30
Figure 2.8.	Physiological heterogeneity in a mixed-species biofilm.....	31
Figure 2.9.	Model of AHL QS in a single generalized bacteria.....	36
Figure 2.10.	Molecular structure of each AHL autodinucers	37
Figure 2.11.	LuxI-directed biosynthesis of AHL autoinducers.....	38
Figure 2.12.	The <i>Vibrio fisheri</i> LuxI/LuxR QS system	43
Figure 2.13.	The <i>Pseudomonas aeruginosa</i> LasI/LasR-RhII/RhIR QS system	47
Figure 2.14.	Epifluorescence and scanning confocal photomicrographs	

	of the WT and the <i>lasI</i> mutant <i>Pseudomonas aeruginosa</i> biofilms containing the GFP expression vector pMRP9	48
Figure 2.15.	A general model for peptide-mediated QS in gram-positive bacteria.....	53
Figure 2.16.	QS control of competence and sporulation in <i>Bacillus subtilis</i>	57
Figure 2.17.	Biosynthetic pathway of AI-2.	69
Figure 2.18.	Current schemes of AI-2 response	70
Figure 2.19.	Three basic AHL QS control strategies	83
Figure 2.20.	QS inhibitors from natural source. (a) penicilic acid, (b) patulin. (c) Diketopiperazines produced by <i>Pseudomonas putida</i> , (d) Cyclo(L-Phe-Pro), (e) Cyclo(L-Leu-L-Val).....	87
Figure 2.21.	Synthetic AHL inhibitors with a change in the acyl side chain.	91
Figure 2.22.	Synthetic AHL inhibitors with an alternation in the lactone structure. (a) 2-amino-3-oxo-C12-(2-aminocyclohexanone), (b) 2-amino-3-oxo-C12-(2-aminocyclohexanol), and (c) <i>N</i> -decanoyl cyclopentylamid.....	92
Figure 2.23.	Non-AHL based QS inhibitors. (a) 2,4,5-tri-bromoimidazole. (b) indole, (c) 3-nitrobenzene-sulfonamide, and (d) 4-nitro-pyridine-N-oxide (4-NPO)	93
Figure 2.24.	Conceptual illustration of QS control by trapping AHLs on cyclodextrins.	104
Figure 2.25.	Enzymatic degradation of AHL autoinducers by lactonase and acylase.	109
Figure 2.26.	Enzyme immobilization onto hydroxyl containing supports via activation with (a) cyanogens bromide, and (b) <i>S</i> -triazine.	127
Figure 2.27.	Activation of a carboxylic acid support with a carbodiimide	

	followed by enzyme coupling	129
Figure 2.28.	Activation of an amine-bearing support with glutaraldehyde followed by enzyme coupling	132
Figure 2.29.	Enzyme immobilization to (a) Eupergit via free amino groups and (b)unmodified polyacrolein via free amino groups, followed by reduction of the Schiff base with sodilum borohydride.....	134
Figure 2.30.	Illustration of the large surface area of nanostructured materials.....	136
Figure 2.31	(a) Comparison of conventional approach using reverse micelles and single enzyme naoparticle (SEN) entrapment. (b) Schematic illustration of enzyme solubilization for SEN synthesis..	140
Figure 2.32.	'Ship-in-a-bottle' approach for the stabilization of enzymes in nanoporous media with a 'bottle-neck' structure, as shown in (a) the TEM image of mesocellular mesoporous silica. (b) Schematic diagram for the preparation.....	145
Figure 2.33.	Assembly of enzyme aggregate coating on electrospun nanofibers.....	148
Figure 3.1	AHL detection mechanism of <i>Agrobacterium tumefaciens</i> A136 (Ti)(pCF218)(pCF372).	159
Figure 3.2	Schematic representation of <i>Agrobacterium tumefaciens</i> A136 bioassay for in situ detection of total AHL.....	160
Figure 3.3	TLC chromatogram and R_f value of AHL standards	161
Figure 3.4	A Schematic diagram of (a) continuous MBR and (b) batch MBR..	166
Figure 3.5	Characterization of bacterial community in MBR. (a) DGGE of bacteria 16S rDNA PCR products. (b) Gram-	

	stained image of biocake detached from membrane module. Both 16S rDNA for PCR-DGGE and biocake for gram staining were obtained at the operation time of 72 h.	170
Figure 3.6	Characterization of the autoinducer signal in biocake. (a) <i>Agrobacterium tumefaciens</i> A 136 bioassay result for the detection of total AHL. (b) TLC chromatogram of AHL extract from membrane-biocake	171
Figure 3.7	Occurrence of AHL signals in biocake during continuous MBR operation. (a) 22 h, (b) 46 h, (c) 58 h and (d) 72 h. .	175
Figure 3.8	Comparison of the AHL level in deposited MLSS and biofilm on membrane. (a) <i>Agrobacterium tumefaciens</i> A136 bioassay, (b) AHL level per biomass	176
Figure 3.9	Calibration curve for the quantification of AHL level in membrane-biofilm using C8-HSL as a standard... ..	177
Figure 3.10	Correlation between QS activity and filtration resistance of biofilm. (a) Experiment scheme. (b) Variation of TMP and AHL levels as a function of biofilm growth time..	178
Figure 3.11	Evidence for membrane biofouling prevention by quorum quenching. (a) TMP profile, and (b) <i>Agrobacterium tumefaciens</i> A136 bioassay results.....	182
Figure 3.12	Change of glucose concentration during the batch reactor operation in a total recycle mode.	183
Figure 3.13	Quantitative analysis of EPS in biocakes in the MBR under various operating conditions..	184
Figure 4.1	Technical problems of free enzyme in the continuous MBR system..	189
Figure 4.2	(a) The magnetic enzyme carrier (MEC) concept and (b) recovery and reuse of the MEC in the MBR under	

	continuous operation.....	190
Figure 4.3	Schematic diagram showing the preparation of the MEC through LBL deposition of PSS/chitosan on MIEX resin and enzyme immobilization via GA treatment..	192
Figure 4.4	Chemical structure of (a) polystyrene sulfonate (PSS) and (b) chitosan.....	193
Figure 4.5	Preparation scheme of the FITC-labeled chitosan..	196
Figure 4.6	Specific binding of SYPRO Orange to acylase in the MEC.	197
Figure 4.7	Enzyme reaction of acylase using <i>N</i> -acetyl-L-methionine as a substrate.....	199
Figure 4.8	Schematic diagram of (a) the batch type MBR in total recycle filtration mode and (b) the MBR in continuous operation... ..	202
Figure 4.9	Change of zeta potential on MIEX support during LBL process ..	207
Figure 4.10	Concentration profile of (a) PSS and (b) chitosan in solution during LBL process ..	208
Figure 4.11	CLSM image of the MEC stained with SYPRO Orange.	209
Figure 4.12	CLSM image of the MIEX-PSS-(FITC labeled chitosan)-acylase stained with SYPRO Orange.....	210
Figure 4.13	(a) Stability of free enzyme, adsorbed enzyme and the MEC under continuous shaking conditions and (b) stability of adsorbed enzyme and the MEC under iterative cycles of enzyme reaction and magnetic separation... ..	213
Figure 4.14	Stability of MEC during 6 days under 29 cycles of enzyme reaction and reuse	214
Figure 4.15	Comparison of TMP profile among each batch MBR during the three operation cycles	217

Figure 4.16	Effect of MEC on the biofilm detachment in batch type MBR ..	218
Figure 4.17	Comparison of TMP build-up between the control and the MEC MBRs under continuous mode.....	222
Figure 4.18	GFC spectrum of (a) SMP (RI), (b) SMP (280 nm), (c) EPS (RI) and (d) EPS (280 nm). ..	223
Figure 4.19	Quantitative analysis of (a) SMP in mixed liquor and (b) EPS in membrane-biocake ..	224

List of Tables

Table 2.1.	Advange and disadvantage of each sidestream and submerged MBR configuration.....	12
Table 2.2.	Advange and disadvantage of each aerobic and anaerobic MBR	13
Table 2.3.	Organisms possessing LuxI/LuxR homologues : the regulatory proteins, the AHL autoinducers, and the regulated functions	39
Table 2.4.	Genes and functions controlled by LuxS in bacteria	71
Table 2.5.	Representative natural and synthetic furanones	101
Table 2.6.	Organisms identified to date exhibiting AHL degrading activity	110
Table 2.7.	List of the patents related to the QS control	113
Table 2.8.	Stabilization effects of immobilization to enzymes.....	118
Table 2.9.	Reactive functional groups in enzym.....	125
Table 3.1.	List of the biosensor for the detection of AHL autoinducers.	158
Table 3.2.	Primers used for the PCR amplification of 16S rDNA	163
Table 3.3.	Continuous MBR operating conditions	165
Table 4.1.	Operating conditions of each control and MEC MBR.....	203

CHAPTER 1

Introduction: Background and Objective

1.1. Background

Over the past two decades, the membrane bioreactor (MBR) has emerged as one of the innovative options in the advanced wastewater treatment technology. For example, about 2,500 MBR plants have been installed worldwide, while more are proposed or under construction¹. Furthermore, the global MBR market value was estimated to \$216.6 million in 2005 and is rising at an average annual growth rate (AAGR) of 10.9%, faster than the larger market for advanced wastewater treatment equipment about 5.5% AAGR². However, membrane biofouling problem which cause severe flux decline, short membrane life-span, and increase of energy consumption still remains as one of the major research issues restricting the innovation and widespread of the MBR technology.

So far, various fouling control techniques have been developed through engineering^{3, 4, 5}, material^{6, 7} and chemical approaches^{8, 9, 10}. Although these conventional fouling control methods have been proven to alleviate membrane fouling efficiently at the early operation stage, they all have an intrinsic limitation of a drastic permeability loss (e.g., increase of the transmembrane pressure at the constant flux) as the operation progresses.

Recent studies with advanced molecular biological techniques have revealed that a main constituent in the fouling layer on the membrane surface is the biocake which consists of both deposition of mixed liquor suspended solid (MLSS) and growth of biofilm on the membrane surface¹¹. Furthermore, the characteristics of the biocake formed on the membrane, such as porosity¹² and bio-volume¹³, are closely associated with the permeability loss in the MBR (membrane biofouling). This suggests that control of biofilm formation, intrinsically a natural biological process, could be a more direct solution to

biofouling than conventional approaches based on the physico-chemical principles.

Meanwhile, bacteria produce small molecules called autoinducers for the purpose of intercellular communication. When the autoinducer concentration reaches the threshold level in proportion to the cell density, it combines with the receptor protein and activates the transcription of specific genes to induce group behaviors such as bioluminescence¹⁴, antibiotic production¹⁵, virulence¹⁶, biofilm formation¹⁷ and sporulation¹⁸ (Quorum sensing, QS). Since Davies et al.¹⁷ first demonstrated that QS mechanism was involved in the differentiation of *Pseudomonas aeruginosa* biofilm formation, many studies have reported that QS control can successfully reduce or prevent biofilm formation on such surfaces as medical devices¹⁹ and plant tissue²⁰.

These results enabled us to hypothesize that, in principle, membrane biofouling originating from biofilm formation could also be alleviated through QS control, e.g., the blocking of intercellular communication to obtain MBR of high performance (Figure 1.1). However, all of the previous QS control researches adopted single defined culture system using model microorganism such as *Pseudomonas aeruginosa*. Microbial world in MBR is the basically undefined mixed culture system whose microbial community consists of various bacterial species. Therefore, no information is currently available on the application of QS to biofouling control in the MBR.

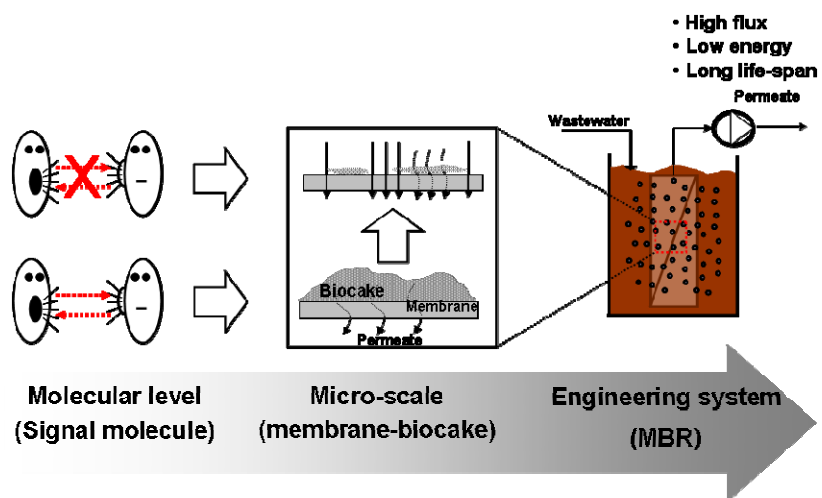


Figure 1.1. Concept of QS-based biofouling control in MBR.

1.2. Objectives

The objective of this study was to develop the new biofouling control method in MBR based on the principle of QS. To achieve this goal, the overall experiments were conducted in the following phases:

(1) Evidence of autoinducer signal

In the 1st phase, the presence of an autoinducer in the mixed cultured MBR was demonstrated and the main autoinducer involved in membrane-biocake was identified.

(2) Correlation between QS and membrane biofouling

In the 2nd stage, a correlation between QS activity and membrane biofouling in MBR was investigated.

(3) Control of membrane biofouling by quorum quenching

In the 3rd phase, the biofouling potential of enzymatic destruction of autoinducer (quorum quenching) was examined in the batch type MBR.

(4) Preparation of magnetic enzyme carrier (MEC)

A 'magnetic enzyme carrier (MEC)' in which quorum quenching enzyme was immobilized on magnetic support was prepared to overcome the technical limitation of free enzyme such as the short catalytic life time and difficulties in recovery.

(5) Application of MEC to MBR in continuous operation

In the final phase, MEC was applied to the MBR under continuous operation to enhance its performance.

CHAPTER 2

Literature Review on Membrane Bioreactor, Quorum Sensing and Enzyme Immobilization

2.1. MBR for Advanced Wastewater Treatment

2.1.1. Concept and Process

The MBR is a technology which combines an activated sludge reactor with a membrane filtration unit for the advanced wastewater treatment and reuse. Wastewater is continuously supplied to the reactor which contains activated sludge. Organic pollutants in wastewater stream are consumed by microorganisms in activated sludge as substrates for growth, maintenance and endogenous metabolism. Simultaneously, this treated water is separated from activated sludge through porous membrane such as microfiltration (MF) or ultrafiltration (UF).

Both biochemical conversion of organic pollutant by microorganism and physical solid-liquid separation through membrane are basic processes which consist of MBR and this provides classification criteria to MBR systems. Firstly, according to the configuration between membrane unit and bioreactor, submerged and side stream type MBRs exist. Secondly, based on biological process type such as redox condition, MBR can be operated in aerobic or anaerobic condition.

2.1.1.1. Submerged and Sidestream MBR

MBR couple membranes with bioreactor in one of two basic configurations: the submerged and side stream MBRs (Figure 2.1). In the case of a side stream system, the membrane unit is independent of the bioreactor. Feed enters the bioreactor where it contacts biomass. This mixture is then pumped around a recirculation loop containing a membrane unit where the

permeate is discharged and the retentate returned to the bioreactor. The transmembrane pressure (TMP) and the crossflow velocity, which define the operation of the membrane, are both generated from a pump. In the submerged configuration, the membrane separation and biodegradation processes are incorporated in the same tank. Under these circumstances, the TMP is derived from the hydraulic head of the water above the membrane. In some systems, this is supplemented by a suction pump to increase the TMP, although this remains significantly less than in sidestream operation.

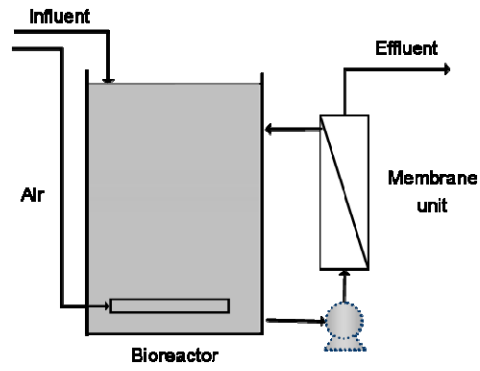
Both submerged and sidestream systems have advantages and disadvantages respectively and these are summarized at Table 2.1. Especially, energy consumption during sidestream MBR operation tends to be greater than during submerged MBR operation due to high rate liquid recirculation required to prevent membrane fouling and maintain high permeate flux rates. In submerged MBR process aeration of the bulk liquid provides the necessary cross-flow velocity at the membrane surface. Outside-in filtration as used in submerged MBR processes can be achieved either under negative pressure, by applying a vacuum to the permeate side of the membrane, or by positive pressure on the bioreactor side of the membrane. More than half of operating MBRs are configured as submerged systems (Figure 2.2a).

2.1.1.2. Aerobic and Anaerobic MBR

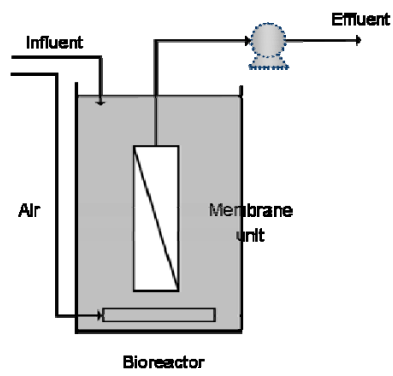
Depending on redox conditions in the bioreactor, systems typically are run as either aerobic or anaerobic processes. In aerobic systems, oxygen supplied as air, is introduced into the biological process using submerged bubble diffusers or surface aeration. Aeration provides the required oxygen transfer for microorganism growth and for mixing in the reactor. In submerged MBR,

coarse bubble diffusers generally are used. The diffusers are not the efficient for oxygen transfer. But the rising bubbles provide turbulent cross flow velocity over the membrane surface, which helps to maintain flux and prevent fouling. Aeration adds to MBR operating costs. In external systems, aeration is accomplished with fine bubble diffusers, a more efficient means of oxygen transfer. However, the operational flux of these systems is higher, so that membrane fouling is more pronounced and vigorous cleaning regimes are necessary.

Anaerobic processes take place in the absence of oxygen. The growth rate of anaerobic bacteria is slower than that of aerobic microbes and requires a longer retention time to treat wastewater effectively. In addition, anaerobic systems typically use external membrane units that need a high recirculation rate. Comparison of each aerobic and anaerobic MBR was summarized in Table 2.2. As illustrated in Figure 2.2b, about 98% of currently installed MBRs are aerobic reactors.



(a)



(b)

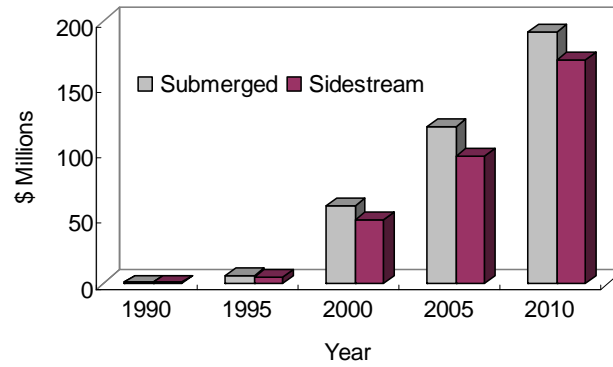
Figure 2.1. Schematics of the (a) sidestream MBR and (b) submerged MBR.

Table 2.1. Advantage and disadvantage of each sidestream and submerged MBR configuration.

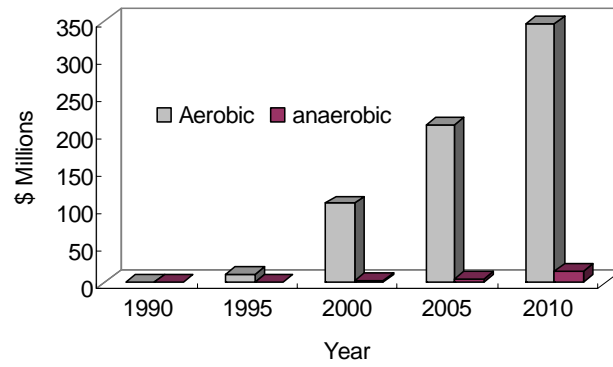
Configuration	Advantage	Disadvantage
Submerged	<ul style="list-style-type: none"> -Low pumping costs -Less frequent cleaning -Lower operating cost 	<ul style="list-style-type: none"> - High aeration costs - Lower flux - Larger footprint - Higher capital costs
Sidestream	<ul style="list-style-type: none"> - Low aeration costs - Higher flux - Smaller footprint - Lower capital costs 	<ul style="list-style-type: none"> - Higher pumping costs - More frequent cleaning - Higher operating costs

Table 2.2. Advantage and disadvantage of each aerobic and anaerobic MBR

Parameter	Aerobic MBR	Anaerobic MBR
Energy consumption	Low	High
Removal efficiency (%)	60 ~ 90	>95
Sludge production	Low	High
Stability	Low ~ Moderate	Moderate ~ high
Alkalinity	High	Low
Biogas production	Yes	No
Nutrients removal	Low	Potentially high



(a)



(b)

Figure 2.2. Estimation of market value of MBR by (a) configuration (submerged vs sidestream) and (b) type of biological process (aerobic vs anaerobic).

2.1.1.3. Advantage and Disadvantage of MBR

The advantages offered by MBR over conventional activated sludge processes (ASP) are widely recognized and of these the ones most often cited are²¹:

- (1) Production of high quality, clarified and largely disinfected permeate product in a single stage; the membrane has an effective pore size <0.1 mm – significantly smaller than the pathogenic bacteria and viruses in the sludge.
- (2) Independent control of solids and hydraulic retention time (SRT and HRT, respectively). In a conventional ASP separation of solids is achieved by sedimentation, which then relies on growth of the mixed liquor solid particles (of flocs) to a sufficient size (>50 mm) to allow their removal by settlement. This then demands an appropriately long HRT for growth. In an MBR the particles need only be larger than the membrane pore size.
- (3) Operation at higher mixed liquor suspended solids (MLSS) concentrations, which reduces the required reactor size and promotes the development of specific nitrifying bacteria, thereby enhancing ammonia removal.
- (4) Reduced sludge production, which results from operation at long SRTs because the longer the solids are retained in the bioreactor the lower the waste solids (sludge) production.

Of these advantages, it is the intensity of the process (i.e. the smaller size of the plant compared to conventional treatment) and the superior quality of the

treated product water that are generally most important in practical wastewater treatment applications. An MBR displaces three or four individual process, demanding only that the initial screening stage be upgraded to limit the impact of large gross solids (>1–3 mm in size) on clogging of the membrane flow channels.

Having said this, compared with conventional biotreatment processes MBRs are to some extent constrained, primarily by:

- (1) Greater process complexity; membrane separation demands additional operational protocols relating to the maintenance of membrane cleanliness.
- (2) Higher capital equipment and operating costs; the membrane component of the MBR incurs a significant capital cost over and above that of an ASP and maintaining membrane cleanliness demands further capital equipment (capex) and operating costs (opex). This is only partly offset by the small size of the plant.

2.1.2. Trends in MBR: Market and Research

2.1.2.1. World Market

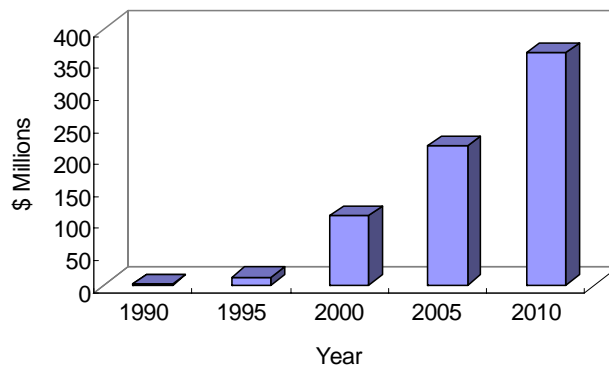
Since first been developed at 1960s, the MBR has been widely used in water reuse systems in building, industry, sanitary treatment and municipal wastewater treatment. In commercial use for little more than a decade, MBR is beginning to realize its market potential in wastewater treatment and water recycling for industrial, municipal, in-building and marine use. For example,

about 2,500 MBR plants have been installed worldwide, while more are proposed or under construction¹. Valued at an estimated \$ 216.6 million in 2005, the global MBR market is rising at an average annual growth rate (AAGR) of 10.9%, faster than the larger market for advanced wastewater treatment equipment, about 5.5% AAGR, and more rapidly than the market for other types of membrane systems, which are increasing at rates from 8% to 10% depending on technology (Figure 2.3a).

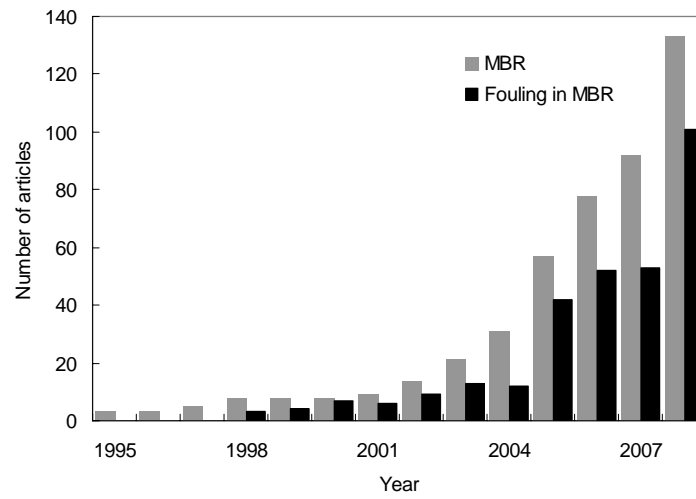
2.1.2.2. Research: Membrane Fouling

The research trend in MBR technology was reviewed by the data on number of articles published since year 1995. As shown in Figure 2.3b, number of published papers increased dramatically since year 2000 in similar way with global market value, which suggests growing acceptance of MBR technology and escalating technical demand to overcome the perceived drawbacks of MBR such as its complex and small scale nature, high costs and operator skill requirements.

The performance of MBR process is mainly deteriorated by the membrane fouling which is the occlusion or blocking of membrane pores at the surface of the membrane. This membrane fouling causes severe operation problems of flux decline, short membrane life-span, and increase of energy consumption and therefore, have been regarded as a main obstacle restricting the development of MBR technology. As clearly shown in Figure 2.3b, over the 70% of MBR researches was dedicated to the topic of fouling including investigation of the mechanism and development of the control techniques.



(a)



(b)

Figure 2.3. Trends in MBR: (a) global market value (Source: BCC. Inc) and (b) number of research articles published since 1995 (Source: ISI)

2.2. Fouling Control in MBR

As previously described, fouling is the most critical factor for the performance of the MBR system. Therefore, during the past two decades, various techniques have been explored to overcome membrane fouling through engineering, material and chemical approach respectively.

2.2.1. Engineering Approach

The basic idea of this approach is to optimize the engineering component in MBR such as aeration intensity, module design, and process configuration.

2.2.1.1. Aeration

Aeration is an indispensable operating factor in MBR to provide the oxygen required for the microbial growth. In addition, the air bubbles rise to the surface of the tank water and create an air lift which recirculates tank water around the membrane module. When the rate of air flow is within an effective range, the rising bubbles and tank water scour and agitate the membranes to inhibit solids in the tank water from fouling the pores of the membranes

Meng et al.²² compared the membrane fouling in three parallel MBRs operated under different aeration conditions and have reported that either small or large aeration intensity had a negative influence on membrane permeability, which implies the presence of the optimum aeration condition.

Phattaranawik et al.³ have suggested the new bubbling method in which bubbling requirements for MBRs are split into fine bubbles for aeration and larger coarse bubbles for fouling control using a bubble-size transformer (BST) comprising converging channels and a tube-bank unit.

2.2.1.2. Module Design

The basic idea of this technique is to enhance the mobility of membrane so as to remove or prevent fouling layer on the membrane surface using physical force induced by hydrodynamics in the bioreactor.

For example, in the US patent 5403479²³, the frameless hollow fiber membrane module was suggested as an efficient physical membrane cleaning method.

Yeon et al.⁵ proposed open-end type hollow fiber module which has higher mobility than conventional closed end type module and reported that this module type use the turbulence in the bioreactor more efficiently, which result in fouling reduction.

Hai et al.⁴ designed hollow fiber membrane module containing a flexible thin spacer which exhibited the optimum rigidity as well as minimize the sludge intrusion.

2.2.1.3. Process Configuration

Membrane fouling can also be controlled by changing the configuration of the system. For example, Kim et al.²⁴ evaluated the effect of the vertical position of the submerged membrane on the fouling and reported that fouling could be alleviated in the upper zone due to the reduced biomass concentration and then applied this configuration to both lab-scale reactor and pilot plant coupled with biological nutrient removal process.

Li et al.²⁵ developed MBR with aerobic granular sludge (MGSBR) in which conventional suspended floc were substituted by the aerobic granules. This

MGSBR showed more enhanced filtration performance compared to the conventional MBR.

2.2.2. Material Approach

Membrane fouling is an interfacial phenomenon between solid membrane surface and mixed liquor containing various organics and microorganisms. Therefore, to increase intrinsic fouling resistance of membrane surface can be a simple and effective fouling control technique. The researches about this topic have been conducted based on the following two principles.

2.2.2.1. Hydrophilicity of the Membrane Surface

Futamura et al.²⁶ carried out filtration experiments with two types of membranes made of same material, polyethylene, but with difference hydrophilicity and reported that the transmembrane pressure (TMP) increase rate of hydrophobic membranes was higher than that of hydrophilic ones. This suggests that fouling resistance of the membrane can be enhanced by regulating the hydrophilicity of the surface.

Sainbayar et al.²⁷ modified the surface of polypropylene membrane by ozone treatment followed by graft polymerization with 2-hydroxy-ethyl methacrylate. This surface modified membrane showed enhanced water permeability in the anaerobic MBR

Yu et al.⁷ modified the surface of polypropylene hollow fiber microfiltration membranes by the photoinduced graft polymerization of acrylamide. This surface modified membrane demonstrated enhanced filtration performance in the submerged MBR compared to the virgin membrane without modification.

2.2.2.2. Antimicrobial surface concept

A surface which can repress the microbial growth (antimicrobial surface) can also be another strategy for fouling prevention. Recently, Tan and Obendorf⁶ imparted an antimicrobial property to microporous polyurethane membrane surface by grafting *N*-halamine precursor and subsequent chlorine bleaching, which showed good bactericidal efficiency but its biofouling control efficiency in the MBR system was not tested. In Korea patent application 10-2006-0136445, chitosan was impregnated to the surface of porous MF/UF membrane to increase the antimicrobial activity of the membrane. When applied to the MBR, these chitosan imparted membranes showed more enhanced water permeability compared to the control membrane without chitosan during 30 days operation²⁸.

2.2.3. Chemical Approach

The basic idea of this approach is to remove the major foulants such as small colloid, biopolymers using chemicals such as zeolite⁹, coagulant²⁹, charged polymer⁸ and activated carbon^{10,30}.

2.2.3.1. Zeolite

Lee et al.⁹ reported that with the addition of natural zeolite, membrane permeability was greatly enhanced by the formation of rigid floc that had lower specific resistance than that of the control activated sludge.

2.2.3.2. Coagulant

Since pore size of MF membrane conventionally used in MBR varies from about 0.04 to 0.4 μm , colloidal particles smaller than this cause pore plugging which increase the filtration resistance. Therefore, addition of coagulant can reduce membrane fouling

Lee et al.⁹ reported that the membrane fouling was reduced remarkably when alum was added into the MBR due to the increase in particle size by coagulation of small colloids.

Chen et al.²⁹ reported that coagulant such as polymeric aluminum chloride and polymeric ferric sulfate could control membrane fouling rate by the restraining of gel layer formation, decelerating the development of membrane foulants and removing stable foulants from the membrane surface.

2.2.3.3. Charged Polymer

Since Chang et al.³¹ have first demonstrated the importance of the microbial physiological state in membrane biofouling, biopolymers produced by microorganisms such as soluble microbial products (SMP) and extracellular polymeric substances (EPS) are currently accepted one of the major foulants in MBR. Furthermore, these biopolymers is generally comprised of polysaccharide, protein, nucleic acid, lipids and humic acids³², most of which has negative charge in the mixed liquor condition. Consequently, water soluble polymers with positive charge have potential of fouling alleviation in MBR.

For example, Nalco company has developed the cationic polymers with the trade mark of 'MPE (Membrane Performance Enhancer)'. MPEs were reported to reduce the biopolymer level especially polysaccharide level⁸ and was successfully applied to pilot- and full-scale MBRs³³.

Koseoglu et al.³⁴ compared the effectiveness of 7 different chemicals of in lab-scale MBR. Although all these additives reduced the membrane fouling, the performance of cationic polymer was independent of small variations in dosing, while for other additives over or under dosing showed detrimental effects on filterability

2.2.3.4. Activated Carbon

When added to the MBRs, activated carbon adsorbs the organic foulants such as slowly biodegradable residual chemical oxygen demand (COD)³⁰, extracellular polymeric substances inside the microbial floc³⁵ and fine colloids³⁰, which results in the performance enhancement in terms of treated water quality and membrane filterability in MBR.

Activated carbon also can change the cake structure which was closely associated with water permeability. For example Kim et al.¹⁰ have reported that the addition of powdered activated carbon (PAC) lead to the decrease of not only the compressibility of sludge floc but also the content of extracellular polymeric substances inside the microbial floc, which increased porosity of cake layer and thus enhanced the membrane flux.

2.2.4. New Perspective: Biofilm on the Membrane Surface

In MBR under constant flux operation, TMP profile, which is an engineering indicator of the membrane fouling, shows a general tendency of a gentle rise up until a transition point and sharp increase thereafter¹¹. Although the conventional fouling control techniques previously reviewed are have been reported to be effective at the fouling prevention in MBR, all of them only extend the operation periods to the transition points and the abrupt TMP

rise-up after transition point, which is more critical problem in MBR, remained to be unchallenged.

In the early stage of the MBR research, the fouling layer established on the membrane surface was considered as abiotic cake layer. Therefore, the fouling mechanism was investigated using physico-chemical concepts such as adsorption of organic foulants on the membrane surface, accumulation of mixed liquor suspended solids, compression of cake according to the operating pressure. However, many reports have shown experimentally the importance of the biological factor on the permeability loss in the MBR (Membrane biofouling) As a result, recent MBR researches placed their research focus on the revealing of the fouling phenomena using biological frame.

Since the year of 2000, the concept of biofilm, ubiquitous surface microbial system, started to be introduced in the interpretation of the biofouling in the MBR and become the main research stream in the area of the MBR for advanced water treatment.

2.2.4.1. Biofilm Basics

Microbial biofilms may be defined as populations of microorganisms that are concentrated at an interface (usually solid/liquid) and typically surrounded by an extracellular polymeric slime matrix³⁶. The general life cycle of biofilm on the solid surface was conceptually depicted in Figure 2.4.

A bacterial biofilm begins to form when individual cells initially attach to a surface. The ability of a cell to perform this “initial attachment event” is controlled by both environmental factors, including nutrient levels, temperature, and pH, and genetic factors, including the presence of genes

encoding motility functions, environmental sensors, adhesins, etc. The combination of factors influencing biofilm development are frequently species-specific, however, there are many features common to most bacteria studied to date. After initial attachment, the cells begin to grow and spread as a monolayer on the surface to form microcolonies. During microcolony formation, cells undergo developmental changes which give rise to the complex architecture of the mature biofilm. Paramount among these changes are the production of the exopolysaccharide matrix, one of the hallmarks of a mature biofilm. As the biofilm continues to grow several things can happen; the biofilm may spread into uninfected areas as environmental conditions allow and, occasionally, cells will detach from the biofilm and re-enter a planktonic mode. These planktonic cells can then repeat the cycle, infecting new surface. Essentially, biofilm may form on any surface exposed to bacteria and some amount of water. Once anchored to a surface, biofilm microorganisms carry out a variety of detrimental or beneficial reactions (by human standards), depending on the surrounding environmental conditions.

A main concept in the study of microbial biofilms is their inherent ‘microscale heterogeneity’. Biofilm heterogeneity is the extent of nonuniform distribution of any selected component in any of the compartments of the biofilm system, such as the distribution of the biomass (structural heterogeneity, Figure 2.5), selected nutrients (chemical heterogeneity, Figure 2.6), selected products of microbial metabolism (physiological heterogeneity, Figure 2.7 and 2.8).

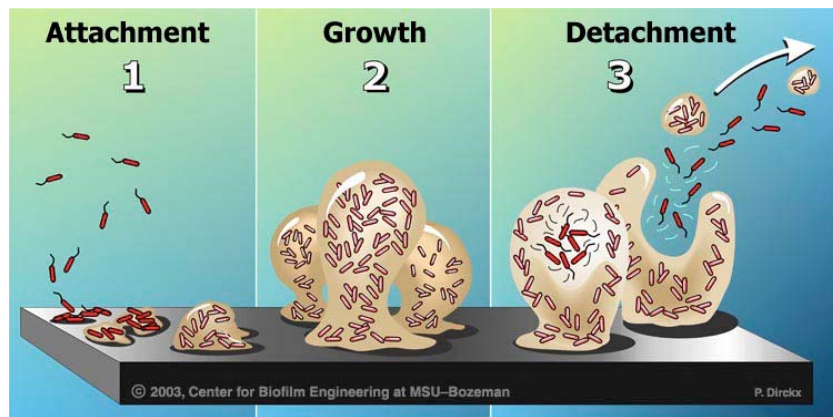


Figure 2.4. The biofilm life cycle in three steps: attachment, growth of micro-colonies, swarming phenomena and detachment in clump. (Image was obtained from the Center for Biofilm Engineering at MSU Bozeman)

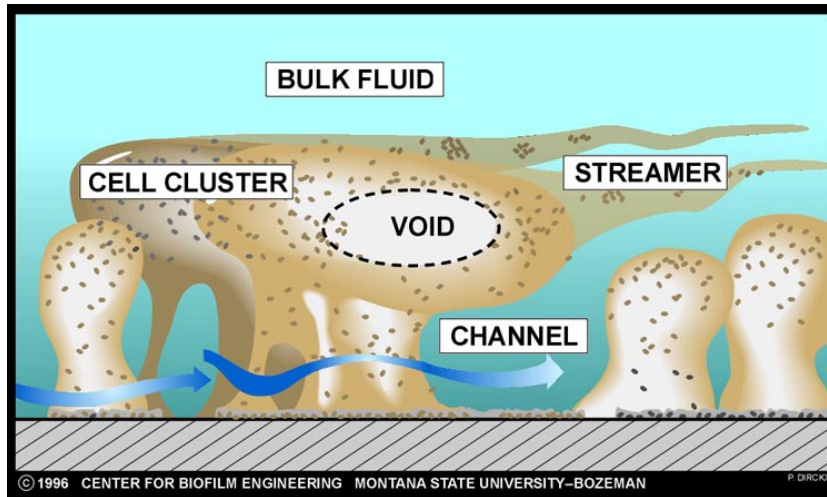


Figure 2.5. Conceptual illustration of the heterogeneity of biofilm structure with bacterial clusters, streamers, and water channels. (Image was obtained from the Center for Biofilm Engineering at MSU Bozeman)

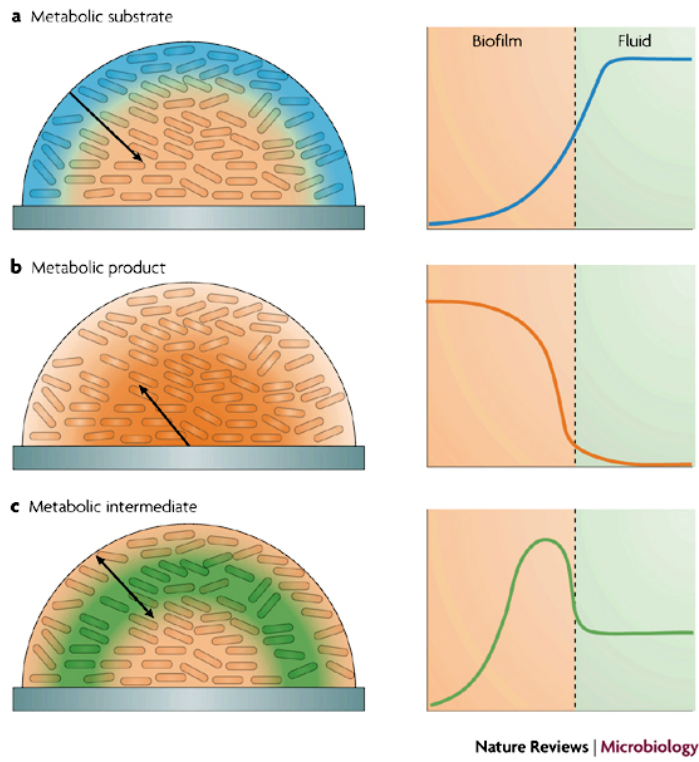
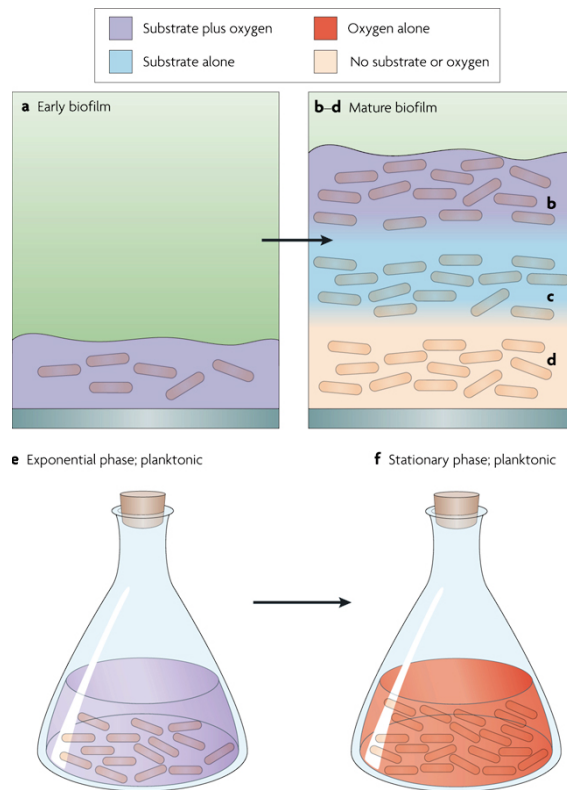
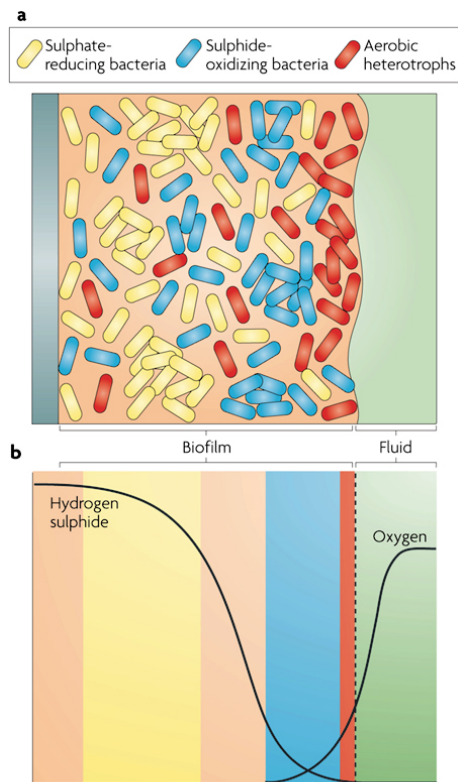


Figure 2.6. Three qualitatively distinct patterns of chemical heterogeneity arise in biofilms. (a) metabolic substrate, (b) metabolic product and (c) metabolic intermediate³⁷



Nature Reviews | Microbiology

Figure 2.7. Physiological heterogeneity in a single-species biofilm. A thin biofilm at an early stage of development (a) is replete with both substrate and oxygen. In the mature biofilm, environments that contain both substrate and oxygen (b), substrate but no oxygen (c) and neither substrate nor oxygen (d) can occur. In an exponential-phase planktonic culture, substrate and oxygen are both present (e), whereas in a shaken stationary-phase culture, substrate can be depleted but oxygen will still be present (f)³⁷



Nature Reviews | Microbiology

Figure 2.8. Physiological heterogeneity in a mixed species biofilm. Three groups of microorganisms are distributed within a biofilm (a), and each experiences a range of chemical microenvironments (b). In panel b, shaded zones denote the regions of oxygen respiration (red), sulphide oxidation (blue) and sulphate reduction (yellow), and the black curves describe the concentration profiles for hydrogen sulphide and oxygen.³⁷

2.2.4.2. Biofilm in the MBR: Current Status of the Arts

Park and Lee³⁸ have experimentally proved that the cake layer formed on the membrane surface was able to biodegrade a certain percentage of the soluble COD. This COD removal fraction increased in proportion to the growth of the cake, which implies that the fouling layer has characteristics of biofilm. Based on these results, Lee¹¹ proposed the concept of biocake which summarizes both the physical deposition of the mixed liquor suspended solids (MLSS) in mixed liquor and biofilm growth on the membrane surface.

Among various biofilm themes, structure, defined as the distribution of biomass in the space occupied by the biofilm, gained the attention of the MBR research. It is because the different biofilms have different structures, and the structure of the same biofilm varies over time. In addition, biofilm structure reflects certain functions of the biofilm such as filtration resistance in the case of the MBR.

Yun et al.¹² analyzed the structure of the membrane-biocake in terms of the internal porosity using the 'biofilm structure analysis technique' which consists of fluorescent staining of biocake components such as bacterial cells and EPS, confocal laser scanning microscopy (CLSM) and image analysis software (ISA-2). They found that high DO concentration conditions induced larger porosity compared to low DO conditions, which resulted in enhanced water permeability in membrane-biocake. Kim et al.³⁹ compared the distribution of EPS in the membrane-biocake in different high and low DO environments using the same techniques and showed that not only the amount of EPS but also its spatial distribution affects the water permeability of the membrane-biocake.

This biofilm structure analysis technique also provided more exact understanding of conventional fouling control techniques. For example, Hwang et al.⁴⁰ monitored the porosity change when conventional fouling reducing cationic polymer was added and found that this chemical induced the more heterogeneous structure with high porosity, which is the main reason for the performance enhancement by addition of the cationic polymer. Lee et al.⁴¹ analyzed the spatial distribution of biocake porosity on the hollow fiber membrane immersed in MBR using biofilm structure analysis technique and investigated a correlation between the biocake porosity and the flux at every local membrane position. Based on these results, they finally suggested the optimum position of an aerator in the reactor to obtain minimal membrane biofouling

All these cases reviewed above clearly demonstrate that this new approach based on the concept of biofilm can be the fundamental solution for biofouling problem in MBR.

2.3. Quorum Sensing

2.3.1. Definition and Mechanism

Bacteria perceives its own cell population density and communicate with each other using small signaling molecules called autoinducers and, as a result, coordinate expression of specific genes to fluctuations in cell-population density. This “bacterial signaling” is generally described as “quorum sensing (QS)” in reference to the frequent observation that the signals only accumulate in environments that support a sufficiently dense population (a quorum) of signal producing bacteria⁴².

QS systems can be divided into three general classes based on the type of autoinducer signal and the apparatus used for its detection;

- (1) Gram-negative bacteria typically have LuxI/LuxR type QS
- (2) Gram-positive bacteria which use modified oligopeptides autoinducers
- (3) Autoinducer-2 (AI-2) for the interspecies communication
- (4).AI-3 and *Pseudomonas* quinolone signal (PQS)

2.3.1.2. Gram-Negative Bacteria: LuxI/LuxR type QS

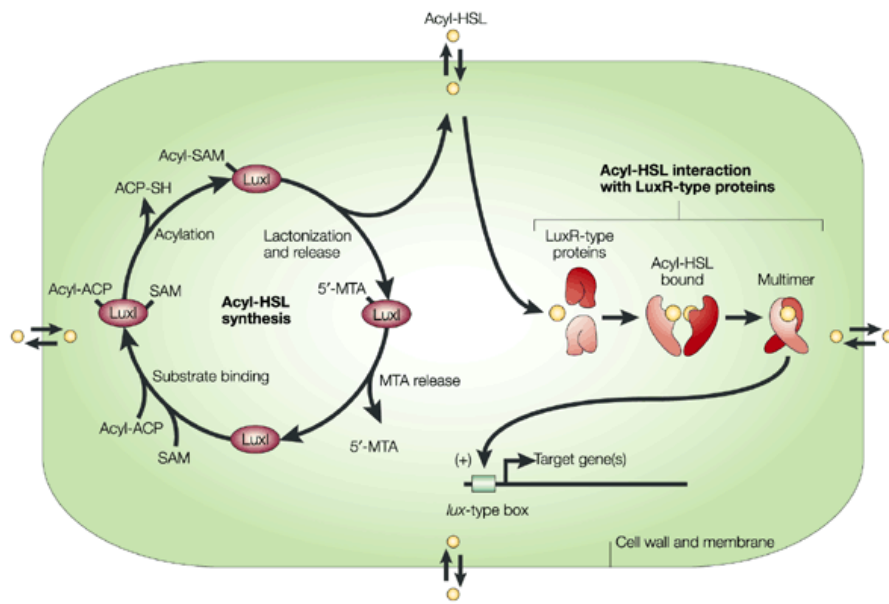
General mechanism of LuxI/LuxR type quorum sensing system of gram - negative bacteria was depicted in Figure 2.9. In this type of QS system, *N*-acylated homoserine lactones (AHLs) which consist of a homoserine lactone ring joined to a fatty acid side that can vary in the number of carbons and modifications on the third carbon is used as an autoinducer (Figure 2.10).

In these gram-negative bacterial QS circuits contain, at a minimum, homologues of two *Vibrio fischeri* regulatory proteins called LuxI and LuxR.

The LuxI-like proteins synthesize a specific AHL signaling molecule ligating a specific acyl moiety from an acyl-acyl carrier protein (acyl-ACP) to the homocysteine moiety of *S*-adenosylmethionine (SAM). In detail, the LuxI-type protein directs the formation of an amide linkage between SAM and the acyl moiety of the acyl-ACP. Subsequent lactonization of the ligated intermediate with the concomitant release of methylthioadenosine occurs. This step results in the formation of the AHL autoinducers (Figure 2.11)

The autoinducer concentration increases with increasing cell-population density. The LuxR-like proteins bind cognate AHL autoinducers that have achieved a critical threshold concentration, and the LuxR-autoinducer complexes also activate target gene transcription

The LuxI/R systems have been identified in over 25 species of gram-negative bacteria and these bacteria were summarized at Table 2.3. Among the 25 species of bacteria that mediate QS by means of a LuxI/LuxR type circuit, the *Vibrio fischeri*, *Pseudomonas aeruginosa*, *Agrobacterium tumefaciens*, and *Erwinia carotovora* systems are the best understood, and descriptions of each of these systems are provided below.



Nature Reviews | Molecular Cell Biology

Figure 2.9. Model of AHL QS in a single generalized bacteria⁴².

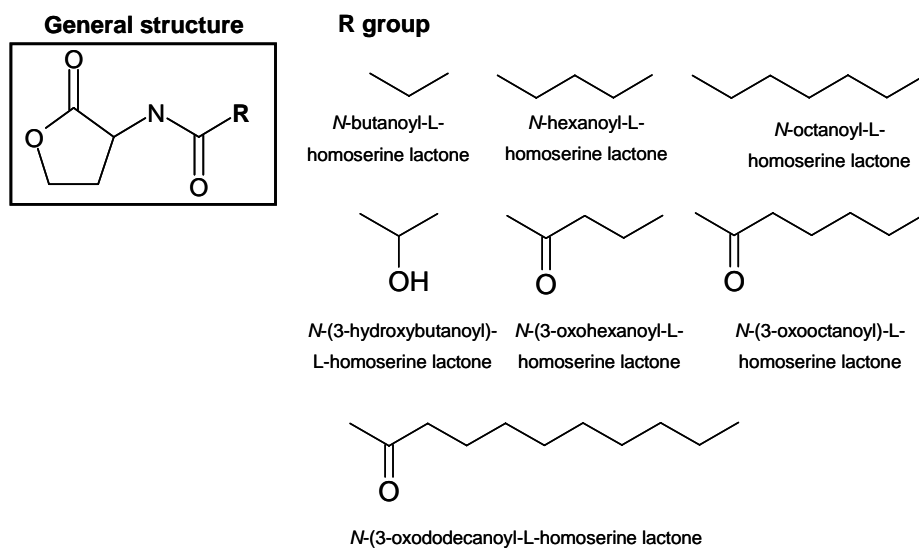


Figure 2.10. Molecular structure of each AHL autoinducer.

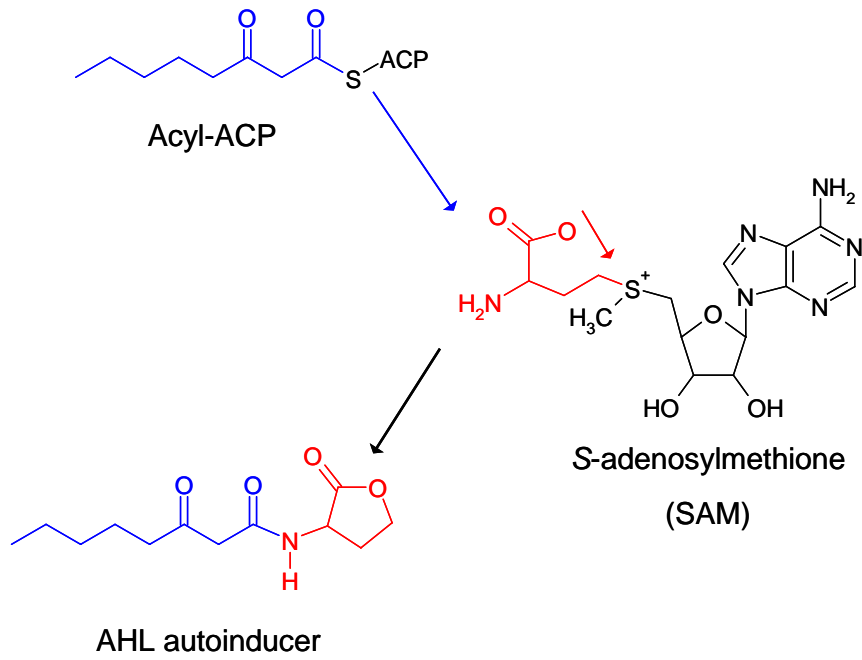


Figure 2.11. LuxI-directed biosynthesis of AHL autoinducers. Shown in the figure is the *N*-(3-oxooctanoyl)-L-homoserine lactone (3-oxo-C8-HSL), which is synthesized by TraI of *Agrobacterium tumefaciens*.

Table 2.3. Organisms possessing LuxI/LuxR homologues : the regulatory proteins, the AHL autoinducers, and the regulated functions⁴³

Organism	LuxI/LuxR Homologue	Autoinducer Identity	Target genes and functions
<i>Vibrio fischeri</i>	LuxI/LuxR	3-oxo-C6-HSL	<i>luxICDABE</i> (bioluminescence) ¹⁴
<i>Aeromonas hydrophila</i>	AhyI/AhyR	C4-HSL	Serine protease and metalloprotease production ⁴⁴
<i>Aeromonas salmonicida</i>	AsaI/AsaR	C4-HSL	<i>aspA</i> (exoprotease) ⁴⁵
<i>Agrobacterium tumefaciens</i>	TraI/TraR	3-oxo-C8-HSL	<i>tra, trb</i> (Ti plasmid conjugal transfer) ⁴⁶
<i>Burkholderia cepacia</i>	CepI/CepR	C8-HSL	Protease and siderophore production ⁴⁷
<i>Chromobacterium violaceum</i>	CviI/CviR	C6-HSL	Violacein pigment, hydrogen cyanide, antibiotics, exoproteases and chitinolytic enzymes ⁴⁸
<i>Enterobacter agglomerans</i>	EagI/EagR	3-oxo-C6-HSL	Unknown ⁴⁹
<i>Erwinia Carotovora</i>	(a) ExpI/ExpR (b) CarI/CarR	3-oxo-C6-HSL	(a) Exoenzyme synthesis ⁵⁰ (b) Carbapenem antibiotic synthesis ⁵¹
<i>Erwinia hrysanthemi</i>	ExpI/ExpR	3-oxo-C6-HSL	<i>pecS</i> (regulator of ectinase synthesis) ⁵²
<i>Erwinia stewartii</i>	EsaI/EsaR	3-oxo-C6-HSL	Capsular polysaccharide Biosynthesis, virulence ¹⁶

Table 2.3. (Continued)

Organism	LuxI/LuxR Homologue	Autoinducer Identity	Target genes and functions
<i>Pseudomonas aereofaciens</i>	PhzI/PhzR	C6-HSL	<i>phz</i> (phenazine antibiotic biosynthesis) ⁵³
<i>Pseudomonas aeruginosa</i>	(a) LasI/LasR (b) RhlI/RhlR	(a) 3-oxo-C12-HSL (b) C4-HSL	(a) <i>lasA</i> , <i>lasB</i> , <i>aprA</i> , <i>toxA</i> (exoprotease virulence factors), biofilm formation ⁵⁴ (b) <i>lasB</i> , <i>rhlAB</i> (rhamnolipid), <i>rpoS</i> (stationary phase) ⁵⁵
<i>Ralstonia solanacearum</i>	SolI/SolR	C6-HSL C8-HSL	Unknown ⁵⁶
<i>Rhizobium etli</i>	RaiI/RaiR	Multiple, unconfirmed	Restriction of nodule number ⁵⁷
<i>Rhizobium leguminosarum</i>	(a) RhiI/RhiR (b) CinI/CinR	(a) C6-HSL (b) 3-OH-7-cis- C14-HSL	(a) <i>rhiABC</i> (rhizosphere genes) and stationary phase ⁵⁸ (b) QS regulatory cascade ⁵⁹
<i>Rhodobacter sphaeroides</i>	CerI/CerR	7,8,-cis-C14-HSL	Prevents bacterial aggregation ⁶⁰
<i>Serratia liquefaciens</i>	SwrI/?	C4-HSL	Swarmer cell differentiation, exoprotease ⁶¹
<i>Vibrio anguillarum</i>	VanI/VanR	3-oxo-C10-HSL	Unknown ⁶²
<i>Yersinia enterocolitica</i>	YenI/YenR	C6-HSL, 3-oxo-C6-HSL	Unknown ⁶³
<i>Yersinia pseudotuberculosis</i>	(a) YpsI/YpsR (b) YtbI/YtbR	(a) 3-oxo-C6-HSL (b) C8-HSL	Hierarchical QS cascade regulating bacterial aggregation ⁶⁴

2.3.1.1.1. *Vibrio fischeri* LuxI/LuxR Bioluminescence System

The first described QS system is that of the bioluminescent marine bacterium *Vibrio fischeri*, and it is considered as the paradigm for QS in most gram-negative bacteria⁶⁵. *Vibrio fischeri* colonizes the light organ of the Hawaiian squid *Euprymna scolopes*. In this organ, the bacteria grow to high cell density and induce the expression of genes required for bioluminescence. The squid uses the light provided by the bacteria for counterillumination to mask its shadow and avoid predation. The bacteria benefit because the light organ is rich in nutrients and allows proliferation in numbers unachievable in seawater

The QS mechanism of *Vibrio fischeri* was shown in Figure 2.12. The luciferase enzymes required for light production in *Vibrio fischeri* are encoded by *luxCDABE*, which exists as part of the *luxICDABE* operon. Two regulatory proteins called LuxI and LuxR comprise the QS. LuxI is the autoinducer synthase, which produces the 3-oxo-C6-HSL¹⁴, and LuxR is the cytoplasmic autoinducer receptor/DNA binding transcriptional activator⁶⁶.

At low cell densities, the *luxICDABE* operon is transcribed at a low basal level. Therefore, a low level of autoinducer is produced via *luxI*, and because the genes encoding luciferase are located directly downstream of the *luxI* gene, only a low level of light is produced. The AHL autoinducer is freely diffusible across the cell membrane, so the concentration of autoinducer in the extracellular environment is the same as the intracellular concentration of the autoinducer

As the *Vibrio fischeri* culture grows, autoinducer accumulates to a threshold level that is sufficient for detection and it is bound by LuxR protein.

Interaction of LuxR with the AHL unmasks the LuxR DNA binding domain, allowing LuxR to bind the *luxICDABE* promoter and activate its transcription. Importantly, the LuxR-AHL complex also induces expression of *luxI* because it is encoded in the luciferase operon. This regulatory configuration floods the environment with the signal. This creates a positive feedback loop that causes the entire population to switch into “QS mode” and produce light.

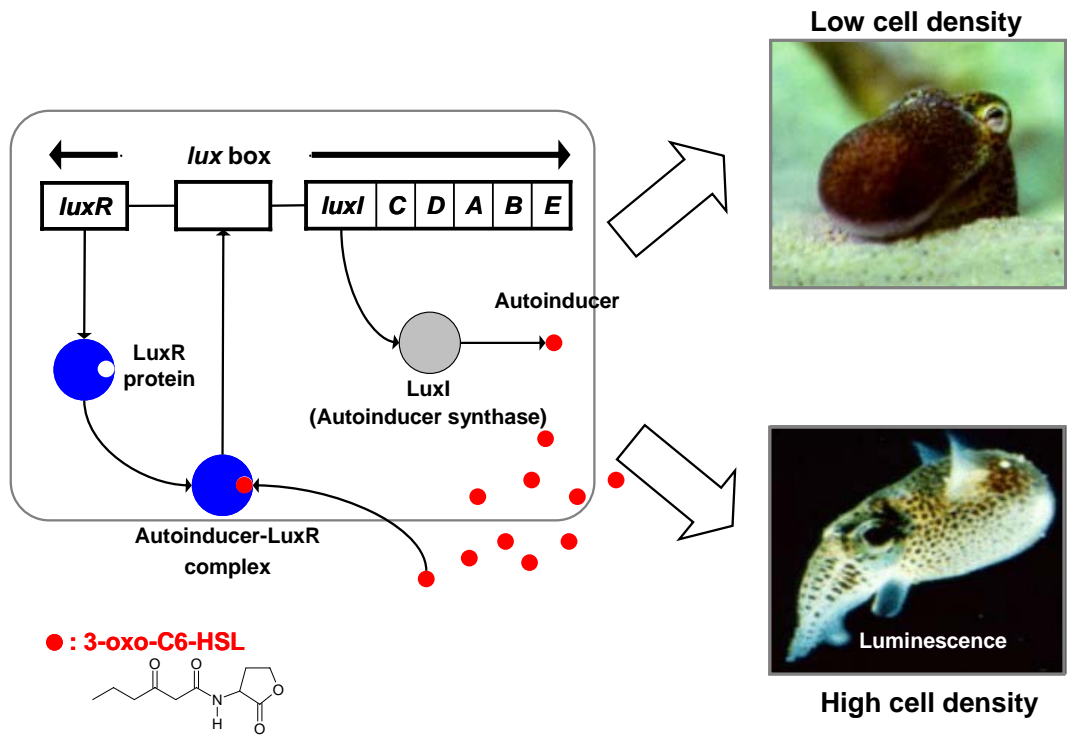


Figure 2.12. The *Vibrio fischeri* LuxI/LuxR QS circuit.

2.3.1.1.2. *Pseudomonas aeruginosa* LasI/LasR-RhII/RhIR Virulence System

In the opportunistic human pathogen *Pseudomonas aeruginosa*, a hierarchical LuxI/LuxR circuit regulates QS. Two pairs of LuxI/LuxR homologues, LasI/LasR⁶⁷ and RhII/RhIR⁶⁸, exist in *Pseudomonas aeruginosa*. Both LasI and RhII are autoinducer synthases that catalyze the formation of 3-oxo-C12-HSL⁵⁴ and C4-HSL⁵⁵, respectively. The two regulatory circuits act in tandem to control the expression of a number of *Pseudomonas aeruginosa* virulence factors. The *Pseudomonas aeruginosa* QS circuit functions as follows. At high cell density, LasR binds its cognate AHL autoinducer, and together they bind at promoter elements immediately preceding the genes encoding a number of secreted virulence factors that are responsible for host tissue destruction during initiation of the infection process. These pathogenicity determinants include elastase, encoded by *lasB*; a protease encoded by *lasA*; ExotoxinA, encoded by *toxA*; and alkaline phosphatase, which is encoded by the *aprA* gene^{17, 69, 70, 67}. Analogous to the *Vibrio fischeri* LuxI/LuxR circuit, LasR bound to autoinducer also activates *lasI* expression, which establishes a positive feedback loop⁷¹. The LasR-autoinducer complex also activates the expression of the second QS system of *Pseudomonas aeruginosa*. Specifically, expression of *rhlR* is induced. RhIR binds the autoinducer produced by RhII; this complex induces the expression of two genes that are also under the control of the LasI/LasR system, *lasB* and *aprA*. Additionally, the RhIR-autoinducer complex activates a second class of specific target genes. These genes include *rpoS*, which encodes the stationary phase sigma factor; *rhlAB*, which encodes rhamnosyltransferase and is

involved in the synthesis of the biosurfactant/hemolysin rhamnolipid; genes involved in pyocyanin antibiotic synthesis; the *lecA* gene, which encodes a cytotoxic lectin; and the *rhlI* gene. Again, similar to LasI/LasR and LuxI/LuxR, activation of *rhlI* establishes an autoregulatory loop. As mentioned above, the LasR-autoinducer complex activates *rhlR* expression to initiate the second signaling cascade. However, the LasR-dependent autoinducer, 3-oxo-C12-HSL, also prevents the binding of the RhlI-dependent autoinducer, C4-HSL, to its cognate regulator RhlR⁷². Presumably, this second level of control of RhlI/RhlR autoinduction by the LasI/LasR system ensures that the two systems initiate their cascades sequentially and in the appropriate order. A model showing the *Pseudomonas aeruginosa* QS circuit is presented in Figure 2.13.

Recent studies on QS in *Pseudomonas aeruginosa* have revealed that QS is crucial for proper biofilm formation. Specifically, *Pseudomonas aeruginosa lasI* mutants do not develop into mature biofilms. Rather, they terminate biofilm formation at the micro-colony stage¹⁷. These mutants can be complemented to wild-type biofilm production by the exogenous addition of the LasI-dependent 3-oxo-C12-HSL autoinducer (Figure 2.14). *Pseudomonas aeruginosa* is the primary pathogen observed in the lungs of people afflicted with cystic fibrosis (CF), and microscopic analysis of CF sputum samples indicates that *Pseudomonas aeruginosa* exists predominantly in biofilms in vivo. Finally, both the LasI- and the RhlI-directed autoinducers have been detected in sputum samples taken from CF patients⁷³. These data indicate that biofilm formation by *Pseudomonas aeruginosa* could be critical for colonization of the lung, and therefore antimicrobial therapies designed to

interfere with quorum sensing, and by analogy with biofilm formation, could be used in the treatment of CF.

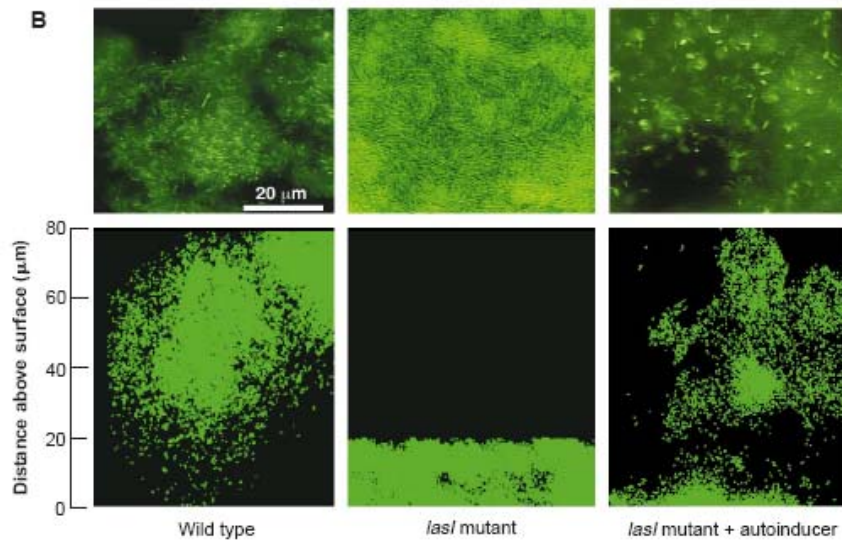


Figure 2.14. Epifluorescence and scanning confocal photomicrographs of the WT and the *lasI* mutant *Pseudomonas aeruginosa* biofilms containing the GFP expression vector pMRP9-1¹⁷.

2.3.1.1.3. *Agrobacterium tumefaciens* TraI/TraR Virulence System

Agrobacterium tumefaciens is a plant pathogen that induces crown gall tumors on susceptible hosts. The transfer of the oncogenic Tumor inducing (Ti) plasmid from the bacterium to the host cell nucleus is required for the tumor formation process.

Upon infection, a region of the Ti plasmid, the T-DNA, is transferred from *Agrobacterium tumefaciens* to the plant cell where it is integrated into the nuclear genome.

Genes on the Ti plasmid direct the biosynthesis and secretion of opines in the plant. Subsequently, opines are consumed as a food source by the invading bacteria. The Ti plasmid also encodes genes that cause the production of phytohormones that induce host cell proliferation resulting in tumors^{74, 75}. In *Agrobacterium tumefaciens*, QS controls the conjugal transfer of the Ti plasmid between bacteria⁴⁶. Both the regulatory components TraI and TraR of the *Agrobacterium tumefaciens* QS system are located on the transmissible Ti plasmid^{76, 77}. Conjugation between *Agrobacterium tumefaciens* cells requires two sensory signals, a host opine signal and the 3-oxo-C8-HSL autoinducer signal, which is the product of the bacterial TraI enzyme. Opines produced at the site of the infection act both as a growth source for the bacteria and to initiate the QS cascade. Opines indirectly induce the expression of TraR via opine-specific regulators. There are two classes of opineregulated conjugal Ti plasmids, octopine-type and nopaline-type. In octopine-type Ti plasmid transfer, the opine octopine acts to induce TraR via the activator OccR, whereas for nopaline-type Ti plasmids, the opines agrocinopine A and B induce TraR expression through the inactivation of the repressor AccR. Note

that OccR and AccR are not LuxR homologues. Thus, QS in *Agrobacterium tumefaciens* is responsive to both host and bacterial signals, indicating that this system has been well adapted for exclusive use at the host-pathogen interface. At a primary level the *Agrobacterium tumefaciens* QS circuit functions analogously to that of *Vibrio fischeri*. Specifically, low, basal-level expression of *traI* results in low levels of autoinducer production. Following opine activation of the expression of *traR*, TraR binds the autoinducer, and the complex induces further expression of *traI* to establish the characteristic positive autoinduction loop. Target genes regulated by the autoinducer-TraR complex include the *tra* operon, the *trb* operon, and a gene called *traM*. The *tra* operon is required for mobilization of the Ti plasmid, and the *trb* operon encodes the genes necessary for production of the mating pore. TraM, while induced by the TraR-autoinducer complex, acts to downregulate QS by binding to TraR and inhibiting TraR from binding DNA and activating target gene expression. TraM therefore adds an additional level of regulation to the *Agrobacterium tumefaciens* circuit that does not appear to exist in the *Vibrio fischeri* circuit.

2.3.1.1.4. *Erwinia carotovora* ExpI/ExpR-CarI/CarR Virulence /Antibiotic system.

The pathogenic bacterium *Erwinia carotovora* causes soft-rot in potato and other plant hosts. The secretion of cellulase and several pectinases that macerate the plant cell walls mediates pathogenicity in *Erwinia carotovora*. A cognate pair of LuxI/LuxR homologues, ExpI/ExpR, is assumed to control secretion of the exoenzymes. Specifically, mutagenesis of *expI* results in a

pleiotropic phenotype that affects several secreted enzymes. No concrete role for ExpR in regulation of the virulence factors has yet been established. Presumably, secretion of exoenzymes only at high cell density, under the control of a QS regulatory cascade, ensures that the bacteria do not prematurely wound the host and thus alert the host to their presence prior to achieving a sufficient bacterial cell number to mount a successful infection.

Similar to *Pseudomonas aeruginosa*, a second LuxI/LuxR-like QS pair exists in *Erwinia carotovora*. The CarI/CarR circuit regulates the biosynthesis of carbapenem antibiotics in response to cell-population density and an AHL autoinducer. In *Erwinia carotovora* antibiotic and exoenzyme production occur simultaneously. It is hypothesized that as the exoenzymes damage the plant cell wall, the antibiotic functions to fend off competitor bacteria that attempt to invade the plant by taking advantage of the wound produced by the *Erwinia carotovora*. Both CarI and ExpI produce the identical autoinducer, 3-oxo-C6-HSL. This result indicates that CarR and ExpR respond to the same signal, which could effectively couple the timing of their individual regulatory activities.

2.3.1.2. Gram-Positive Bacteria: Peptide Mediated QS

Gram-positive bacteria also regulate a variety of processes in response to increasing cell-population density. However, in contrast to gram-negative bacteria, which use AHL autoinducers, gram-positive bacteria employ secreted peptides which are generally secreted via a dedicated ATP-binding cassette (ABC) transporter as autoinducers for QS. A general model for QS in gram-positive bacteria was shown in Figure 2.15. Gram-positive bacteria use two-component adaptive response proteins for detection of the autoinducers. In gram-positive bacteria, a peptide signal precursor locus is translated into a precursor protein (black and white diamonds) that is cleaved (arrows) to produce the processed peptide autoinducer signal (black diamonds). Generally, the peptide signal is transported out of the cell via an ABC transporter (gray protein complex).

When the extracellular concentration of the peptide signal accumulates to the minimal stimulatory level, a histidine sensor kinase protein of a two-component signaling system detects it. The sensor kinase autophosphorylates on a conserved histidine residue (H), and subsequently, the phosphoryl group is transferred to a cognate response regulator protein. The response regulator is phosphorylated on a conserved aspartate residue (D). The phosphorylated response regulator activates the transcription of QS target gene(s).

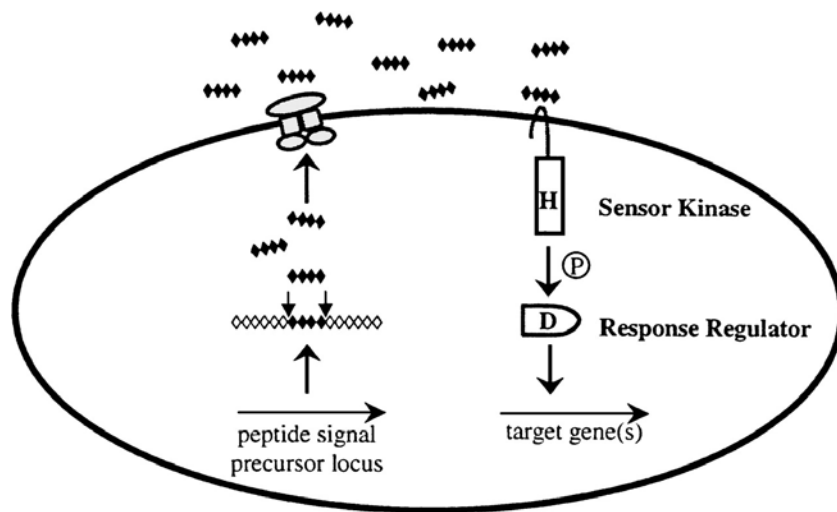


Figure 2.15. A general model for peptide-mediated QS in gram-positive bacteria⁴³.

2.3.1.2.1. *Bacillus subtilis* ComP/ComA Competence/Sporulation System

Bacillus subtilis is a soil organism that uses an elaborate peptide QS system to choose between development of the competent state and the sporulation process. Only 10% of a given population of *Bacillus subtilis* cells become competent, and in contrast to *Streptococcus pneumoniae*, the competent state is achieved at the transition between logarithmic and stationary phase growth.

Presumably, increased levels of exogenous DNA are available as the population enters stationary phase owing to cell lysis. Tuning the onset of the competent state to a later stage of growth (i.e. higher cell density) probably ensures that *Bacillus subtilis* inherits its own species' DNA. It is hypothesized that the small subpopulation of cells that are competent for DNA uptake use the DNA they acquire as a repository of genetic material that can be exploited for repair of damaged/mutated chromosomes. Sporulation in *Bacillus subtilis* occurs when environmental conditions have deteriorated and the bacteria are depleted for nutrients. The bacteria undergo an asymmetric cell division, resulting in the formation of dormant, environmentally resistant spores. Sporulation occurs only poorly at low cell density, even if the *Bacillus subtilis* cells are starved. Regulation of sporulation at high cell density requires several extracellular/environmental signals, but as described below, part of this control is certainly via a QS mechanism. Commitment to vegetative growth, competence, or the sporulation process is irreversible, and an incorrect choice by the *Bacillus subtilis* cell would likely have fatal consequences.

Two peptides mediate QS control of competence and sporulation in *Bacillus subtilis*. The peptides are called ComX and CSF (competence and sporulation factor). Both peptides are secreted and accumulate as the cell density increases. The ComX peptide is 10 amino acids long, and it contains a hydrophobic modification on a tryptophan residue that is required for signaling activity. The processed ComX peptide is derived from a 55-amino acid precursor peptide that is encoded by the *comX* gene⁷⁸⁻⁸⁰. Although the machinery that is required for secretion of ComX has not been identified, a protein called ComQ is required for production of the peptide. The specific role of ComQ remains unknown. Detection of accumulated ComX signal is via the two-component ComP/ComA sensor kinase/response regulator pair. Phospho-ComA activates the expression of the *comS* gene, and ComS inhibits the proteolytic degradation of the ComK protein. ComK is a transcriptional activator that controls the expression of structural genes required to develop competence. ComK is subject to several modes of regulation, one of which is a transcriptional autoregulatory loop. This positive feedback mechanism likely promotes the commitment of the cells to the competence pathway.

The second QS peptide in *Bacillus subtilis*, CSF, is a pentapeptide. The five amino acids at the C-terminus of the precursor peptide PhrC are cleaved to form the CSF signal molecule⁸⁰. CSF accumulates extracellularly as a function of increasing cell density. However, the signaling role of CSF is intracellular. Extracellular CSF is imported into *Bacillus subtilis* by an ABC-type oligopeptide transporter called Opp. When the intracellular concentration of CSF is low, CSF binds to and inhibits a ComA-specific phosphatase called RapC. As mentioned, phospho-ComA is the response regulator controlling the

expression of genes required for competence. Inhibition of RapC by CSF causes a net increase in the level of phospho-ComA. Therefore, low levels of internal CSF promote competence development.

Whereas low internal concentrations of CSF promote competence, high internal levels of CSF inhibit competence and induce sporulation. At high concentration CSF inhibits the expression of *comS*, which results in increased proteolysis of ComK, the protein required for the decision to commit to competence. Furthermore, at high internal concentration, CSF promotes sporulation. The mechanism by which CSF stimulates sporulation is analogous to the mechanism for CSF stimulation of competence. In this case CSF inhibits a phosphatase called RapB.

RapB dephosphorylates a response regulator (Spo0A) that is involved in promoting sporulation. Therefore, inhibition of the RapB phosphatase activity increases the levels of phospho-Spo0A, favoring a switch in commitment from competence to the sporulation pathway. Presumably, adjustment of the concentration of CSF above or below some critical level tips the balance in favor of one lifestyle over another, allowing *Bacillus subtilis* to correctly choose to commit to one of two very different terminal fates. Figure 2.16 shows the interconnected competence/sporulation QS pathway of *Bacillus subtilis*.

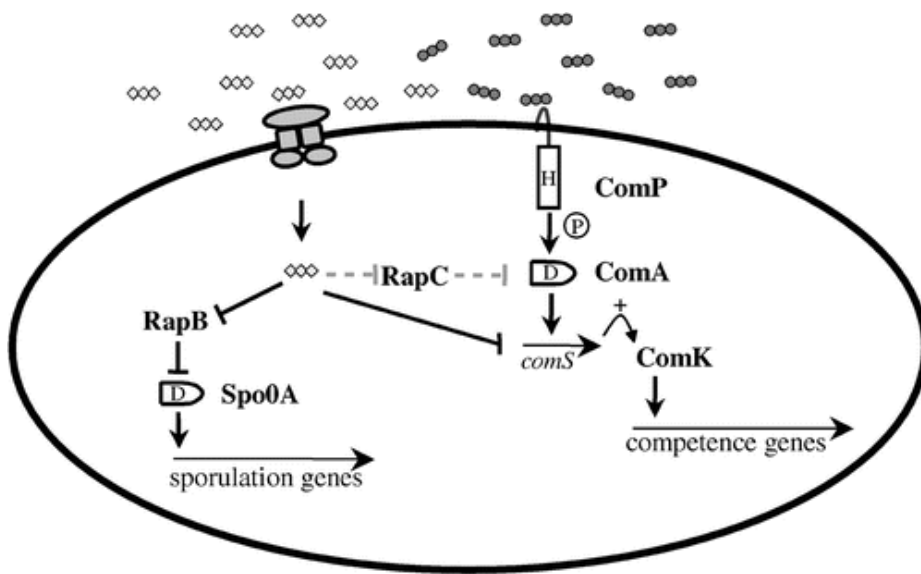


Figure 2.16. QS control of competence and sporulation in *Bacillus subtilis*⁴³.

2.3.1.2.2. *Staphylococcus aureus*: AgrC/AgrA Virulence System

The invasive pathogen *Staphylococcus aureus* causes a variety of human illnesses, including skin infections, toxic shock syndrome, endocarditis, and food poisoning. This multitasking bacterium can promote disease in almost any tissue in the human body. Primarily compromised individuals are susceptible to *Staphylococcus aureus* infection.

A variety of pathogenicity determinants are required for successful invasion by *Staphylococcus aureus*, many of which are regulated by peptide QS. An RNA molecule called RNA III regulates density-dependent pathogenicity in *Staphylococcus aureus*^{81, 82}. The *agrBDCA* operon encodes the components of a peptide QS system that is partially responsible for regulating the levels of RNAIII. The *agrBDCA* locus is adjacent to and transcribed divergently from the *hld* gene. The *hld* gene encodes a hemolysin, and *hld* also encodes the RNAIII transcript. The *agrD* gene specifies the 46-amino acid precursor peptide AgrD that is processed to a final octapeptide by an AgrB-dependent mechanism^{83, 84}. The processed autoinducing peptide (AIP) contains a thiolactone ring that is absolutely required for full signaling activity⁸⁵. AgrC is the sensor kinase and AgrA is the cognate response regulator of the two-component system. Phospho-AgrA, via an unknown mechanism, increases the concentration of RNAIII. RNAIII functions as an effect or to activate the expression of an array of secreted virulence factors.

Tremendous strain-to-strain variation exists in the AIPs of *Staphylococcus aureus*. The variability in the AIPs determines their specificity for interaction with a particular AgrC sensor kinase. *Staphylococcus aureus* strains can be categorized into four different groups based on the specificity of their AIPs. A

remarkable feature of the *Staphylococcus aureus* QS system is that each AIP, while initiating the *agr* virulence cascade in its own group, specifically inhibits the *agr* response in the other *Staphylococcus aureus*⁸⁶. It is hypothesized that this interference with virulence allows the invading *Staphylococcus aureus* strain that is first to establish its quorum sensing circuit to out-compete secondary invading strains.

2.3.1.3. Autoinducer-2 (AI-2) for the Interspecies Communication

Vibrio harveyi makes a typical gram-negative type AHL autoinducer AI-1; however, response to the AHL is mediated by a gram-positive like two-component phospho-relay system. Additionally, *Vibrio harveyi* produces and detects a second autoinducer, AI-2. This autoinducer is produced by a remarkably wide variety of gram-negative and gram-positive bacteria, and in every case production requires a protein called LuxS. Unlike for AHL and oligopeptide autoinducers, the biosynthetic pathway and chemical intermediates in AI-2 production, and possibly the AI-2 molecule itself, are identical in all AI-2-producing bacteria studied to date. These findings have led to the proposal that AI-2 is a ‘universal’ signal, which functions in interspecies cell-to-cell communication⁴³. The structure of *Vibrio harveyi* AI-2 was recently determined to be a novel furanosyl borate diester with no similarity to other autoinducers.

2.3.1.3.2. Biosynthesis and Structure of AI-2

AI-2 is produced from *S*-adenosylmethionine (SAM) in three enzymatic steps (Figure 2.17). SAM is an essential cofactor for processes such as DNA, RNA and protein synthesis. The use of SAM as a methyl donor in these and other metabolic processes produces the toxic intermediate *S*-adenosylhomocysteine (SAH), which is hydrolyzed to *S*-ribosylhomocysteine (SRH) and adenine by the nucleosidase enzyme Pfs (50methylthioadenosine/*S*-adenosylhomocysteine nucleosidase). LuxS catalyzes the cleavage of SRH to 4,5-dihydroxy 2,3-pentanedione (DPD) and homocysteine⁸⁷. Combining purified Pfs and LuxS proteins with SAH in vitro yielded high quantities of

AI-2 activity. Nuclear magnetic resonance (NMR) spectroscopy and mass spectral analyses of the reaction product suggested that it did not contain a significant amount of DPD, but instead contained a mixture of compounds. This finding led to the hypothesis that, following formation, DPD cyclizes to a mixture of furanone rings, which are more stable than the linear DPD. It was assumed that one of the furanones must give rise to the observed AI-2 activity^{87,88}.

The studies described above revealed that AI-2 was produced from the ribosyl moiety of SRH, and previous genetic analyses had demonstrated that the primary sensor for AI-2 in *Vibrio harveyi* (LuxP) was a homolog of the *Escherichia coli* ribose-binding protein. These two findings led to the idea that, if a mixture of products was formed by rearrangement of DPD, LuxP could be used to bind specifically the molecule with AI-2 activity.

Thus, Chen et al.⁸⁹ successfully determined the structure of AI-2 by crystallizing LuxP in a complex with the autoinducer. The crystal showed that AI-2 is a novel furanosyl borate diester.

The presence of a boron atom in AI-2 is especially intriguing because little is known regarding the functional role of boron in biological systems. Boron is ubiquitous in the environment and it is known to be essential in many organisms; however, what role it plays remains mostly a mystery. The current evidence suggests that to form the AI-2 signal molecule, borate is added to one of the products resulting from the spontaneous cyclization of DPD⁸⁹. Boron addition could occur spontaneously; however, it is also possible that an unidentified enzyme catalyzes this modification in vivo. One possibility is

that the LuxP protein plays the dual role of borate-addition enzyme and AI-2 sensor.

At present only the *Vibrio harveyi* AI-2 structure has been determined. To date, the biosynthetic route to DPD production has been shown to be identical in *Escherichia coli*, *Salmonella typhimurium*, *Vibrio harveyi*, *Vibrio cholerae*, and *Enterococcus faecalis*, *Neisseria meningitides*, *Porphyromonas gingivalis* and *Staphylococcus aureus*^{87,90}. Thus, it is assumed that all LuxS containing bacteria make the DPD precursor. However, as all the subsequent steps have not been characterized, we do not know if all AI-2s are identical, or if DPD cyclizes to a variety of furanones that, in turn, undergo different adduct reactions to generate a diverse array of 'AI-2' signal molecules. Another possibility is that LuxS-containing bacteria release DPD or a specific cyclized DPD product, and then each recipient species acts on the precursor to generate a unique AI-2 signal. Finally, some bacteria could produce more than one AI-2 derivative and/or have multiple sensory apparatuses that detect variously modified forms of AI-2. Diversity in AI-2 signal generation and detection could be used as the basis of an extensive chemical lexicon that encodes information about the number of members and species composition of a given community.

2.3.1.3.3. Mechanism of AI-2 Response

Response to AI-2 was graphically depicted in Figure 2.18. The clearest evidence that demonstrates that AI-2 can control gene expression through QS comes from studies of *Vibrio* spp., in particular the organism in which it was first identified, *Vibrio harveyi*. AI-2 is one of three QS signal molecules

produced by *Vibrio harveyi* that control bioluminescence. AI-2 can gain access to the periplasm of *Vibrio harveyi*, where it interacts with the periplasmic binding protein LuxP, which in turn interacts with a membrane-bound histidine protein kinase, LuxQ. In the absence of AI-2, LuxQ autophosphorylates and transfers a phosphate to LuxU, which subsequently passes it to the response regulator, LuxO. Phospho-LuxO, with σ_{54} , activates expression of small regulatory RNA (sRNA), which, with the help of the chaperone Hfq, destabilizes the mRNA that encodes the activator protein LuxR_{Vh}. As LuxR_{Vh} is required for transcription of the luciferase-encoding genes, no light is generated. At high AI-2 concentrations (indicating high cell density), LuxQ functions as a phosphatase, reversing the flow of phosphates and turning on light production. The sensors of the other two autoinducers (AI-1 and cholerae AI-1) feed into the same pathway at the level of LuxU. The components of the AI-2 response network are shared by other *Vibrio* species (including *Vibrio cholerae*, *Vibrio parahaemolyticus*, *Vibrio vulnificus* and *Vibrio fischeri*, as well as the renamed *Listonella anguillarum*). This mechanism integrates the sensory inputs from all the autoinducers; however, *Vibrio harveyi* can distinguish between conditions in which all autoinducers are present (the ‘coincidence state’, characterized by complete dephosphorylation of LuxO) and all other variations. So, in *Vibrio harveyi*, the individual presence of an autoinducer initiates a phosphatase activity that exceeds the remaining kinase activity, but is not sufficient to deplete phospho-LuxO completely.

Therefore, the simultaneous presence of all three autoinducers will result in a more dramatic effect on gene regulation. The sensitivity of this system

might even enable *Vibrio harveyi* to respond to changes in the ratio between AI-1 and AI-2. The involvement of sRNAs in this system might impart the ability to behave as a sensitive, definitive on/off switch leading to an all-or-nothing response. Moreover, it is not dedicated to the control of bioluminescence, but can modulate other phenotypes in *Vibrio harveyi*.

In *Salmonella enterica* Serovar Typhimurium, instead of initiating a phosphorylation cascade, AI-2 seems to be taken up by an ABC TRANSPORTER. As observed with other bacteria, AI-2 is only transiently found in culture supernatants¹⁹. Although AI-2 might undergo inactivation or degradation in the supernatant or on the cell surface (either spontaneously or enzymatically), some bacterial cells can actively take up AI-2, and the genes encoding an ABC transporter were identified as an operon that is differentially expressed in a *Salmonella enterica* Serovar Typhimurium luxS mutant (the luxS-regulated *lsr* operon). Immediately upstream of this *lsrACDBFGE* operon are the divergently transcribed *lsrR* gene (encoding a repressor for the *lsr* operon), and *lsrK* (encoding a kinase responsible for AI-2 phosphorylation). Deletion of *lsrR* results in rapid and complete removal of AI-2 from the supernatant, presumably because the *lsr* operon is maximally expressed and the encoded proteins transport all the AI-2 into the cell. The combined effect of the ABC transporter and adjacent genes is to phosphorylate AI-2 and then further convert it to currently uncharacterized product(s).

Recently, the *Escherichia coli* genes homologous to *lsr* have been shown to have similar functions. As *lsr* transporter mutants retain the ability to slowly internalize AI-2, it appears that there is a second, inefficient AI-2 transporter.

Given the structure of AI-2 and the similarity of the *lsr* operon with riboseuptake systems (*rbs*), it is possible that the latter could function in this regard. However, the *rbs* operon of *Escherichia coli* does not seem to have this function. An alternative transporter normally used to transport other molecules with a similar structure to AI-2 could perform this role. Although also described as a QS related response, the similarity (both by sequence homology and function, that is, uptake followed by phosphorylation) of the Lsr transporter with the uptake mechanisms of other sugars strongly indicates a primarily metabolic role for AI-2.

2.3.1.3.4. Function of AI-2

It has been clear for several years that AI-2 production is widespread in the bacterial kingdom. However, demonstrations that it acts as a signal in bacteria other than *Vibrio harveyi* have not been as readily established. Many recent reports clearly show that both gram-negative and gram-positive bacteria sense and respond to AI-2, and further, that AI-2 controls an assortment of apparently 'niche-specific' genes. The functions of AI-2 that have been reported in the literature are listed in Table 2.4. In nearly all cases, AI-2 acts in conjunction with other regulatory factors. Thus, the delay between the identification of LuxS/AI-2 and its designation as a signaling molecule can be explained by the difficulty required to tease out its exact function in redundant hierarchies.

As mentioned, AI-2 was discovered as one of two redundant QS signals controlling bioluminescence in *Vibrio harveyi*⁹⁰⁻⁹². AI-2 is also a member of a complex QS circuit controlling the virulence cascade in the related bacterium

*Vibrio cholerae*⁹³. The QS system of *Vibrio cholerae* resembles that of *Vibrio harveyi*, but the *Vibrio cholerae* circuit is composed of three parallel signaling channels⁹³.

Clostridium perfringens uses AI-2/LuxS to regulate toxin production⁹⁴. The timing of toxin production is critical for virulence in *Clostridium perfringens* and occurs at mid-late exponential phase. Interestingly, this coincides with the timing of maximal AI-2 production. Analysis of toxin mRNA levels shows that compared with the wild-type, *Clostridium perfringens* luxS mutants have reduced toxin transcription at mid-log phase, whereas at stationary phase, mutant and wild type toxin mRNA levels are similar. Apparently, redundant regulatory mechanisms exist for controlling toxin expression and timing. Stevenson et al.⁹⁵ showed that LuxS from *Borrelia burgdorferi* complements an *Escherichia coli* luxS mutant, and several *Borrelia burgdorferi* proteins showed altered expression following exogenous addition of AI-2. However, *Borrelia burgdorferi* did not produce detectable AI-2, suggesting that it is not made under laboratory conditions and/or that AI-2 production requires a signal from the tick host. *Photobacterium luminescens* has a complex life cycle that includes a symbiosis with a nematode, and a pathogenic phase involving infection of an insect by the bacteria-containing nematode. Antibiotic production by *Photobacterium luminescens* is critical for ensuring monoxenic conditions for nematode reproduction at the moment of insect death. LuxS controls the timing of biosynthesis of the antibiotic and restricts it to mid-log phase, while other factors control the level of production of the drug⁹⁶. In most bacteria examined, extracellular AI-2 activity peaks in mid-late exponential phase and declines precipitously in stationary phase. This

phenomenon has been most thoroughly studied in *Escherichia coli* and *Salmonella enterica* Serovar Typhimurium, where AI-2 levels are further influenced by environmental factors such as osmolarity, pH and carbohydrates^{97, 98}. There is no evidence for the regulation of AI-2 activity at the level of luxS transcription, translation or LuxS protein stability. Fluctuations in AI-2 levels can be partially attributed to alterations in *pfs* expression, which correlate with maximal extracellular AI-2 levels, suggesting that production of AI-2 is controlled at the level of LuxS substrate availability⁹⁹. The rapid disappearance of AI-2 in stationary phase is controlled by another mechanism. Accumulation of extracellular AI-2 at midlog phase induces expression of genes encoding an ABC transporter called Lsr ('LuxS-regulated'), and Lsr transports AI-2 into the cells¹⁰⁰.

We do not yet understand the benefit enteric bacteria derive from producing and releasing AI-2, only to internalize it at later times. It appears that AI-2 cannot be used as a carbon source, suggesting that the bacteria are not 'eating' AI-2¹⁰⁰. Internalization of the signal could be a mechanism for rapidly terminating AI-2-controlled behaviors. Thus, the transient nature of AI-2 could permit a cascade of differently timed behaviors. For example, one set of behaviors could initiate on AI-2 appearance and terminate when AI-2 is internalized, while a different set of behaviors could be induced upon AI-2 internalization.

This use of the AI-2 signal is in contrast to canonical autoinducers that accumulate in stationary phase and thereby produce all-or-none responses. Another possibility is that *Escherichia coli* and *Salmonella enterica* Serovar Typhimurium internalize AI-2 to interfere actively with the signaling

processes of the commensal gut microflora. Perhaps, pathogenic *Escherichia coli* and *Salmonella enterica* Serovar Typhimurium produce AI-2 in early stages of growth to ‘go along with the crowd’, but at later times, eliminating their own signal and that of the commensals could impair the commensals’ ability to communicate effectively, which could provide the intruders with a colonization advantage.

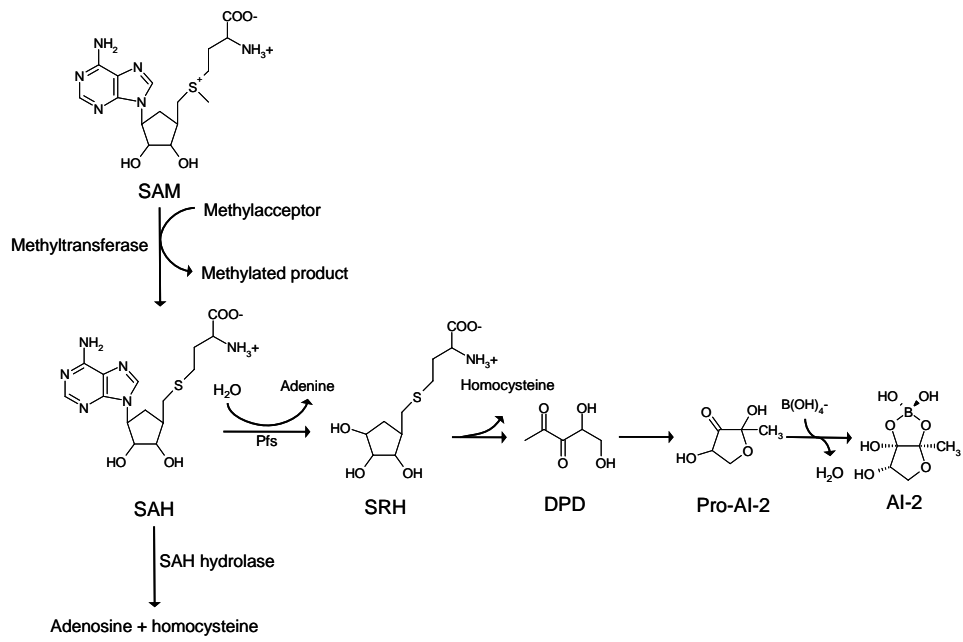
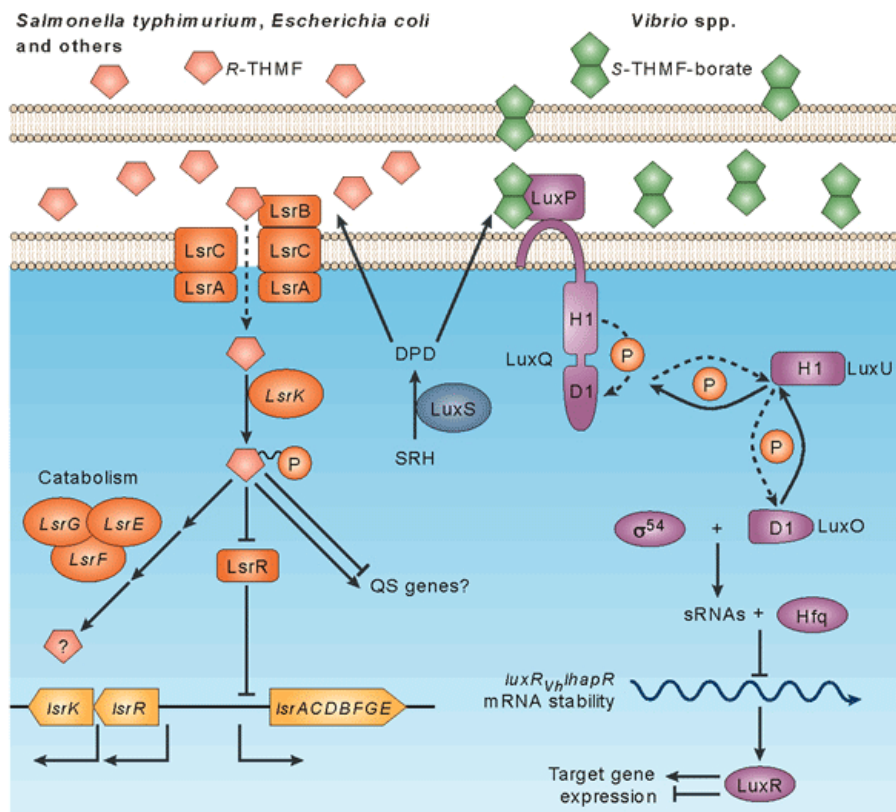


Figure 2.17. Biosynthetic pathway of AI-2.



Nature Reviews | Microbiology

Figure 2.18. Current schemes of AI-2 response¹⁰¹.

Table 2.4. Genes and functions controlled by LuxS in bacteria.

Species	Functions	Genes regulated
<i>Actinobacillus actinomycetecomitans</i>	Virulence factors : leukotixin, iron acquisition	<i>afuA</i> ¹⁰²
<i>Borrelia burgdorferi</i>	Expression of many proteins on two-dimensional	Unknown ⁹⁵
<i>Campylobacter jejuni</i>	Motility	Unknown ⁹⁷
<i>Clostridium perfringens</i>	Virulence factors : alpha, kappa and theta toxins	<i>pfo</i> ⁹⁴
<i>Escherichia coli</i> . W3110	Cell division, DNA processing, cell shape and morphology	242 genes (microarray) ¹⁰³
<i>Escherichia coli</i> . EHEC(O157:H7)	Virulence factors : type-III secretion, Shiga toxin, flagella, motility, cell division	LEE operon, <i>stx</i> , <i>ptsN</i> , <i>sulA</i> , <i>fihD</i> , <i>fiiA</i> , <i>fliC</i> , <i>motA</i> , <i>qseA</i> , <i>qseBC</i> 404 genes (microarray) ^{104, 105, 106}
<i>Escherichia coli</i> . EHEC(O127:H6)	Motility (flagellin expression)	Unknown ¹⁰⁷
<i>Neisseria meningitides</i>	Bacteremic infection	Unknown ¹⁰⁸
<i>Photobacterium luminescens</i>	Carbapenem biosynthesis	<i>cpm</i> ⁹⁶

Table 2.6 (Continued)

Species	Functions	Genes regulated
<i>Photorhabdus luminescens</i>	Carbapenem biosynthesis	<i>cpm</i> ⁹⁶
<i>Porphyromonas gingivalis</i>	Virulence factors: protease, hemagglutinin activities, hemin acquisition	<i>uvrB</i> , <i>hasF</i> ^{102, 109, 110}
<i>Salmonella typhi</i>	Biofilms	Not identified ¹¹¹
<i>Salmonella typhimurium</i>	AI-2 ABC transport system	<i>lsrACDBFGF</i> ¹⁰⁰
<i>Shigella flexneri</i>	Transcription factor involved in controlling virulence	<i>virB</i> ¹¹²
<i>Streptococcus pyogenes</i>	Virulence factors: secreted protease hemolysin	<i>speB</i> and <i>sagA</i> ¹¹³
<i>Vibrio cholerae</i>	Virulence factors: Cholera toxin, toxin-coregulated pilus	<i>tcpP</i> , <i>tcpA</i> , <i>ctxAB</i> , ~70 virulence genes (microarray) ^{93, 114}
<i>Vibrio cholerae</i>	Light production, colony morphology, siderophore production	<i>luxCDABE</i> ^{91, 92, 115}

2.3.1.4. Other QS systems.

At least, two additional QS systems have been identified in gram-negative bacteria. These include autoinducer 3 (AI-3), which is associated with virulence regulation in EHEC O157:H7¹⁰⁴ and the *Pseudomonas* quinolone signal (PQS), which is associated with *Pseudomonas aeruginosa*¹¹⁶.

AI-3 is associated with luxS homologs in EHEC O157:H7, but this signal itself is hydrophobic and thus chemically distinct from the polar AI-2 signals¹⁰⁴. AI-3 is also biologically distinct from AI-2. During EHEC pathogenesis, both AI-3 and host epinephrine, but not AI-2 stimulate expression of the locus of enterocyte effacement (LEE) genes and thus provide evidence of bacteria and host cross-talk during this infection¹¹⁷.

A novel, additional autoinducer has recently been demonstrated to be involved in quorum sensing in *Pseudomonas aeruginosa*. This signal is noteworthy because it is not of the homoserine lactone class. Rather, it is 2-heptyl-3-hydroxy-4-quinolone (denoted PQS for *Pseudomonas* quinolone signal)¹¹⁸. PQS partially controls the expression of the elastase gene *lasB* in conjunction with the Las and Rhl QS systems. The expression of PQS requires LasR, and PQS in turn induces transcription of *rhlI*. These data indicate that PQS is an additional link between the Las and Rhl circuits. The notion is that PQS initiates the Rhl cascade by allowing the production of the RhlI-directed autoinducer only after establishment of the LasI/LasR signaling cascade. PQS molecules are quite hydrophobic and have been shown to be transported between cells by outer membrane vesicles. There is also strong evidence that the PQS actually induces the formation of these vesicles through interference with Mg²⁺ and Ca²⁺ ions in the outer membrane¹¹⁶. In a recent

review, it was suggested that membrane vesicles may represent a mechanism for interkingdom signaling in the plant rhizosphere.

2.3.2. Role of QS in Biofilm

In general, biofilm cells encounter much higher local cell densities than free-floating, planktonic cell populations. An obvious consequence of this is the elevated levels of metabolic by-products, secondary metabolites and other secreted or excreted microbial factors that biofilm cells encounter. Of particular interest are intercellular signaling or QS molecules. Because biofilms generally consist of aggregates of cells, one could argue that they represent an environmentally relevant context for QS. This idea that the biofilms are optimum sites for expression of phenotypes regulated by QS has led to numerous studies of QS mechanism in the bacterial biofilms including its various phenotypes.

2.3.2.1. Attachment

Attachment of a bacterium to a surface, or substratum, is the initial step in the formation of a biofilm. The nature of the attachment surface in addition to several microbial factors have been shown to affect adherence¹¹⁹.

In general, the cyclic-peptide-dependent accessory gene regulator (*agr*) QS system in *Staphylococcus aureus* represses several surface adhesins that mediate contact with the host matrix¹²⁰. These include fibrinogen- and fibronectin-binding proteins. Under certain conditions, *agr* mutants adhere more efficiently than wild-type strains to both biological and abiotic surfaces^{121, 122, 123}.

The gastrointestinal pathogen *Helicobacter pylori* has a luxS homolog that has been implicated in attachment. A luxS mutant was shown to adhere approximately twice as well as the wild-type strain¹²⁴. Conversely, LuxS of the pathogen *Salmonella enterica* serovar Typhimurium was shown to be required for biofilm formation on human gallstones¹¹¹.

2.3.2.2. Maturation

The maturation of a biofilm community occurs downstream of adherence. The architecture of mature biofilms can vary from flat, homogenous biofilms, to highly structured biofilms, characterized by void spaces and towers of cells encased in an extracellular matrix. The architecture of a biofilm affects the distribution of chemical gradients and potentially the antimicrobial tolerance profiles of bacteria in the biofilm, although the latter remains to be tested experimentally³⁶. Several factors have been shown to influence biofilm architecture, including motility, extracellular polymeric substance matrix production and rhamnolipid production^{125, 126, 127}.

AHL-based QS has been shown to influence biofilm maturation for the gram-negative bacterium *Serratia liquefaciens*¹²⁸. QS regulates swarming motility in *Serratia liquefaciens*¹²⁹. Wild-type *Serratia liquefaciens* biofilms are heterogenous, consisting of cell aggregates and long filaments of cells. A mutation in the AHL synthase gene, *swrI*, resulted in thin biofilms that lacked aggregates and filaments. Two QS regulated genes, *bsmA* and *bsmB*, were also implicated in biofilm development. The BsmA and BsmB proteins showed no homology to proteins of known function. The CepI/R QS system of *Burkholderia cepacia* H111 has also been shown to control biofilm maturation. Huber et al.¹³⁰ showed that strains with mutations in either *cepI* or

cepR formed biofilms that were arrested at the microcolony stage of growth, whereas the wild-type strain formed more robust biofilms that covered the attachment surface. The AhyI/R AHL QS system of *Aeromonas hydrophila* has also been shown to be required for biofilm maturation¹³¹. A strain harboring an *ahyI* mutation formed biofilms that were structurally less differentiated than the wild-type strain. Interestingly, the *ahyI* mutant also showed a gradual reduction in biofilm associated viable counts, leading the authors to suggest that the *ahyI* mutant biofilm cells were more susceptible to biofilm-related stress. This phenotype could be partially overcome by exogenous addition of C4-HSL, the cognate AHL of the system. For all three of the systems mentioned, the functional consequence of this altered architecture is unclear.

The LuxS type QS system in *Streptococcus* mutants is also involved in biofilm development. A mutation in *luxS* resulted in mature biofilms with less overall biomass¹³². The architecture of the mature biofilm was different for the mutant strain. A *luxS* mutant biofilm grown on hydroxyapatite disks was loose and rough in appearance compared with the wild-type strain, which formed biofilms that were smooth and confluent. A two-component regulatory system, *smu486* and *smu487*, was also identified as potentially being involved in the QS dependent biofilm phenotype¹³².

2.3.2.3. Aggregation and Dissolution or Dispersal

Aggregation in liquid culture has been correlated with a propensity to form biofilm communities. Liquid-culture aggregates probably have many of the same characteristics as a biofilm community, including cells held together by an extracellular matrix and steep chemical gradients within the aggregate. Cell

aggregates, or flocs, are observed in both industrial (e.g. wastewater treatment plants) and natural (e.g. marine snow) settings.

There is growing appreciation within the biofilm field that individual cells of a variety of bacterial species are capable of actively leaving a biofilm. Presumably, this dispersal process could serve to enable bacteria to colonize new surfaces and reinitiate the biofilm developmental process^{133, 134}. Using QS to regulate this process makes sense. In crowded conditions, where resources are becoming limited, QS would be an ideal way to mediate exodus from a biofilm. As described below, there is some evidence to support the notion that for certain bacterial species QS controls dispersal.

AHL based quorum sensing in the phototroph, *Rhodobacter sphaeroides*, has been shown to control cellular aggregation⁶⁰. Mutations in the AHL synthase of the *Rhodobacter sphaeroides* QS system, called *cer* (for community escape response), resulted in hyper aggregation of cells in liquid culture. The ecological role of QS in this organism remains unclear.

The enteric pathogen, *Yersinia pseudotuberculosis*, shows a similar phenotype for QS mutants in its AHL YpsI/R QS system⁶⁴. Mutations in the regulator *ypsR* cause the organism to aggregate in liquid culture. Expression of a 42 kDa surface protein with homology to flagellin was found to be activated in the *ypsR* background and might mediate aggregation. Mutations in both the regulator and the AHL synthase resulted in increased swimming motility.

The plant pathogen, *Xanthomonas campestris*, has a novel QS system that has been implicated in biofilm dispersal¹³⁵. The signal for this system, DSF (for diffusible signal factor) has not yet been identified, however, the gene

responsible for its production (*rpfF*) and a two-component system that senses the signal (encoded by *rpfC* and *rpfG*) have been identified¹³⁶.

Mutations in this system result in aggregates in liquid culture and increased biofilm formation. The secreted polysaccharide, known as xanthan, mediates intercellular aggregation in this organism. *Xanthomonas campestris* produces an extracellular mannosidase, responsible for cleaving xanthan, which is regulated by the DSF/*rpf* QS system and contributes to dissolution of aggregates¹³⁷.

Similar to *Xanthomonas campestris*, the enteric pathogen *Vibrio cholerae* uses QS to regulate production of the secreted exopolysaccharide encoded by the *vps* operon. This exopolysaccharide mediates intercellular aggregation and adherence to surfaces. A homolog of a repressor involved in luxS-based signaling, designated HapR, represses expression of *vps* exopolysaccharide biosynthesis, and a *hapR* mutation results in exopolysaccharide overproduction and a smaller, wrinkled colony, or 'rugose' phenotype when grown on solid medium^{138, 139, 140}. The current model is that attaining a quorum leads to reduction in *vps* exopolysaccharide synthesis. In addition to stimulating biofilm formation and aggregation, it has been suggested that *vps* overproduction might enable *Vibrio cholerae* to survive navigation across the acid pH barrier of the stomach and ultimately promote infection.

2.3.2.4. Current Opinions in the Correlation between QS and Biofilm

Many studies have successfully shown that QS affects the biofilm development for several bacterial species. However, whether QS is absolutely involved in control of the biofilm development is still controversial. For

example, Davies et al.¹⁷ showed that *lasI* mutant of *Pseudomonas aeruginosa* formed flat, undifferentiated biofilms. In striking contrast, Heydorn et al.¹⁴¹ demonstrated that a wild-type biofilm of *Pseudomonas aeruginosa* is indistinguishable from a biofilm formed by a *lasI* mutant, using COMSTAT-assisted image analysis. They also reported that when a biofilm of *Pseudomonas aeruginosa* QS mutant was grown on glucose as the carbon source, a difference in biofilm architecture could be found using image analysis. However, when carbon source was changed to citrate, no difference could be detected¹⁴¹.

An interesting point when considering these data is the criteria that are used to determine the role that QS plays in biofilm formation. A common theme in the studies discussed above is that mutants are constructed in key QS regulators and then biofilm phenotypes are evaluated. Perhaps it is not surprising that QS has been found to be important for biofilm formation under these conditions. There is growing evidence that QS constitutes a global regulatory system in many different species. Generating a mutation in a global regulator would produce pleiotropic phenotypes, and anything that affects motility, surface appendage expression or the chemistry of the cell surface might translate to a biofilm phenotype. Perhaps the best way to evaluate the role of QS is to monitor the signaling process in situ in a developing biofilm of a wild-type strain and determine if the onset of QS corresponds to any discernible transition in development, such as changes in structure or an increase in antimicrobial tolerance. Although this type of analysis would not be trivial, a more accurate understanding of QS in biofilm development might be achieved.

Whether QS is involved in forming one type of biofilm or another is probably of less importance. More interesting are the properties or function of the biofilm. For example, many previous researches found a link between biofilm tolerance against various antibiotics, biocides, peroxide and QS. In detail, biofilms formed by QS mutants or biofilm treated with quorum sensing inhibitors were much more susceptible to the actions of these compounds. These findings, in conjunction with QS control of virulence factor, point out that QS can be a highly attractive target for chemotherapy against biofilm chronic infections.

2.4. QS Control Strategy

AHL type QS system of gram-negative bacteria generally offers three points of attack: The signal generator (LuxI homologue), the signal molecule (AHL) and the signal receptor (LuxR homologue). Therefore, AHL QS inhibition strategy can be divided into blockage of AHL synthesis, interference with signal receptor and inactivation of AHL molecules (Figure 2.19).

2.4.1 Blockage of Signal Synthesis

To date, the least investigated strategy to interfere with quorum sensing is blockage of AHL production. As shown in Figure 2.11, the LuxI family proteins use *S*-adenosylmethionine (SAM) and specific acyl-acyl carrier proteins (acyl-ACP) as substrates for AHL autoinducer biosynthesis. The LuxI type proteins direct the formation of an amide linkage between SAM and the acyl moiety of the acyl-ACP. Subsequent lactonization of the ligated intermediate with the concomitant release of methylthioadenosine occurs. This step results in the formation of the AHL.

Parsek et al.¹⁴² have found that analogues of these AHL building blocks such as holo-ACP, *L/D-S*-adenosylhomocysteine, sinefungin and butyryl-*S*-adenosylmethionine (butyryl-SAM) were able to block AHL production *in vitro*. However, none of them have been tested on bacteria *in vivo* and how these analogues of AHL building block, SAM and acyl-ACP, which are also used in central amino acid and fatty acid catabolism, would affect other cellular functions is presently unknown.

In addition, Rudrappa et al.¹⁴³ have reported that curcumin inhibits PAO1 virulence factors such as biofilm formation, pyocyanin biosynthesis, elastase/protease activity, and AHL production. However, the exact inhibition mechanism of curcumin was not revealed.

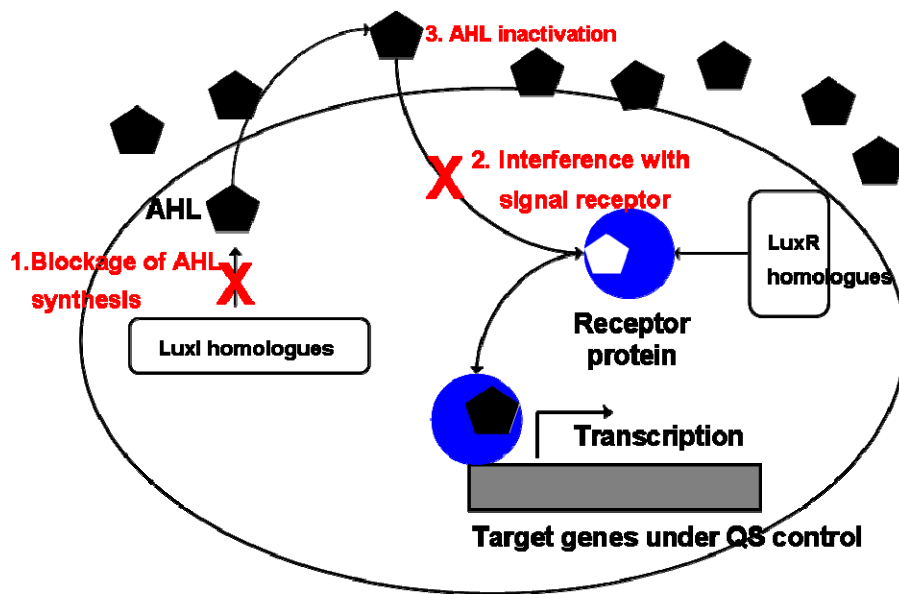


Figure 2.19. Three basic AHL QS control strategies.

2.4.2. Interference with Signal Molecules

A second QS control approach is to prevent the signal from being perceived by the bacteria using chemicals (QS inhibitor). These QS inhibitors can be obtained from both natural source and chemical synthesis.

2.4.2.1. Natural QS Inhibitor

In a recent screening of 50 *Penicillium* species grown on different growth media, a remarkably high fraction, 66% were found to produce secondary metabolites with QS inhibition activity. Two of the compounds were identified as penicilic acid (Figure 2.20a) and patulin (Figure 2.20b) produced by *Penicillium Radicicola* and *Penicillium coprobium*, respectively. A target validation analysis performed by DNA microarray-based transcriptomics showed that patulin targets 45% of the QS genes in *Pseudomonas aeruginosa*.

Extract of garlic was found to act as a potent inhibitor of QS regulated genes such as alginate and elastase in *Pseudomonas aeruginosa*¹⁴⁴. For example, addition of garlic extract to *Pseudomonas aeruginosa* resulted in a flat, undifferentiated biofilm which is very similar with that formed by the quorum sensing mutant. When examined in detail, garlic extract proved to contain a minimum of three different quorum sensing inhibitors, one of which has been identified to be a cyclic disulphur compound.

Diketopiperazines (DKPs) are a family of cyclic dipeptides that have been isolated in the supernatant of numerous cultures of bacterial species, including *Pseudomonas aeruginosa*, *Proteus mirabilis*, *Citrobacter freundii*, and *Enterobacter agglomerans*¹⁴⁵, as well as from protein hydrolysates and fermentation broths from yeast, lichen, and fungi¹⁴⁶. Some Diketopiperazines (DKPs) share structural similarity to endogenous signaling peptides, such as

thyrotropin-releasing hormone¹⁴⁶, and one DKP (cyclo- (L-His-LPro)) has been identified in mammalian tissues.

Holden et al.¹⁴⁵ reported that DKPs can modulate quorum-dependent phenotypes in several different species of bacteria by acting as AHL antagonists in some LuxR-based QS systems and as agonists in others¹⁴⁵. Differential recognition of various DKPs by different LuxR homologues suggests that these AHL mimics may play a role in both intra- and interspecies QS regulation. Chemical structure of DKPs which can act as AHL antagonist was shown in Figure 2.20c-e.

Many higher plant species also secrete substances that mimic AHL signals and affect QS behaviors in bacteria. As in animal cells, these mimics may serve a defensive function by preventing the production of virulence factors in pathogenic organisms. Interestingly, plant derived AHL mimics include substances that both stimulate and inhibit bacterial QS systems. For instance, components of pea seedling exudates inhibited AHL induced violacein synthesis in *Chromobacterium violaceum*, induced swarming activity in *Serratia liquefaciens* MG44, which is defective in AHL synthesis, and induced luminescence in *Escherichia coli* reporters containing plasmids encoding either LuxR from *Vibrio fischeri*, AhyR from *Aeromonas hydrophila*, or LasR from *Pseudomonas aeruginosa*¹⁴⁷. In addition, extracts from rice, soybean, tomato, crown vetch, and *Medicago truncatula* all contain AHL mimics^{148, 149, 150}. The unicellular green alga *Chlamydomonas reinhardtii* also produces substances that interfere with bacterial QS systems¹⁴⁹. Interestingly, a subset of compounds fractionated from *Chlamydomonas reinhardtii* extracts using an ethyl acetate-based extraction procedure similar

to that used to purify AHLs from bacterial culture supernatants stimulated the activity of LuxR-type proteins.

One such compound, selected as a LasR activator, elicited similar, although not identical, changes in gene expression in *Sinorhizobium meliloti* as bonafide AHLs, suggesting that these ethyl acetate-extractable compounds are structurally related to AHLs. A second set of compounds isolated from *Chlamydomonas reinhardtii* that functioned as QS inhibitors did not co-fractionate with these stimulatory activities, suggesting that they are likely to be structurally distinct from AHLs. Although the exact structures of these compounds have not yet been determined, the genetic amenability and the availability of the complete genome sequence of *Chlamydomonas reinhardtii* should permit the rapid identification of genes associated with these responses.

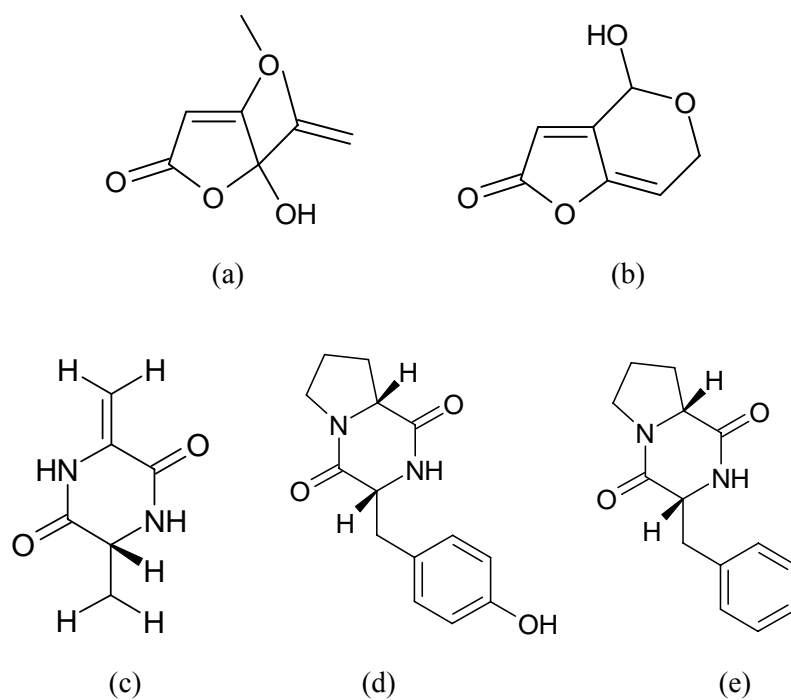


Figure 2.20. QS inhibitors from natural source. (a) penicilic acid, (b) patulin, (c) Diketopiperazines produced by *Pseudomonas putida*, (d) Cyclo(L-Phe-Pro), (e) Cyclo(L-Leu-L-Val).

2.4.2.2. Synthetic QS Inhibitor

2.4.2.2.1. AHL based Inhibitor

One widely explored method is to block the receptor with an analogue of the AHL autoinducer molecule. AHL analogs can be substituted in either the side chain or the ring moiety. Analogs of the 3-oxo-C6 HSL molecule with different substituents in the side chain (Figure 2.21) are able to displace the native signal from the LuxR receptor. However, most of these compounds also exhibit agonists effects, which limit their use as QS inhibitor¹⁵¹. If the C-2 atom in the side chain is replaced by a sulfur atom (Figure 2.21a), it will produce a potent inhibitor of both the *lux* and *las* systems¹⁵². Likewise, if the C-1 atom is replaced by a sulfonyl group, a QS inhibitor is also generated (Figure 2.21b)¹⁵³.

Another strategy to modify the AHL signal molecules is to place atoms or groups at the end of the side chain. Substituting secondary alkyl groups at the C6 atom of 3-oxo-C6 HSL gives rise to agonists, whereas positioning of a secondary aryl group on that location gives rise to an antagonist (Figure 2.21c). Because the size difference between the two types of molecules is negligible, the differences in activity are probably due to the ability of the aryl compounds to interact hydrophobic ally with aromatic amino acids in the protein. If the size of the substituents is increased to include tertiary alkyl derivatives or even larger alkyl and aryl moiety, agonistic activity of the molecules is lost, indicating that they are too bulky to enter the AHL binding site in the receptor protein.

Instead of substitutions at acyl side chain, the entire ring can be exchanged with another cyclic structure. For example, 3-oxo-C12-(2-

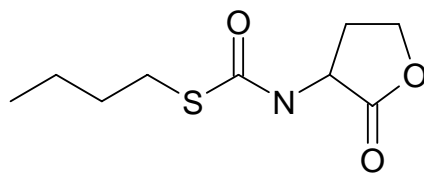
aminocyclohexanone, Figure 2.22a) is an inhibitor of the LasR-based QS system. It is able to downregulate LasR dependent expression of LasI AHL synthase. When applied in a concentration of 100 μ M (which is relatively high for a QS inhibitor), the compound significantly reduced the production of exoproteins. An even more potent inhibitor of LasR is 3-oxo-C12-(2-aminophenol, Figure 2.22b)), which is able to abolish production of pyocyanin and elastase; in addition, it can disrupt normal biofilm formation by *Pseudomonas aeruginosa*. Interestingly, the very similar molecule 3-oxo-C12-(2-aminocyclohexanol), with the phenol replaced by a hexane ring, is a potent agonist of the *las* system. A similar situation is seen with analogs of 3-oxo-C6 HSL from the lux system. If the HSL ring is replaced by a hexane ring, the ability to activate LuxR is retained. On the other hand, if the HSL ring is replaced by a benzyl group, an inhibitor of LuxR is generated¹⁵⁴.

Ishida et al.¹⁵⁵ have synthesized a series of structural analogs of *N*-octanoyl cyclopentylamide with 4~12 carbon. They also have reported that *N*-decanoyl cyclopentylamide (Figure 2.22c) inhibited production of virulence factors, including elastase, pyocyanin, rhamnolipid, and biofilm formation without affecting growth of *Pseudomonas aeruginosa* PAO1.

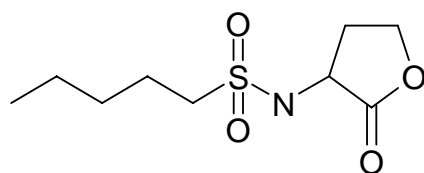
2.4.2.2.2. Non-AHL based Inhibitor

QS inhibitors have also been identified by screening of random compound libraries. Using the above-mentioned screens, Rasmussen¹⁴⁴ identified several QS inhibiting compounds with structures unrelated to the signal molecules, including 2,4,5-tribromo-imidazole, indole, and 3-nitrobenzene sulphone amide, and 4-nitro-pyridine-N-oxide (4-NPO) (Figure 2.23), the first being the most effective. 4-NPO treatment was found to block the *Escherichia coli*

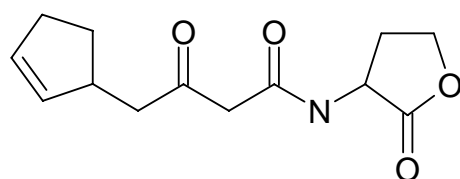
established hybrid LuxR QS system, and further analysis demonstrated a similar effect on *Pseudomonas aeruginosa* cells harbouring a *lasB-gfp* fusion. However, this does not necessarily mean that the compound blocks the quorum sensing regulon in *Pseudomonas aeruginosa*. By the use of DNA micro array-based transcriptomics it was established that 4-NPO significantly lowers expression of 37% of the QS regulated genes in *Pseudomonas aeruginosa*, including several virulence factors known to be regulated by LasR and RhlR. The analysis was based on sample points taken at an optical density of 2.0 and only changes in gene expression greater than fivefold were taken into consideration. Taking into account that genes of the quorum sensing regulon are expressed as a continuum during the planktonic growth cycle the results strongly suggest that the LasR and RhlR receptors were targeted by the compound.



(a)

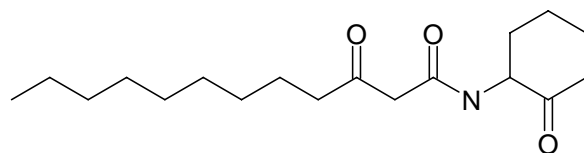


(b)

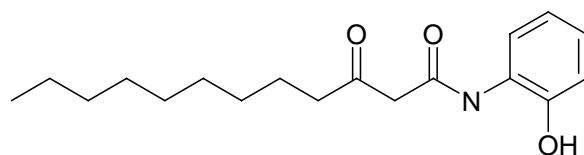


(c)

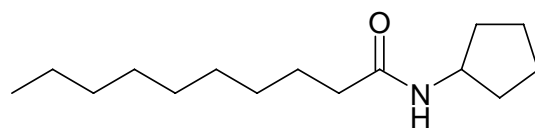
Figure 2.21. Synthetic AHL inhibitors with a change in the acyl side chain.



(a)



(b)



(c)

Figure 2.22. Synthetic AHL inhibitors with an alternation in the lactone structure. (a) 2-amino-3-oxo-C12-(2-aminocyclohexanone), (b) 2-amino-3-oxo-C12-(2-aminocyclohexanol), and (c) *N*-decanoyl cyclopentylamide.

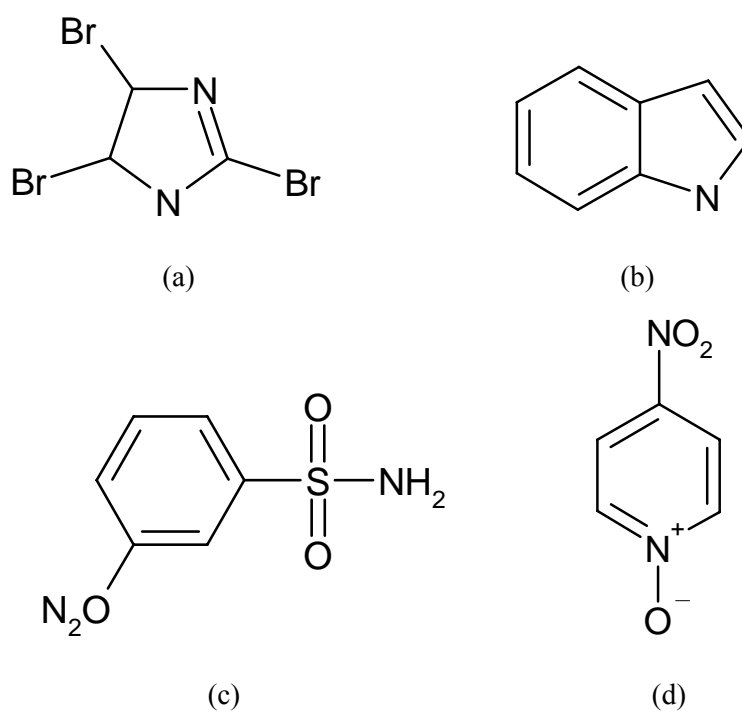


Figure 2.23. Non-AHL based QS inhibitors. (a) 2,4,5-tri-bromo-imidazole. (b) indole, (c) 3-nitrobenzene-sulfonamide, (d) 4-nitro-pyridine-N-oxide (4-NPO)

2.4.2.3. Halogenated Furanones: Novel QS Inhibitor

The marine macro alga *Delisea pulchra* has been found to possess some remarkable antifouling features¹⁵⁶. More than 30 brominated furanones, which was known as fimbrolides, are produced by *D.pulchra* as secondary metabolites on the surface of this seaweed and protect it from the colonization by both prokaryotes and eukaryotes¹⁵⁶. Since this discovery, methods have been developed to synthesize the natural furanones and their synthetic derivatives in laboratory conditions¹⁵⁷. Table 2.5 summarizes the chemical structure of these furanone compounds and their activities on gram-negative and Gram-positive bacteria

2.4.2.3.1 Inhibition of Gram-Negative Bacteria Biofilm Formation

Furanone #1 was reported to inhibit the biofilm formation of *Escherichia coli* XL1-blue on mild steel surfaces in batch experiments¹⁵⁸. The analysis with confocal laser scanning microscopy (CLSM) and staining with the LIVE/DEAD demonstrated that this compound at 60 µg/mL decreased the biofilm thickness by 52% and reduced the percentage of live cells by 87%. However, they showed no effect on the cell growth in suspension cultures with concentrations up to 100 µg/mL, suggesting that the inhibition was not caused by repression of general metabolism. The confocal images of the vertical sections of biofilms revealed that the presence of this furanone compound led to damage of the biofilm structure such as decreased water channels. Hence, the cell death may be caused by nutrient depletion and accumulation of toxic waste. In a later study, Ren et al.¹⁵⁹ reported that this furanone also inhibited the air-liquid biofilm formation of *Escherichia coli* JM109 in 96 well plates without affecting suspension growth.

Hentzer et al.¹⁶⁰ studied the effect of the furanone #3 on the biofilm formation of *Pseudomonas aeruginosa* PAO1. Furanone #3 showed no apparent effect on day 1. By day 7, however, furanone #3 at 5 µg/mL had significantly lowered the amount of biomass. The biofilm in the presence of furanone #3 was strongly similar to that of *Pseudomonas aeruginosa* PAO1 *lasI* mutant, supporting the mechanism that furanone treatment promotes sloughing of the biofilm and leads to defects in the maturation of *Pseudomonas aeruginosa* biofilm.

2.4.2.3. Inhibition of Gram-Positive Bacteria Biofilm Formation

In addition to the phenotypes of gram-negative bacteria discussed above, furanones have also been found to control biofilm formation of gram-positive bacteria. However, furanones appear to be toxic to gram-positive cells, and the mechanism of inhibition is not yet understood.

Ren et al.¹⁶¹ reported that furanone #1 inhibits biofilm formation of *Bacillus subtilis* BE1500 on mild steel surfaces in a concentration dependent manner. The presence of 40 µg/mL of furanone led to significant cell death (64%) and decreased biofilm thickness (25%). Because this furanone was found to have bactericidal effects on *Bacillus subtilis*, the inhibition of biofilm was likely due to the toxicity of furanone #1.

Furanone #1 was also tested for inhibiting biofilm formation of a sulfate-reducing bacterium, *Desulfotomaculum orientis*. Furanone # 1 at concentrations of 20 and 40 µg/mL inhibited 58% and 96% of the *Desulfotomaculum orientis* growth, respectively. Consequently, biofilm formation on mild steel surfaces was inhibited as evidenced by surface analysis using scanning electron microscopy and the weight loss was reduced

up to 80%¹⁶². These results suggest that biofilm inhibition by furanones also has engineering applications.

In addition to the experiments in free solution, furanones have been studied to develop novel coating methods. Baveja et al.¹⁹ modified surfaces with furanone #7 through physical adsorption. Six polymer materials were tested, including poly(vinylchloride), silicone, polyethylene, polypropylene, polyether polyurethane, and polytetrafluoroethylene. All of the modified materials were found to reduce the bacterial load and slime production of *Staphylococcus epidermidis* 24 h after inoculation. No apparent changes in surface hydrophobicity or roughness were identified, suggesting that the effects were due to the inhibitory effects of furanone #7.

To further improve the surface modification, Hume et al.¹⁶³ modified materials with furanone #7 through covalent binding, either by copolymerizing into polystyrene or by coating catheters by plasma-1-ethyl-3-(dimethylaminopropyl) carbodiimide reaction. The modified materials were found to reduce the biofilm formation of *Staphylococcus epidermidis*. *epidermidis* by 89% (polystyrene-furanone disks) and 78% (furanone coated catheters), respectively. In an in vivo study using a graft sheep model, furanone-coated catheters inhibited biofilm formation for 65 days. However, the furanone leached off between 65 and 84 days after implementation¹⁶³.

In addition to biofilm formation, furanones have been shown to inhibit the growth of *Bacillus anthracis*¹⁶⁴ as well as the growth and swarming of *Bacillus subtilis*¹⁶¹. Compared with the well described QS inhibition in gram-negative bacteria, the inhibitory effects of furanones on growth of gram-positive bacteria are less understood. Recent study has shown that deletion of the *Bacillus anthracis luxS* gene leads to apparent defects in cell growth¹⁶⁵.

Hence, furanones may interfere with some signaling pathways of gram-positive bacteria. Ren et al.¹⁶⁶ used DNA micro arrays to study the effects of furanone #1 on *Bacillus subtilis* gene expression at a sub lethal concentration (5 µg/mL). Consistent with the furanones' inhibition on growth, heat-shock genes were induced. This study, however, was based on a single time point and single furanone concentration. More studies with multiple conditions could be helpful for understanding the molecular basis of growth inhibition by furanones.

2.4.2.3. Inhibition Mechanism of Halogenated Furanone

Unlike traditional antibiotics, furanones inhibit the biofilm formation and other phenotypes of gram-negative bacteria at concentrations non inhibitory to growth. The structural similarity between furanones and AHLs led to the hypothesis that furanones may interrupt the QS circuits. QS is based on specific chemical (autoinducer)-protein (transcriptional activator) interactions, and changes in autoinducer structure could lead to low affinity or inhibitory effects¹⁵¹.

Using ³H-labeled 3-oxo-C6-HSL and the *Vibrio fischeri* LuxR overexpressed in *Escherichia coli*, Manefield et al.¹⁶⁷ demonstrated that furanones displaced the ³H-laebelled 3-oxo-C6-HSL from *Escherichia coli* cells overexpressing LuxR protein and that the effect was dose dependent. Furanone #6 was found to have the highest inhibitory activities, followed by furanone #1 and #2. It is worth noticing that no reaction was found between ³H-laebelled 3-oxo-C6-HSL and furanone #6, and furanones had no apparent effects on general metabolic activities as evidenced by comparison of protein expression profiles using two-dimensional gel electrophoresis. These data

suggest that the inhibition was a result of competition between the ³H-labelled 3-oxo-C6-HSL and furanones.

Because furanones disrupt the QS circuit of gram-negative bacteria with no effect on general cell growth and metabolism, it is a conceivable hypothesis that furanones may affect the fate of the transcriptional regulator R protein. To test this hypothesis, Manefield et al.¹⁶⁸ studied the effects of natural and synthetic furanones on the stability of LuxR of *Vibrio fischeri* overexpressed in *Escherichia coli*. It was found that furanones increased the turnover of LuxR in a concentration dependent manner.

Furanones #4 and #6 exhibited the strongest effects, followed by furanones #1 and #3 with moderate activity. Furanone #2 showed no apparent effect. Consistent with the inhibitory effects of furanones on QS, the 3-oxo-C6-HSL was found to protect the LuxR from turnover by furanone. However, the protection could be obtained only if the 3-oxo-C6-HSL was added before furanone.

Inhibition of QS was also observed in biofilms. Hentzer et al.¹⁶⁹ used the synthetic furanone #3 to study the inhibition of QS in *Pseudomonas aeruginosa* biofilms. To investigate the expression level of QS controlled virulence gene *lasB*, a reporter was constructed by fusing the *lasB* promoter to an unstable *gfp* gene and monitoring fluorescence. The unstable version of *gfp* gene was constructed by adding a short peptide sequence to its C-terminal, making it more susceptible to the protease activity.

In the suspension culture of *Pseudomonas aeruginosa* PAO-JP2 (the *lasI rhII* double mutant of the wild type *Pseudomonas aeruginosa* PAO1), it was found that furanone #3 inhibited the QS-mediated fluorescence in a concentration-dependent manner; for example, furanone #3 repressed the

florescence by 50% in the presence of 100 nM 3-oxo-C12-HSL. The effect was reversible by the addition of pure 3-oxo-C12-HSL. Furanone #3 at 10 µg/mL affected neither the growth of *Pseudomonas aeruginosa* PAO1 and PAO-JP2 nor the protein synthesis of PAO 1, suggesting that the inhibition was specifically on the *las* QS system. In support of this hypothesis, the inhibition was found to be titrated with increasing concentrations of 3-oxo-C12-HSL and intensified with increasing concentrations of furanone. However, complete inhibition was not achieved. To ensure the constant dosage of the reporter gene, the *lasB-gfp* was also integrated into the PAO-JP2 chromosome. The PAO-JP2 cells were allowed to grow for 24 h in flow cells before the 3-oxo-C12-HSL and furanone were applied. As expected, the addition of 3-oxo-C12-HSL induced the florescence of the cells. However, furanone #3 at 2 µg/mL repressed the florescence with the presence of 40 nM 3-oxo-C12-HSL. This inhibitory effect was found to be dose dependent; for instance, the inhibition was rescued with 80 nM 3-oxo-C12-HSL and regained when furanone concentration was increased to 4 µg/mL.

Wu et al.¹⁷⁰ studied QS inhibition by furanone #3 and #4. Using luxR-*PluxI-gfp*-labeled *Escherichia coli* MTI 02 in a mouse model, they found that both furanone #3 and #4 could repress 3-oxo-C6-HSL –based QS, while furanone #4 was more efficient. In addition, the inhibition by furanones was found to be titrated by increasing concentrations of the 3-oxo-C6-HSL, suggesting that the furanone compounds inhibited the GFP by interrupting QS.

In addition to the above studies using traditional methods, the novel DNA micro array technology has been used to identify the genes controlled by AHL and furanones on a genome-wide scale. Hentzer et al.¹⁶⁰ used DNA micro arrays to study the *Pseudomonas aeruginosa* genes affected by furanone #4

and compared them with the genes differentially expressed when in contact with the quorum sensing signals. It was found that furanone #4 repressed 85 genes and induced 10 genes more than fivefold. Interestingly, 80% of the genes repressed by furanone were also induced by QS, suggesting that furanone #4 specifically interrupts the QS circuit of *Pseudomonas aeruginosa*.

Overall, both the in vitro and in vivo experiments suggest that furanones are specific blockers of AHL-mediated QS, where some may and others may not compete with the AHLs for binding to the transcriptional activator¹⁷¹. Binding, however, disrupts the function of the receptor and consequently represses the expression of QS regulated genes. Furanones do not kill the cells directly; however, they can disrupt the bacterial multicellular structure and ease the clearance of bacteria by other drugs and the host's immune system.

Table 2.5. Representative natural and synthetic furanones

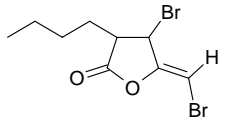
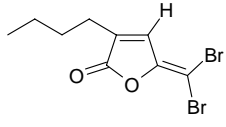
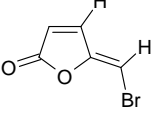
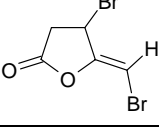
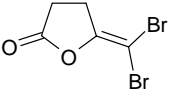
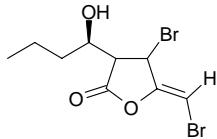
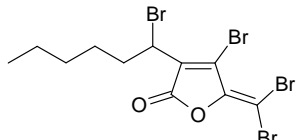
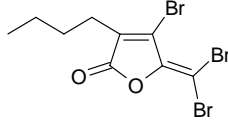
Structure	Functions
<p>1</p> 	<ul style="list-style-type: none"> - Inhibit swarming of <i>Serratia liquenfaceins</i>¹⁷² - Bioluminescence and virulence of <i>Vibrio harveyi</i>¹⁷³ - AI-2 quorum sensing, swarming and biofilm formation of <i>Escherichia coli</i>¹⁵⁸ - Represses siderphore synthesis of <i>Pseudomonas putida</i>¹⁷⁴ - Stimulates the siderphore synthesis of <i>Pseudomonas aeruginosa</i>¹⁷⁴ - Accerlates the turnover of <i>Vibrio fisheri</i> LuxR¹⁶⁸ - Inhibits swarming of <i>Proteus mirabilis</i>¹⁷⁵. - Inhibits the growth of <i>Bacillus anthracis</i>¹⁶⁴ - Inhibits growth, swarming, and biofilm formation of <i>Bacillus subtilis</i>¹⁶¹ - Inhibits the corrosion of mild steel by <i>Desulfotomaculum orientis</i>¹⁶²
<p>2</p> 	<ul style="list-style-type: none"> -Inhibits the growth of <i>Bacillus antharcis</i>.
<p>3</p> 	<ul style="list-style-type: none"> -Affects biofilm development of <i>Paeruginosa</i> and promotes sloughing¹⁶⁹ -Accerlates the turnover of <i>Vibiro fisheri</i> LuxR¹⁶⁸
<p>4</p> 	<ul style="list-style-type: none"> -Represses quorum sensing and virulence factor expression of <i>Pseudomonas aeruginosa</i> PAO1. - Increases its susceptibility to SDS and tobramycon. - Improve clearance of PAO1 from mouse lungs.

Table 2.5. (Continued)

Structure	Functions
<p>5</p> 	<p>-Inhibits the growth of <i>Bacillus anthracis</i></p>
<p>6</p> 	<p>Inhibits QS controlled exoenzyme virulence factor production and carbapenem antibiotic synthesis in <i>Erwinia carotovora</i>. Acceraltes the turnover of <i>Vibrio fischeri</i> LuxR expressed I <i>Escherichia coli</i></p>
<p>7</p> 	<p>Inhibits quorum sensing controlled exoenzyme virulence factor production and carbapenem antibiotic synthesis in <i>Erwinia carotovora</i>. Accelerates the turnover of <i>Vibrio fischeri</i> LuxR expression in <i>Escherichia coli</i>.</p>
<p>8</p> 	<p>Inhibits quorum sensing regulated swarming of <i>Serratia liquefaciens</i>¹⁷².</p>

2.4.2.4. Cyclodextran for the Trapping of AHLs

Cyclodextrins make up a family of cyclic oligosaccharides, composed of 5 or more α -D-glucopyranoside units linked 1 \rightarrow 4. As shown in Figure 2.24, the hydrophobic acyl chain of the AHLs could be included in the interior cavity of cyclodextrins via hydrophobic interactions and hence exclude them from the bacterial sensing network Kato et al.¹⁷⁶ tested *Serratia marcescens*, an opportunistic pathogen that produces a red tripyrrole pigment, 2-methyl-3-pentyl-6-methoxy prodigiosin, via an AHL mediated QS mechanism at the stationary phase. When the bacteria were grown in the presence of an optimum concentration of cyclodextrins in the growth medium, it was observed that the production of prodigiosin was reduced by approximately 40% suggesting a reduction of the AHLs available to be detected by the bacteria.

They also immobilized this cyclodextrin to the cellulose ether hydrogel. This cyclodextrin immobilized gel was shown to form inclusion complex with AHL autoinducers in the culture media of *Pseudomonas aeruginosa*. As a result, this cyclodextrin immobilized gel and successfully inhibited the *rhlA* transcription of *Pseudomonas aeruginosa*¹⁷⁷.

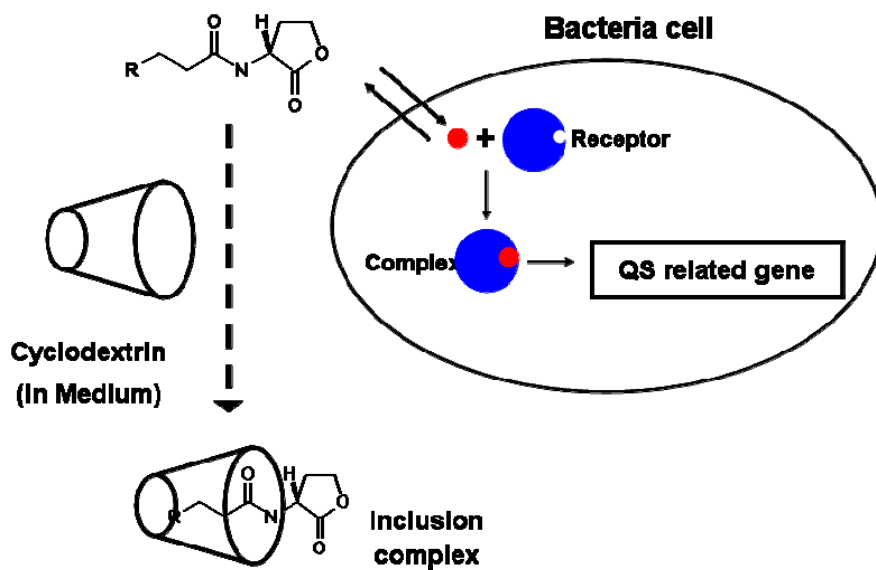


Figure 2.24. Conceptual illustration of QS control by trapping AHLs on cyclodextrin.

2.4.3. Inactivation of Signal Molecules

The third QS control strategy is inactivation or complete degradation of the AHL molecules. This can be achieved by both chemical degradation and enzymatic destruction.

2.4.3.1. Chemical Degradation: Lactonolysis

A simple way to achieve inactivation of the AHL signal molecules is by increasing the pH to above 7¹⁷⁸. This causes ring opening of the AHL (lactonolysis). A number of higher organisms employ this strategy in defense against invading quorum sensing bacteria. Plants that are infected with the tissue-macerating plant pathogen *Erwinia carotovora* will as a first response at the site of attack actively increase pH. This alkalization will in turn prevent expression of quorum sensing controlled gene and virulence factors. A temperature increase accelerates ring opening but this effect is counteracted by the length of the side chain, which decreases the rate of lactonolysis.

2.4.3.2. Enzymatic Degradation: Quorum Quenching

Another AHL inactivation scheme is the ‘quorum quenching’, which is defined as the enzymatic degradation of signal molecules. Some bacteria produce lactonase and acylase, which can disrupt cell-to-cell communication by hydrolyzing the cyclic ester or amide linkage of the AHL autoinducers respectively. Figure 2.25 shows quorum quenching pathways by lactonase and acylase respectively. Microorganisms which have quorum quenching activity were summarized in Table 2.6.

2.4.3.2.1. Quorum Quenching by Lactonase

Lactonolysis of AHLs can also be accomplished by enzymatic activity. Members of the genus *Bacillus* including *Bacillus cereus*¹⁷⁹, *Bacillus mycoides*¹⁸⁰, and *Bacillus thuringiensis*¹⁸¹ produce an enzyme, AiiA, specific for degradation of AHLs. The activity of these enzymes lowers the amount of bioactive AHL signal molecules by catalyzing the ring-opening reaction. Within 2 h, up to 20 mM 3-oxo-C6 HSL can be completely inactivated by a suspension culture producing the enzyme. When *Erwinia Carotovora* is transformed with a plasmid carrying the *aiiA* gene, its virulence against potatoes and eggplants is attenuated.

In addition, when the plant-colonizing bacterium *Pseudomonas fluorescens* was transformed with the *aiiA* gene it was able to prevent soft rot in potatoes caused by *Erwinia Carotovora* and crown gall disease in tomatoes caused by *Agrobacterium tumefaciens*.

Furthermore, expression of *aiiA* in transgenic tobacco plants made them much less vulnerable to infection by *Erwinia Carotovora* compared to their wild type counterparts

This indeed indicates that enzymatic degradation of AHLs would be useful as a means of biocontrol. Production of AHL lactonases is not limited to *Bacillus* species. Several bacteria including *Pseudomonas aeruginosa* PAI-A¹⁸², *Arthrobacter* sp.¹⁸³, *Klebsiella pneumoniae*¹⁸³, *Agrobacterium tumefaciens*¹⁸⁴ and *Rhodococcus* sp.¹⁸⁵ have been found to produce AiiA homologues.

A drawback of this lactonolysis reaction is that it is reversible at acidic pH. That is to say, a ring-opened AHL molecule spontaneously undergoes ring formation if the environment is not alkaline, regardless of the method by

which it was opened (chemical or enzymatic)¹⁸⁶. One way to prevent this could be by chemically modifying the ring-opened AHL (e.g. by mild nucleophilic substitution or reduction of the carboxylic acid), thus preventing reconversion to the ring form. Blocking QS in the environment may have the unintentional effect of interfering with beneficial bacteria.

Pseudomonas chlororaphis controls production of an antibiotic with QS. Under normal circumstances, this bacterium and its antibiotic can be used to control tomato vascular wilt caused by *Fusarium oxysporum*. In an experiment where the bacterium was co-cultured with an AiiA-producing bacterium, the biocontrol activity was lost, rendering the plants susceptible to infection¹⁸⁷.

2.4.3.2.2. Quorum Quenching by Acylase

AHL autoinducers can also be degraded by the acyl-amide cleavage which is catalyzed by acylase. Various microorganisms including *Ralstonia*¹⁸⁸ and *Variovorax* species¹⁸⁹ have been reported to produce quorum quenching acylase.

Especially, Park et al.¹⁹⁰ found the *Streptomyces* species strain M664 which secrete an AHL degrading enzyme. They also have reported that the addition of AhlM protein to the growth medium reduced the accumulation of AHLs and decreased the production of virulence factors including elastase, total protease, and LasA in *Pseudomonas aeruginosa*.

Xu et al.¹⁹¹ have shown that porcine kidney acylase I was able to degrade *N*-acyl homoserine lactones and can reduce the biofilm growth in aquarium water sample.

2.4.3.2.3. Other Quorum Quenching Method

A different, enzyme-based method to inactivate the signal molecules is simply to metabolize the AHLs. Both *Variovorax paradoxus*¹⁸⁹ and *Pseudomonas aeruginosa* PAO1¹⁹² are able to proliferate with AHLs as sole source of energy, carbon and nitrogen. The bacteria produce an amino acylase which cleaves the peptide bond of the signal molecule. The side chain is used as carbon source, the nitrogen from the amide bond is made available as ammonium via the action of lactonase and the ring part is used as energy donor.

Chowdhary et al.¹⁹³ have reported that CYP102A1, a widely studied cytochrome P450 from *Bacillus megaterium*, is capable of very efficient oxidation of AHLs and their lactonolysis products acyl homoserines.

Marin et al.¹⁹⁴ have reported the antibody, XYD-11G2, catalyzed hydrolysis of *N*-(3-oxo-acyl) homoserine lactones using a reactive immunization strategy with a squaric monoester monoamide hapten.

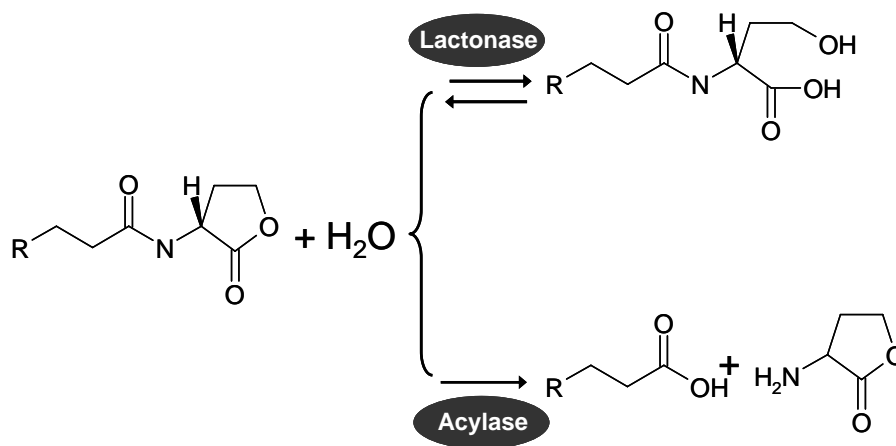


Figure 2.25. Enzymatic degradation of AHL autoinducers by lactonase and acylase.

Table 2.6. Organisms identified to date exhibiting AHL-degrading activity

Strains	Activity	Notes
<i>Bacillus sp.</i> 240B1	Lactonase	<i>aiiA</i> gene, 3-oxo-C6-HSL, 3-oxo-C8-HSL, 3-oxo-C10-HSL ¹⁷⁹
<i>Bacillus strain</i> COT1	Lactonase	<i>aiiA</i> homologues, 3-oxo-C6-HSL with different efficiency ¹⁸⁰
<i>Bacillus thuringiensis</i>	Lactonase	<i>aiiA</i> homologues, 3-oxo-C6-HSL with different efficiency ^{180, 181}
<i>Bacillus cereus</i>	Lactonase	<i>aiiA</i> homologues, 3-oxo-C6-HSL with different efficiency ¹⁸⁰
<i>Bacillus mycoides</i>	Lactonase	<i>aiiA</i> homologues, 3-oxo-C6-HSL with different efficiency ¹⁸⁰
<i>Arthrobacter sp.</i> IBN110	Lactonase	<i>ahlD</i> gene, C6-HSL, 3-oxo-C6-HSL, 3-oxo-C12-HSL, C4-HSL, C10-HSL ¹⁸³
<i>Klebsiella pneumoniae</i>	Lactonase	<i>ahlK</i> gene ¹⁸³
<i>Agrobacterium tumefaciens</i> C58	Lactonase	<i>attM</i> , <i>aiiB</i> gene, C6-HSL, 3-oxo-C8-HSL ¹⁸⁴
<i>Rhodococcus strain</i> LS31	Lactonase	Rapidly degraded a wide range of AHLs ¹⁸⁵
<i>Rhodococcus strain</i> PI33	Lactonase	Less activity towards 2-oxo substituents ¹⁸⁵
<i>Comamonas strain</i> D1	Acylase	AHLs with acyl side chains ranging from 4~16 carbons ¹⁹⁵
<i>Ralstonia strain</i> XJ12B	Acylase	<i>aiiD</i> gene, C4-HSL, 3-oxo-C6-HSL, 3-oxo-C8-HSL, 3-oxo-C12-HSL ¹⁸⁸
<i>Pseudomonas aeruginosa</i> PAO1	Acylase	PA2385 gene encode an acylase ¹⁹⁶
<i>Streptomyces sp.</i> strain M664	Acylase	has a broad substrate specificity. ¹⁹⁰
<i>Streptomyces albus strain</i> A66	Not identified	Attenuated the biofilms and inhibited QS of <i>Vibrio</i> strains ¹⁹⁷
<i>Bacillus megaterium</i>	CYP101A1	Oxidation at the ω -1, ω -2, ω -3 carbons of the acyl chain ¹⁹³

2.4.4. Patent Analysis

Patent analysis was conducted to survey the current status of the QS control technology and to predict its future development. Total 61 patents were issued to the present in EU, Korea, and US (Table 2.7). These data were evaluated both quantitatively and qualitatively.

First, the overwhelming majority of current patents, 60, were granted for using chemical QS inhibitors such as furanone compounds and AHL derivatives and 4,5-dihydroxy- 2-cyclopenten-1-one. 12 patents relate to the degradation of autoinducer in biological way such as bacterial species and enzyme.

Second, most of current patents on QS control by chemical inhibitor such as halogenated furanone suggest the similar application example of adding or injecting solution containing QS inhibitors. Even though this method is still effective at some application area such as preventing plant pathogen, it also had difficulties in being applied to the facility with continuous fluid flow such as water tank or pipeline, which require the periodic supply of these compounds. This technical limitation can be overcome by the surface coating or incorporation with these chemicals with quorum sensing control activity. In US patent 2001-4456826, polymers imparted with furanones showed excellent antifouling efficacy and significantly reduced fouling for more than 100 days.

All of the patents on quorum quenching technique place their focus on the autoinducer degrading activity of the microorganism or enzyme itself. Most of the application example was conducted under the laboratory condition and relatively short periods such as overnight. One major issue in the industrial use of enzyme is to maintain enzyme activity as long as possible. However,

current patents only suggest the simple use of solution containing enzyme, cell culture and cell extract, which was not suitable techniques in the engineering system such as MBR. Furthermore, in the case of the enzyme, the technical consideration about how to stabilize enzyme and maintain its activity in harsh condition is lacking. Therefore, enzyme technology such as immobilization would be expected to be the key element of the applying the quorum quenching technique to the engineering field.

Table 2.7. List of patents related to the QS control.

Number	Title	Country
04731333	Blockers of the quorum sensing system of gram-negative bacteria	EU
06720161	Compounds and methods for modulating communication and virulence in quorum sensing bacteria	EU
03713993	Effect of treatment with 4,5-dihydroxy- 2-cyclopenten-1-one (dhcp) on gene expression and quorum-sensing in bacteria	EU
03010185	Blockers of the quorum sensing system of gram-negative bacteria	EU
01906508	Control of bacterial infection by quenching quorum-sensing of plant pathogenic bacteria	EU
07121933	Bacterial strains, genes and enzymes for control of bacterial diseases by quenching quorum-sensing signals	EU
04021176	Control of the gene expression in eukaryotic cells	EU
00966667	Bacterial strains, genes and enzymes for control of bacterial diseases by quenching quorum-sensing signals	EU
20060028763	New quorum sensing inhibitor	Korea
20047013065	Antibacterial amide derivative and method of preventing a biofilm formation using the same	Korea
20060121650	Homoserine lactone derivative for a quorum sensing antagonist and method of preventing a biofilm formation)	Korea
20060028763	Microorganism degrading AHL and method of using thereof)	Korea
20050004633	Anti-bacterial composition comprising a compound inhibiting acyl-homoserine lactone synthase activity)	Korea
20067026346	Methods for reducing biofilm formation in infectious bacteria)	Korea
20040014110	Enzyme decomposing AHL, and method for controlling pathogenic disease using thereof	Korea
20037002587	Bacterial strains, genes and enzymes for control of bacterial diseases by quenching quorum-sensing signals	Korea
20030073320	<i>Rhodococcus</i> sp. PI-33 Decomposing Acylated Homoserine Lactone	Korea
20030073319	<i>Rhodococcus</i> sp. LS-31 Decomposing Acylated Homoserine Lactone	Korea
20020068797	Microorganism and gene degrading AHL, and method of using thereof	Korea
20020017167	Method for controlling pathogenic disease using <i>Bacillus thuringiensis</i>	Korea
20010073348	Microorganism decomposing AHL, and method of using thereof	Korea

Table 2.7. (Continued)

Number	Title	Country
20040068207	New quorum sensing inhibitor	Korea
20057002431	Methods for the treatment of an infectious bacterial disease with an anti-lactone or lactone derived signal molecules antibody	Korea
1998-159305	Preparation of cross-linked 2-dimensional polymers with sidedness from .alpha.,.beta.-lactones	US
2001-961458	Compositions and methods for regulating bacterial pathogenesis	US
2001-961452	Compositions and methods for regulating bacterial pathogenesis	US
2001-885379	Methods for eliminating the formation of biofilm	US
2001-870934	Preparation of 4-hydroxy-3[2H]-furanones	US
2001-853832	Compounds and methods for regulating bacterial growth and pathogenesis	US
2001-445682	Antifouling polymers	US
2001-035318	Hard surface cleaners containing chitosan and furanone	US
2002-164446	Quorum sensing and biofilm formation	US
2001-381271	Method, system and computer program product for technical management and biocontrol of disease in animal production systems	US
2006-560669	Modulation of Pathogenicity	US
2008-044135	<i>B. Anthracis</i> prevention and treatment: mutant <i>B. anthracis</i> lacking LuxS activity and furanone inhibition of growth, AI-2 quorum sensing, and toxin production	US
2007-834380	Combinatorial libraries of autoinducer analogs, autoinducer agonists and antagonists, and methods of use thereof	US
2007-711935	Crystals of LuxP and complexes thereof	US
2006-561729	Modulation of pathogenicity	US
2006-561715	Modulation of pathogenicity	US
2002-094301	Selective antibacterial agents	US
2006-561275	Method of inhibiting bacterial growth and biofilm formation with natural quorum sensing peptides	US
2006-460946	Method and process of using controlled gas environments to inhibit microbial growth	US
2006-435978	Anti-bacterial agents based upon oxoanion binding	US
2005-907166	Method for modulating microbial quorum sensing	US
2005-228707	AI-2 compounds and analogs based on <i>Salmonella typhimurium</i> LsrB structure	US
2002-502351	<i>Ralstonia</i> AHL-acylase gene	US
2006-561701	Modulation of pathogenicity	US
2002-227400	Crystals of LuxP and complexes thereof	US

Table 2.7. (Continued)

Number	Title	Country
2005-104681	AI-2 compounds and analogs based on <i>Salmonella typhimurium</i> Lsrb structure	US
2003-312039	Bioactive food complex, method for making bioactive food complex product and method for controlling disease	US
2003-456696	Local delivery of agents for disruption and inhibition of bacterial biofilm for treatment of periodontal disease	US
2003-506778	Effect of treatment with 4,5-dihydroxy-2-cyclopenten-1-one (dhcp) on gene expression and quorum-sensing in bacteria	US
2003-637940	Combinatorial libraries of autoinducer analogs, autoinducer agonists and antagonists, and methods of use thereof	US
2003-676770	Anti-bacterial agents based upon oxoanion binding	US
2004-577119	Proteins Involved in signal transduction	US
2004-823396	<i>B. anthracis</i> prevention and treatment: mutant <i>B. anthracis</i> lacking LuxS activity and furanone inhibition of growth, AI-2 quorum sensing, and toxin production	US
2005-044285	Quorum sensing and biofilm formation	US
2003-524082	Methods for the treatment of an infectious bacterial disease with an anti-lactone or lactone derived signal molecules antibody	US

2.5. Enzyme Immobilization

Enzyme immobilization is generally defined as "the imprisonment of an enzyme molecule in a distinct phase that allows exchange with, but is separated from, the bulk phase in which substrate effect or inhibitor molecules are dispersed and monitored"

The advantage of enzyme immobilization was listed in Table 2.8. The principal advantage of immobilizing enzymes is to retain the catalyst in the reactor. This can greatly improve the economics of a process. For a continuous process, a soluble enzyme would be washed out of the reactor along with the product stream. A process like this would not be economically feasible if the biocatalyst is very expensive (as is often the case) and cannot be reused. Although an ultrafiltration setup could be used to retain the enzyme, it is often too costly, both in capital and operation, on a large scale. Also, having a soluble enzyme in the product would not be desirable if the biocatalyst can cause the product to undergo side reactions or if there are toxicity effects associated with the catalyst, as will often be the case if the product is an intravenous drug. Another advantage of immobilizing enzymes is to increase enzyme activity or stability especially under denaturing conditions. Thermal stability can often be improved by many orders of magnitude compared to the soluble enzyme. Activity of an enzyme in nonaqueous media can also be significantly higher than the native enzyme. Another important advantage is the ability to control the microenvironment of the immobilized enzyme. For example, by immobilizing an enzyme on an acidic support (such as poly acrylic acid), the catalyst can be used at higher pHs, where the substrate may be more soluble, while the pH of the microenvironment surrounding the enzyme could be much closer to the enzyme's optimum pH.

There are also limitations to immobilizing enzymes. Some inherent catalytic activity is almost always lost during the immobilization procedure. Enzymes possess highly defined, yet relatively fragile three-dimensional structures that must come in contact and interact with the rigid support. These binding forces, such as covalent bonds or adsorptive interactions, are often more powerful than the secondary forces, such as hydrogen bonding and hydrophobic and ionic interactions, which hold proteins in their proper configuration for enzymatic activity. In addition, no covalent immobilization method is able to bind only the nonessential elements of every enzyme (if they even exist) to the support, and all supports create asymmetric force fields and change the water activity around the biocatalyst. In addition, apparent activity can be decreased by mass transfer limitations. However, the increase in stability and ease of removal from the product stream and reuse often more than make up for any decrease in activity.

Table 2.8. Stabilization effects of immobilization to enzymes.

-
1. Prevention of either proteolysis or aggregation by spatial fixation of enzyme molecules to the support.
 2. Unfolding of the enzyme is reduced due to multipoint covalent or adsorptive attachment to the support, and/or intramolecular crosslinking of the enzyme.
 3. Multimeric enzymes would have a lower likelihood to dissociate if all subunits are attached to the support.
 4. Denaturing agents (e.g., chemical inactivators) can be excluded from the enzyme by the support or inactivated by the support before reaching the enzyme (e.g., decomposition of hydrogen peroxide, produced during the oxidation of glucose by glucose oxidase, catalyzed by activated carbon).
 5. Shifting by a charged support of the local pH, thus preventing pH inactivation of the enzyme.
 6. Exclusion by the support (e.g., an encapsulation membrane) of proteases from the enzyme's environment.
 7. Increased thermal stability due to multipoint attachment of enzyme to support.
-

2.5.1. Conventional Methods

There is no one universal immobilization system; instead, a range of methodologies must be evaluated depending on the enzyme to be immobilized and the overall process in which the immobilized enzyme is to be used. Also, most immobilization methods, although conceptually distinct, often overlap to a certain extent, and in some cases, multiple immobilization methods are employed. In general the following techniques have been described for immobilization of enzymes.

2.5.1.1. Adsorption

Adsorption is the simplest method and involves reversible surface interactions between enzyme and support material. The forces involved are mostly electrostatic, such as van der Waals forces, ionic and hydrogen bonding interactions, although hydrophobic bonding can be significant. These forces are very weak, but sufficiently large in number to enable reasonable binding. The procedure consists of mixing together the biological component(s) and a support with adsorption properties, under suitable conditions of pH, ionic strength, and so on, for a period of incubation, followed by collection of the immobilized material and extensive washing to remove non bound biological components.

Enzyme immobilization by adsorption has the following advantages:

- (1) Little or no damage to enzymes/cells.
- (2) Simple, cheap, and quick to obtain immobilization.
- (3) No chemical changes to support or enzyme/cell.
- (4) Reversible to allow regeneration with fresh enzymes/cells.

Disadvantages include:

- (1) Leakage of enzymes from the support/contamination of product
- (2) Nonspecific binding.
- (3) Overloading on the support.
- (4) Steric hindrance by the support.

The most significant disadvantage is leakage of biocatalyst from the support. Desorption can occur under many circumstances, and environmental changes in pH, temperature, and ionic strength will promote desorption. Sometimes an enzyme, firmly adsorbed, is readily desorbed during reaction as a result of substrate binding, binding of contaminants present in the substrate, product production, or other conditions leading to change in protein conformation. Physical factors, such as flow rate, bubble agitation, particle-particle abrasion, and scouring effect of particulate materials on vessel walls, can lead to desorption.

Nonspecific binding can become a problem if substrate, product, and/or residual contaminants are charged and interact with the support. This can lead to diffusion limitations and reaction kinetics problems, with consequent alteration in parameters V_{\max} and K_m . Further, binding of protons to the support material can result in an altered pH microenvironment around the support with consequent shift in pH optimum (1-2 pH units), which may be important for enzymes with precise pH optimum requirements. Unless carefully controlled, overloading the support can lead to low catalytic activity, and the absence of a suitable spacer between the enzyme molecule and the support can produce problems related to steric hindrance

2.5.1.2. Entrapment

The entrapment method of immobilization is based on the localization of an enzyme within the lattice structure of the support such as polymeric gel. The porosity of the gel lattice is controlled to ensure that the structure is tight enough to prevent leakage of enzyme, yet at the same time allow free movement of substrate and product. Inevitably, the support will act as a barrier to mass transfer, and although this can have serious implications for reaction kinetics, it can have useful advantages since harmful cells, proteins, and enzymes are prevented from interaction with the immobilized biocatalyst .

There are several major methods of entrapment:

- (1). Ionotropic gelation of macromolecules with multivalent cations.
- (2). Temperature-induced gelation.
- (3). Organic polymerization by chemical/photochemical reaction
- (4). Precipitation from an immiscible solvent

Entrapment can be achieved by mixing an enzyme with a polyionic polymer material and then crosslinking the polymer with multivalent cations in an ion-exchange reaction to form a lattice structure that traps the enzymes/cells (ionotropic gelation). Temperature change is a simple method of gelation by phase transition using 1-4% solutions of agarose or gelatin. However, the gels formed are soft and unstable. A significant development in this area has been the introduction of x-carrageenan polymers that can form gels by ionotropic gelation and by temperature-induced phase transition, which has introduced a greater degree of flexibility in gelation systems for immobilization.

Alternatively, it is possible to mix the enzyme with chemical monomers that are then polymerized to form a crosslinked polymeric network, trapping the enzyme in the interstitial spaces of the lattice. The latter method is more

widely used, and a number of acrylic monomers are available for the formation of hydrophilic copolymers. For example, acrylamide monomer is polymerized to form polyacrylamide and methylacrylate is polymerized to form polymethacrylate. In addition to the monomer, a crosslinking agent is added during polymerization to form crosslinkages between the polymer chains and help to create a three-dimensional network lattice. The pore size of the gel and its mechanical properties are determined by the relative amounts of monomer and crosslinking agent. It is therefore possible to vary these concentrations to influence the lattice structure. The formed polymer may be broken up into particles of a desired size, or polymerization can be arranged to form beads of defined size. Precipitation occurs by phase separation rather than by chemical reaction, but does bring the cells/enzymes into contact with a water-miscible organic solvent, and most cells/enzymes are not tolerant of such solvents. Thus, this method is limited to highly stable/previously stabilized enzymes or nonliving cells.

2.5.1.4. Covalent Bonding

Covalent attachment of enzymes to an insoluble support is an often-used method of enzyme immobilization. It is especially useful when leaching of enzyme from the support is a concern. The enzyme is usually anchored via multiple points and this generally imparts greater thermal, pH, ionic strength, and organic solvent stability onto the enzyme since it is more rigid and less susceptible to denaturation. Covalently immobilized enzymes are also often more resistant to degradation by proteolysis.

There are, however, some drawbacks to covalent enzyme immobilization. Typically it is more expensive and complex to covalently immobilize an

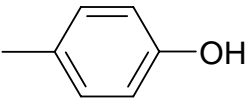
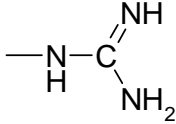
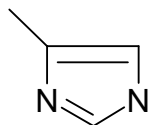
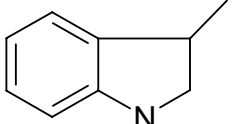
enzyme compared to the other methods due to the higher costs of the support. The support often needs to be activated prior to immobilization. The increased stability and typically minimal enzyme leaching often more than make up for these shortcomings.

Enzymes contain a number of functional groups capable of covalently binding to supports. Table 2.9 lists these groups along with their relative frequency in a typical protein. Of the functional groups of enzymes listed, $-NH_2$, $-CO_2H$, and $-SH$ are most frequently involved in covalent immobilization. Amines and sulfhydryls are good nucleophiles, while the ability to activate carboxylates so they are reactive toward nucleophiles makes these groups important as well. The phenolic ring of tyrosine is also extremely reactive in diazo-coupling reactions, and its hydroxyl group can be an excellent nucleophile at basic pH. Aldehydes can react with the guanidino group of arginine and, although histidine displays a lower nucleophilicity, it can react in some cases with supports activated with tosylates, tresylates, or other good leaving groups.

The supports to which the enzymes are attached can vary greatly. They can be either natural polymers, such as modified cellulose, starch, dextran, agar polysaccharides, collagen, and gelatin; or they can be synthetic, such as polystyrene, polyacrylamide, polyacrylates, hydroxyalkyl methacrylates, and polyamides. Inorganic supports can also be used, such as porous glass, metal oxides, metals, sand, charcoal, and porous ceramics. The variety of chemistries available for covalent attachment allows the conditions of immobilization to be tailored to each enzyme system. This also allows the microenvironment of the enzyme to be tailored by appropriate modification of

the support surface; hydrophobic moieties or ionically charged groups may be used to alter the support to enhance the enzyme-catalyzed reaction of interest.

Table 2.9. Reactive functional groups in enzyme.

Reactive group	Chemical structure
ϵ -Amino of lysine and N-terminus	$-\text{NH}_2$
Carboxylate of glutamic acid, aspartic acid, and C-terminus	$-\text{COOH}$
Thiol of cystein	$-\text{SH}$
Phenolic of tyrosine	
Guanidino of arginine	
Imidazole of histidine	
Disulfide of cystine	$-\text{S}-\text{S}-$
Indole of tryptophan	
Thioether of methionine	$-\text{C}(\text{H}_2)-\text{S}-$
Hydroxyl of serine and threonine	$-\text{CH}_2\text{OH}$

2.5.1.4.1. Covalent Attachment onto Polyhydroxyl Supports.

Polyhydroxyl supports such as porous glass polysaccharides are among the most commonly used materials for enzyme immobilization. Because hydroxyl groups are poor leaving groups, they must first be activated. This is typically done with cyanogens bromide. Other activating agents such as *S*-triazine derivatives have also been used. Once the support is activated, it is able to covalently couple to an enzyme usually through the α -amino group of lysine or through the amino terminus. The mechanism of derivation polyhydroxyl supports with above two derivatizing agents and subsequent enzyme immobilization is shown in Figure 2.26.

Supports that have been preactivated with cyanogens bromide can be stored for periods up to 1 year at freezer temperatures. Preactivated supports are also available commercially. Once the support is activated, coupling of the enzyme requires no more than exposing the enzyme to the activated support in an aqueous solution for a few hours, followed by extensive washing to remove any protein that is not covalently bound.

This method is extremely popular in the laboratory scale. However, it has not been widely used in large scale applications. The activating agent, cyanogens bromide, is extremely toxic and most carbohydrate supports such as cellulose, agarose and dextran have poor mechanical stability compared to other support materials. Also, since the supports are natural polysaccharides, microbial contamination and degradation are a concern. Finally, the bond between the enzyme and the support is potentially susceptible to hydrolytic cleavage, which would cause leaching of the enzyme from the support over time

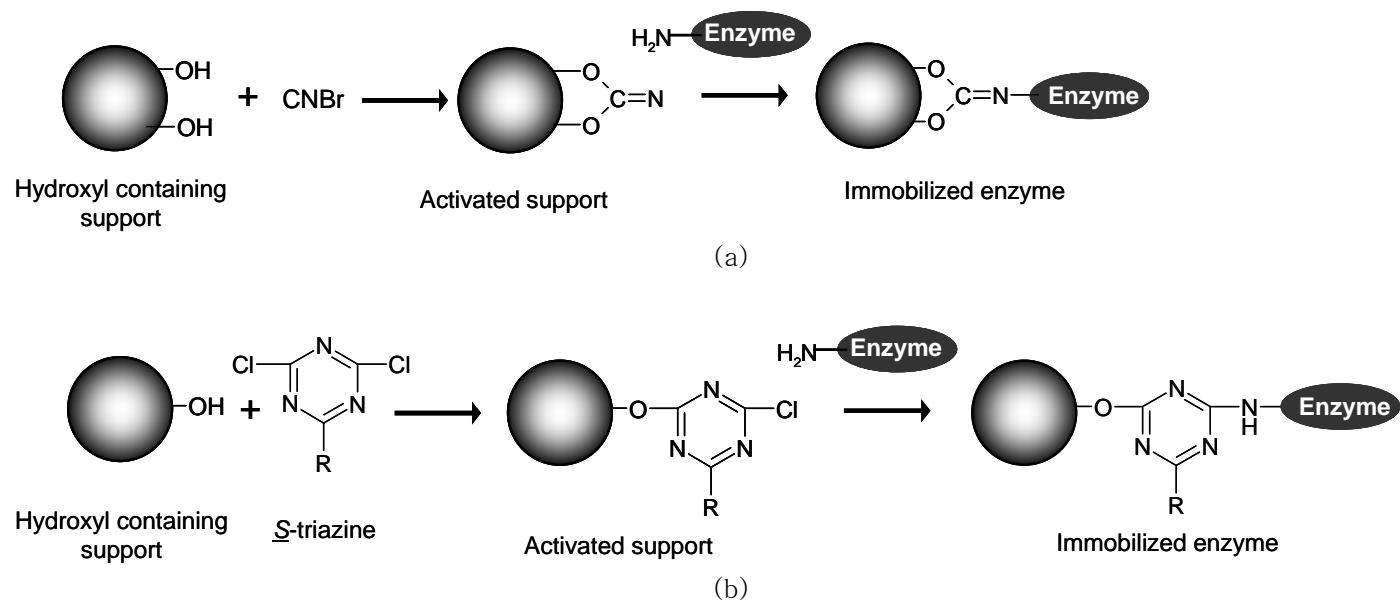


Figure 2.26. Enzyme immobilization onto hydroxyl containing supports via activation with (a) cyanogens bromide and (b) *S*-triazine.

2.5.1.4.2. Covalent Attachment on Carboxylic Acid Bearing Supports.

Carboxylic acid containing supports such as copolymer of acrylic acids with acrylic esters have been also been used as an immobilization support. These must be activated and this is usually done with a carbodiimide reagent. Under slightly acidic conditions (pH 4.75~5.0) carbodiimide react with carboxylic acid groups to give the highly reactive O-acylisourea derivatives. The support are then washed to remove excess reagent and the enzyme is coupled to the activated support at neutral pH to give stable amide, thioester, or ester linkage, depending on the residue reacting with the support. The most widely used water soluble carbodiimides are 1-ethyl-3-(3-dimethylaminopropyl)-carbodiimide (EDC) and 1-cyclohexyl-3-(2-morpholino-ethyl)- carbodiimide (CDC), both of which are commercially available. The reaction scheme for activating a carboxylic acid containing support and subsequent enzyme coupling is shown in Figure 2.27.

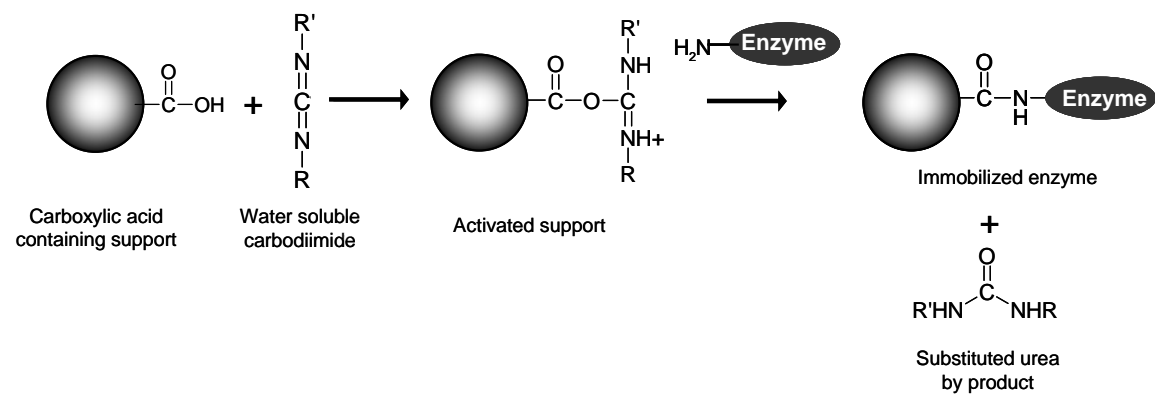


Figure 2.27. Activation of a carboxylic acid support with a carbodiimide followed by enzyme coupling.

2.5.1.4.3. Covalent Attachment on Amine Bearing Supports.

Amine containing supports are among the most used and the most useful support for covalent enzyme immobilization. These supports can either be organic or inorganic supports bearing amine functionality. The most frequent technique for introducing amine groups on inorganic supports is via aminosilane attachment. Another common amine-bearing support is polyethyleneimine-coated particles. This polymer can be coated onto various supports including alumina, carbon, diatomaceous earth and polyvinyl chloride-silica composite.

The coupling of an enzyme to amine-bearing supports can be done in a number of ways. The most common way is through the use of difunctional reagents such as diimidate ester, diisocyanates and dialdehyde. Glutaraldehyde (GA) is often used as it is one of the least expensive difunctional reagents available in bulk. This reagent reacts in a complex fashion to form Schiff bases with amine groups on the support and produces pendant Aldehydes and α, β -unsaturated carbonyl functionalities through which enzymes may attach. Enzyme attachment is simply accomplished by mixing the enzyme with the activated support. A simplified example of this was shown in Figure 2.28. The acid-labile Schiff base can be reduced to more stable secondary amine bonds with sodium borohydride to increase the stability of the enzyme-support linkage.

Enzymes can also be covalently bonded directly to amine-bearing supports via enzyme's carboxylic groups. These must previously be activated with a carbodiimide or similar reagent prior to immobilization. The activation step can cause enzyme inactivation and thus this method is not used as often.

Diisocyanates have also been used as a coupling agent between amine-bearing supports and enzymes. If alkaline conditions are used, a substituted

urea bond is formed between an amine on the enzyme and the isocyanate. If moderately acidic conditions are employed, the isocyanate will react with a hydroxyl group on the enzyme and form a urethane bond.

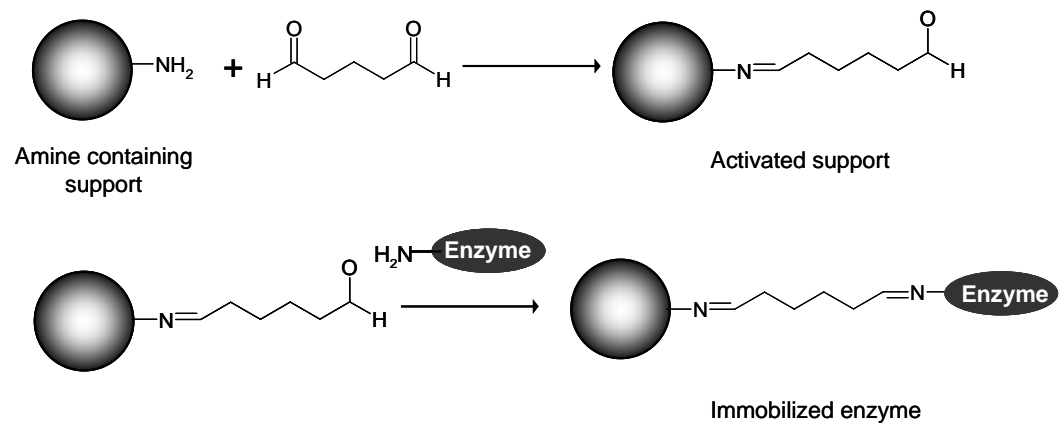


Figure 2.28. Activation of an amine-bearing support with glutaraldehyde followed by enzyme coupling

2.5.1.4.4. Covalent Attachment on Reactive Polymer Supports

Due to the preactivated nature of epoxy-containing supports, these materials have gained considerable attention as commercially useful support matrices for enzyme immobilization. A commercial epoxy-containing support is available under the trade name of 'Eupergit'

This material is a crosslinked copolymer of methacrylamide and oxirane containing monomers and consists of spherical beads of about 200 μm in diameter. Enzyme immobilization to Eupergit is relatively simple. The enzyme solution is brought in contact with the Eupergit beads either quiescently or with slight mixing for 24~96 h. This can be done either at room temperature or if the enzyme is unstable, 4 will also work. Various pHs can be used for the binding. Under neutral and alkaline conditions, the amino groups on the enzyme are principally responsible for binding the support. Under acidic and neutral conditions sulfhydryl and carboxyl groups take part in binding (Figure 2.29a).

Polyacrolein bead is another used reactive polymer carrier for covalent enzyme attachment. Binding of enzymes to unmodified polyacrolein is shown in Figure 2.29b. Various oligomers such as polyglycine have been attached to the polyacrolein beads to act as spacers between the particles and enzymes

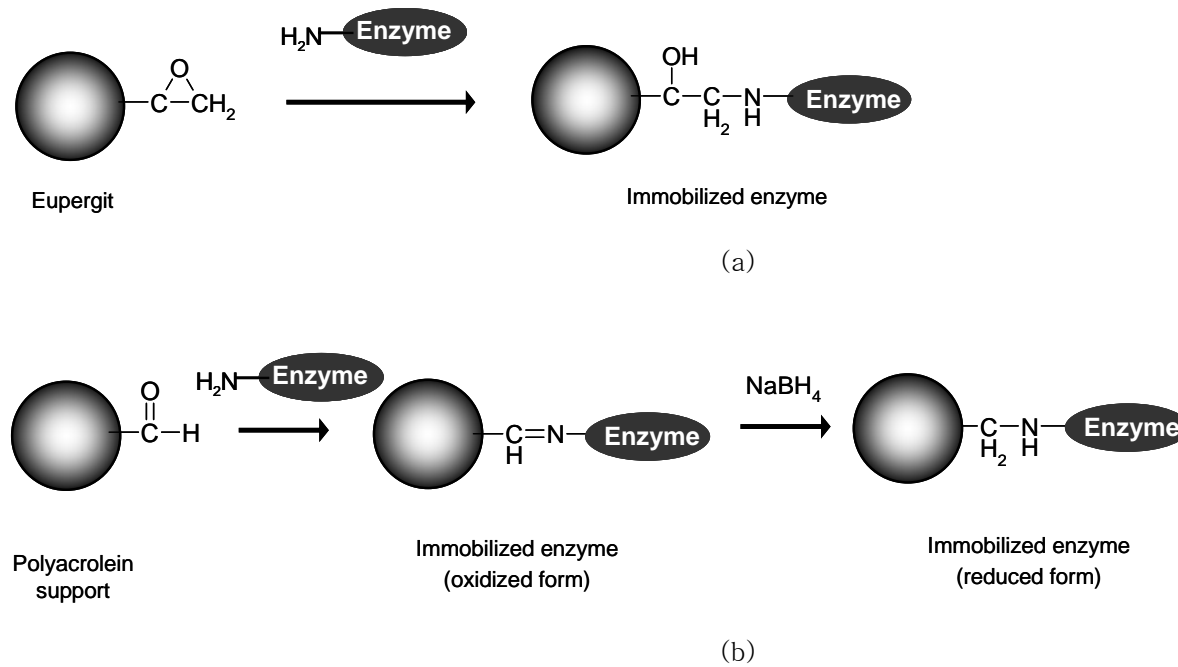


Figure 2.29. Enzyme immobilization to (a) Eupergit via free amino groups and (b) unmodified polyacrolein via free amino groups, followed by reduction of the Schiff base with sodium borohydride.

2.5.2. Nanobiocatalysis: New Trends in Enzyme Technology

‘Nanobiocatalysis’ can be defined as the incorporation of the enzymes into nanostructured materials such as nanoporous materials, electrospun nanofibers and magnetic nanoparticles¹⁹⁸. In the beginning stages of nanobiocatalysis, enzymes were immobilized on various nanostructured materials using conventional approaches, such as simple adsorption and covalent attachment. This approach gathered attention by immobilizing enzymes onto a high surface area of nanostructured materials (Figure 2.30). This large surface area resulted in improved enzyme loading, which in turn increased the apparent enzyme activity per unit mass or volume compared to that of enzyme systems immobilized onto conventional materials. However, it did not take much time for scientists and engineers to look for additional advantages of nanostructured materials other than their high surface area.

One of the particularly advantageous features of nanostructured materials is the control over size at the nanometer-scale, such as the pore size in nanopores, thickness of nanofibers or nanotubes and the particle size of nanoparticles. The uniform size distribution of nanomaterials and their similarity in size with enzyme molecules, together with other advantageous nanomaterial properties such as conductivity and magnetism, have revolutionized nanobiocatalytic approaches in various areas of enzyme technology and led to improved enzyme properties in nanobiocatalytic systems, particularly with regard to enzyme stability and activity.

Recently, nanobiocatalytic approaches have evolved beyond simple enzyme immobilization strategies to include enzyme stabilization¹⁹⁹, wired enzyme²⁰⁰, the use of enzymes in sensitive biomolecular detection²⁰¹, artificial enzymes²⁰², nanofabrication²⁰³ and nanopatterning²⁰⁴.

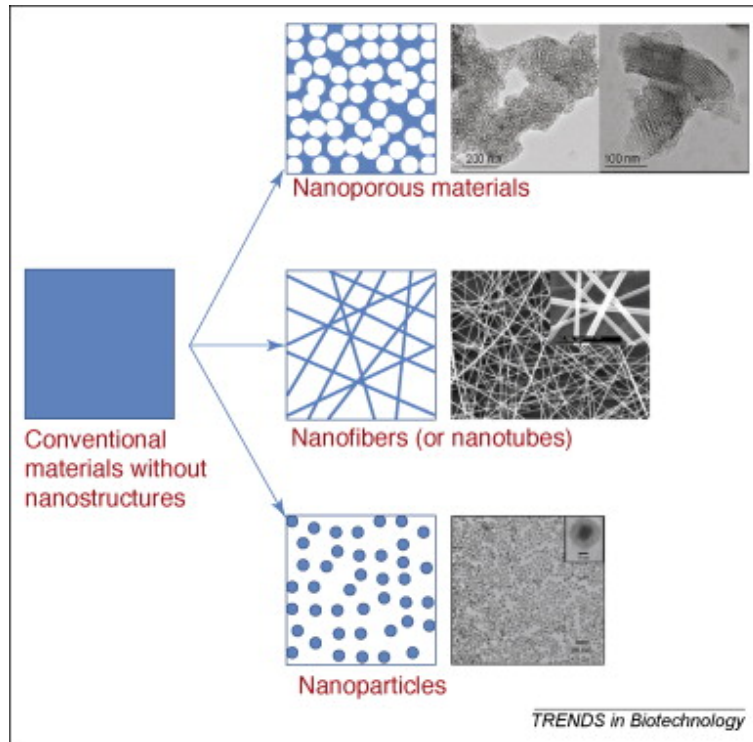


Figure 2.30. Illustration of the large surface area of nanostructured materials.

Shown are transmission electron microscope (TEM) images of nanoporous silica (top panel) and magnetic nanoparticles (bottom panel), as well as scanning electron microscope (SEM) images of electrospun nanofibers (middle panel)¹⁹⁸.

2.5.2.1. Enzymes in Nanomaterials: Nanoentrapment

Most techniques for obtaining nanoparticles that contain enzymes have been based on the so-called ‘nanoentrapment’ approach using the water-in-oil microemulsion system (reverse micelles), which leads to discrete nanoparticles through polymerization in the water phase or water–oil interface^{205, 206, 207, 208, 209}. One of the challenges of this approach is the difficulty in controlling the size of reverse micelles, as well as the number of enzyme molecules within each reverse micelle, which will directly affect the final properties of enzyme-entrapped nanoparticles. Thus, success in this approach requires rigorous optimization processes that address these issues. This approach of enzyme nanoentrapment was used to incorporate magnetic nanoparticles together with enzymes into spherical silica nanoparticles²⁰⁹.

In 2003, a new synthetic approach was reported under the name of ‘single enzyme nanoparticles (SENs)’, in which an organic-inorganic hybrid polymer network of a thickness of less than a few nanometers was built up from the surface of the enzyme²¹⁰. This approach is therefore in stark contrast to the conventional nanoentrapment described above. SEN synthesis consists of three steps(Figure 2.31a):

- (1) The enzyme surface is modified in water by acryloylation;
- (2) The vinyl polymer is grown from the enzyme surface in hexane;
- (3) The attached polymer chains undergo orthogonal polymerization via silanol condensation crosslinking

One of the crucial steps is the solubilization of the modified enzymes from water into hexane.

Chymotrypsin and trypsin are solubilized into hexane by ion pairing with low concentration of an anionic surfactant in the absence of reverse micelles.

The ion-paired enzyme–surfactant complex in hexane thus remains dissolved without any aggregation, maintaining the native structure of the enzymes and exhibiting high enzyme activity²¹¹. This solubilization technique requires much smaller amounts of surfactants than the formation of reverse micelles and allows the extraction of individual enzyme molecules into a hydrophobic organic solvent (Figure 2.31b)

As a result, the surfaces of the solubilized enzyme molecules are well exposed to the organic solvent²¹², thereby enabling the synthesis of the vinyl polymer directly from the enzyme surface and leading to the covalent linkages between the enzyme molecule and the final polymer network. The significant stabilization of chymotrypsin and trypsin in the form of SENs can be attributed to these covalent linkages, as well as to the crosslinked network that confines the enzyme to prevent unfolding and denaturation. Kinetic studies with the SENs of chymotrypsin revealed that there was no serious mass transfer limitation on the substrate of *N*-succinyl-Ala-Ala-Pro-Phe *p*-nitroanilide²¹⁰, suggesting that the thin polymer network is sufficiently porous for the easy transfer of this substrate, which is ~1 nm in size. Due to the small size of the resulting SENs, it is also possible to place them into nanoporous silica²¹³.

Traditionally, enzyme stabilization by adsorption in nanoporous media requires matching the pore size to that of the enzyme to retard enzyme unfolding. It has been shown to be of particular advantage if the radius of curvature for the pore is similar to that of native enzyme, thereby confining the enzyme and, furthermore, allowing multiple points of covalent attachment in the silica nanopore²¹⁴. However, in the immobilization of SENs into nanoporous silica, the modified enzyme molecules are already stabilized

within a thin polymer network, and the silica pore size can be independently selected to provide other desirable attributes, such as rapid mass transfer to and from enzyme catalysts, with no concern of enzyme stabilization. Thus, larger silica pores can be selected that would not provide extended stabilization of an unmodified enzyme but allow for rapid diffusion. A modified approach using a simplified protocol was reported under the name of 'single enzyme nanogels' and consists of two steps: enzyme acryloylation followed by aqueous polymerization and crosslinking to entrap a single enzyme within each nanogel formed²¹⁵. This approach stabilizes the enzyme by the same principles as described for the SENSs, that is, covalent linkage to a crosslinked polymer network that retards enzyme unfolding. The simplified synthesis of the nanogel-confined enzyme was made possible by using water-soluble acrylamide as a monomer and obviated the need to solubilize the enzyme in an organic solvent. Another interesting approach for creating a nanostructure around an enzyme molecule is the self assembly of organoclay-wrapped enzymes. In this approach, each enzyme molecule can be wrapped with a thin layer of cationic organoclay oligomers by simply mixing the enzyme and the organoclay²¹⁶.

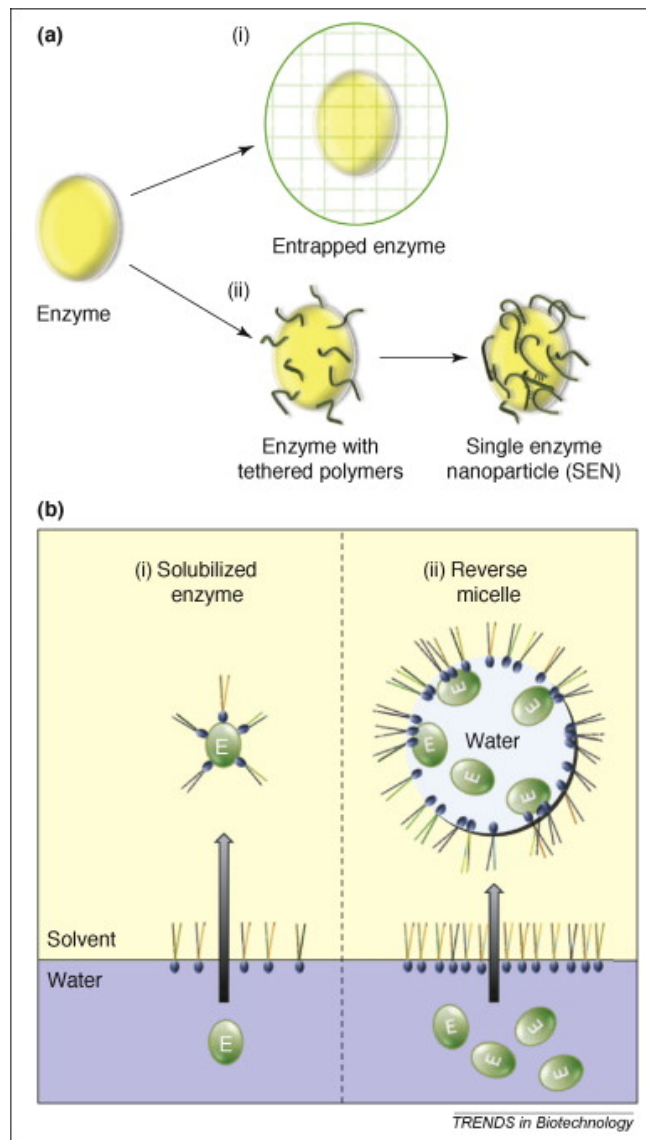


Figure 2.31. (a) Comparison of conventional approach using reverse micelles and single enzyme nanoparticle (SEN) entrapment. (b) Schematic illustration of enzyme solubilization for SEN synthesis¹⁹⁸.

2.5.2.2. Enzyme Immobilization into Nanoporous Media: Ship-in a-Bottle Approach

Nanoporous media with pores 2–50 nm in size have attracted a lot of attention as hosts for enzyme immobilization owing to their controlled porosity and high surface area. Most frequently, simple adsorption approaches have been used to immobilize enzymes into nanoporous media^{217, 218, 219, 220, 221, 222, 223}. These approaches, however, have a serious problem: the continuous leaching of adsorbed enzyme molecules from nanoporous media. In particular, enzyme loss during the initial washing steps results in a significantly reduced enzyme loading, which is not desirable because the activity per unit mass of biocatalytic materials is reduced.

Therefore, larger enzyme reactors are required to accomplish a given conversion. The recovery rate of adsorbed enzymes in subsequent reaction cycles is also reduced owing to continuous enzyme leaching and poor enzyme stability under the shaking conditions that are normally employed to reduce the mass transfer limitation in the operation of reactors with immobilized enzymes.

To prevent the leaching of enzymes, covalent linkage has traditionally been used to attach the enzyme molecules to the inner surface of nanoporous media. Wang et al.²²⁴ hypothesized that the nanopore nanoenvironment surrounding the enzyme with its concave surface would improve the enzyme stability by providing an ideal configuration for multiple covalent linkages between enzyme molecules and the inner surface of nanopores. However, the final enzyme loadings achieved with this approach were generally poor due to two reasons. Firstly, only the inner surface of nanopores could be used for the attachment of enzyme molecules, rather than the entire pore volume. Secondly,

the earlier attachment of enzyme molecules on the inlet of nanopores could exert a serious steric hindrance against the penetration of the other additional enzyme molecules into nanopores behind the inlet, which is crowded with pre-attached enzyme molecules.

Recently, a ‘ship-in-a-bottle’ approach was employed as a simple but effective means of enzyme immobilization into nanoporous media (Figure 2.32). This approach improved both enzyme loading and enzyme activity by effectively preventing the leaching of enzyme²²⁵. The first step involves the adsorption of enzymes into nanoporous material, which results in a high degree of enzyme loading. The second step is glutaraldehyde (GA) treatment, which covalently links the enzyme molecules, resulting in crosslinked enzyme aggregates at the nanometer-scale within the nanopores. In successful applications of this ship-in-a-bottle approach, specially designed nanoporous media have been employed. One of these media is mesocellular mesoporous silica (MMS), which has a unique pore structure that is composed of spherical 37 nm-sized mesocellular pores connected by 13 nm-sized mesopores^{225, 226, 227}.

Another media is nanoporous carbon, in which the main pores (31 nm) are connected via window pores (21 nm). These smaller connecting pores effectively prevent the leaching of enzyme aggregates, hence the ‘ship-in-a-bottle’ description. We termed this method of enzyme immobilization the ‘nanoscale enzyme reactor (NER)’ approach. The NER approach could stabilize the enzyme activity by combining the ship-in-a-bottle arrangement with enzyme crosslinking. The former prevents the leaching of enzyme from nanoporous media while the latter inhibits the denaturation of enzyme molecules owing to multiple covalent linkages via chemical crosslinking.

As an extension of the NER approach, magnetic nanoparticles have been entrapped within the crosslinked enzyme aggregates in nanoporous media²²⁶. This double-ship-in-a-bottle approach has enabled highly stable enzyme systems that can also be easily recycled for repetitive use via a simple magnetic separation. In addition, the NERs of lipase with entrapped magnetic nanoparticles showed a good resistance to proteolytic digestion, which is an important feature for successful applications of enzyme catalysts in the presence of proteases. Proteases, which irreversibly inactivate enzymes via proteolysis, are often present during *in vitro* and *in vivo* biocatalysis reactions involving biological fluids, cellular extracts or implantable biosensors and devices. Most enzymes in NERs would not be accessible to proteolytic digestion due to the steric hindrance against the penetration of proteases into crosslinked enzyme aggregates in nanoporous media. At the same time, multiple covalent linkages between enzyme molecules would also contribute to the resistance to proteolytic digestion. Recently, it was confirmed that the NERs of chymotrypsin are also resistant to proteolytic digestion²²⁷. These systems have been proven to be magnetically separable, highly loaded with enzymes, stable under rigorous shaking, resistant to proteolytic digestion and recyclable for iterative uses. These advantageous features can be easily expanded to many other enzymes, which will lead to successful enzyme applications in many areas of enzyme technology.

In addition to this approach, immobilized enzymes in nanoporous media have already been employed in various applications, such as in biosensors²²⁸,²²⁹, peptide synthesis²³⁰, kinetic resolution²³¹, pulp bio-bleaching²³², magnetically switchable bioelectrocatalytic systems²³³ and trypsin digestion

for proteomic analysis^{234, 235, 236}, and are expected to lead to further advances in more diversified fields of enzyme technology.

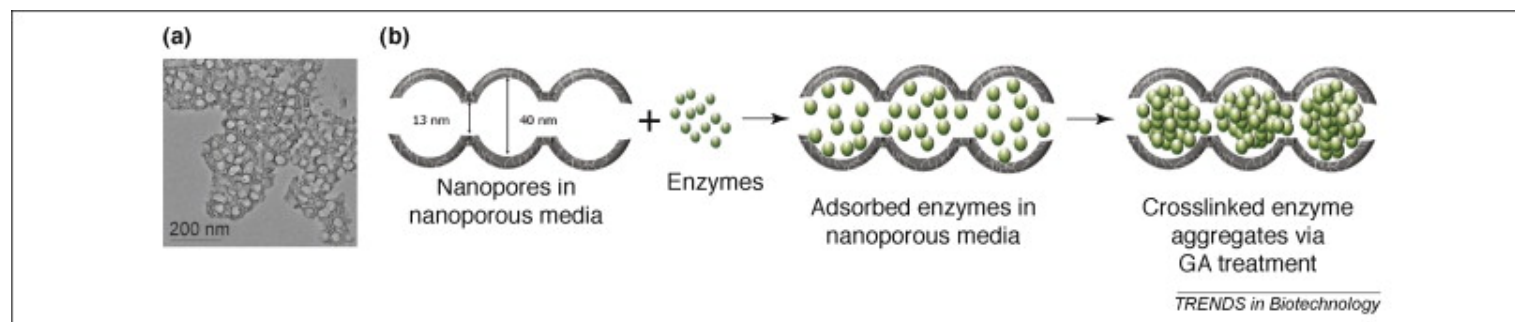


Figure 2.32. 'Ship-in-a-bottle' approach for the stabilization of enzymes in nanoporous media with a 'bottle-neck' structure, as shown in (a) the TEM image of mesocellular mesoporous silica (MMS). (b) Schematic diagram for the preparation¹⁹⁸.

2.5.2.3. Enzyme Aggregate Coating on Nanomaterial.

Enzyme aggregate coating combines covalent enzyme attachment on various nanomaterials with enzyme crosslinking, leading to an increase in enzyme loading, overall enzyme activity and enzyme stability. Figure 2.33 schematically shows the assembly of such an enzyme coating on the surface of electrospun polymer nanofibers. In a first step, enzyme molecules are covalently attached to the surface of nanofibers and serve as ‘seed’ sites. The second step involves the addition of further enzyme molecules and their crosslinking to the seed enzyme molecules, thereby leading to a crosslinked enzyme aggregate coating. This approach has successfully been applied for various nanomaterials, including nanofibers^{237, 238, 239}, carbon nanotubes²⁴⁰ and magnetic nanoparticles²⁴¹. These nanomaterials provide a large surface area for enzyme immobilization, leading to high enzyme loading, which is further increased by one to two orders of magnitude by multiple-layer enzyme coating. The high degree of enzyme stabilization observed suggests that the enzyme coating is tightly bound to the surface of nanomaterials and resistant to washing, even under rigorous shaking conditions, thereby providing excellent operational stability. The intrinsic enzyme stability was also improved by multiple covalent linkages, preventing the enzyme denaturation^{242, 243}.

Enzyme-coating systems could be repeatedly recycled^{237, 241} and have been successfully tested in continuous reactors over long periods of operation^{238, 239}. These systems have already been employed for chemical drug modification and in biofuel cells²⁴⁰. The stabilized activity of glucose oxidase coating on carbon nanotubes enabled the continuous operation of a biofuel cell for more than 16 h. This high operational stability is anticipated to pave the way for the

increased use of biofuel cells, the operation of which is currently restricted owing to their short lifetime.

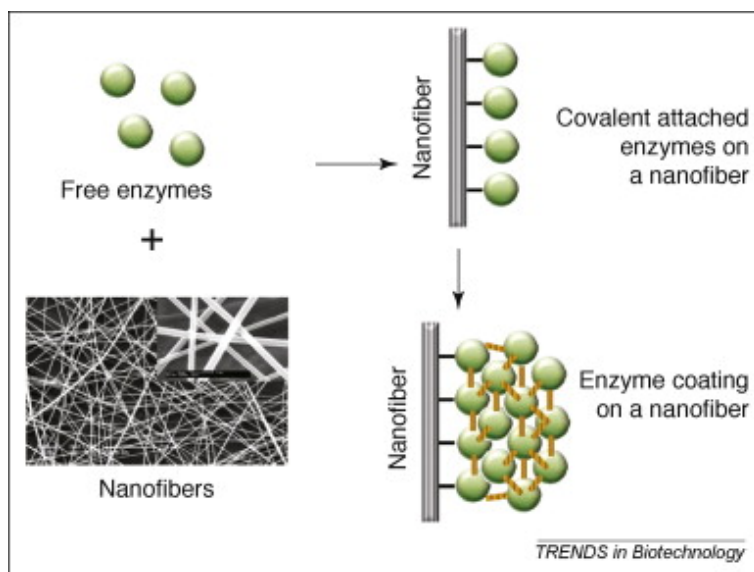


Figure 2.33. Assembly of enzyme aggregate coating on electrospun nanofibers¹⁹⁸.

2.5.2.4. Interfacial Biocatalysis

Most industrial enzymes generally lack the ability of interfacial assembling, which is desired for in vitro biotransformations between immiscible chemicals in biphasic reaction media. Nanoscale fabrication of enzymes can introduce desired affinity interactions to drive the assembly of enzyme molecules at oil–water interfaces. For example, enzymes properly conjugated with hydrophobic polymer groups were able to self-assemble at oil–water interfaces, where they could catalyze interfacial reactions between chemicals dissolved in the oil and water phases^{244, 245}. The catalytic efficiency of the enzyme is significantly improved because the interface-assembled biocatalysts have simultaneous access to chemicals dissolved in both phases. Recently, carbon nanotubes and several other types of nanoparticles were also found to be able to assemble at the interface when they were conjugated with enzymes²⁴⁶. Interfacial enzyme assemblies can be in the form of either a monolayer or multiple layers, but higher enzyme activities were realized when thinner assemblies were formed^{244, 245}. It was suspected that thick assemblies might present an increased mass-transfer barrier across the interface, therefore preventing reactants being able to reach the active site of the enzymes.

Enzymes that have been assembled at the interface showed improved stability when compared to native enzymes simply placed in the same oil–water biphasic systems. This has been attributed to a reduction in interfacial stress caused by the conjugated enzymes acting as macromolecular surfactants²²⁴. The stability of the interface-assembled enzymes could be further improved by adding stabilizers such as polyols and sugars, which create a more favorable environment for enzyme assemblies²⁴⁷.

Assemblies of enzyme-carrying nanoparticles on solid surfaces have been further explored for the development of bioactive materials^{248, 249}. In one example, a 2D assembly of silica nanoparticles with covalently attached enzymes was achieved in a pattern-controlled manner on the surface of silica plates²⁴⁸. It is expected that such assemblies might find applications in the development of biosensors and biochips through the combination of the highly selective activities of the enzymes and the optical and/or electrochemical properties of the supporting materials. Moreover, multiple layers of nanoparticles could also be formed, thus introducing unique optical or electrical properties to the surface in addition to their enzymatic bioactivity²⁴⁹.

2.5.2.5. Nanoenvironment and Enzyme Stability

The effect of the nanoscale environment on enzyme stability has been investigated for various nanomaterials. A series of studies using carbon nanotubes and silica nanoparticles have established a new degree of understanding on the interaction of enzymes with the surface curvature of nanomaterials. It was shown that the effect of the nanoscale environment on enzyme stability is enzyme specific.

For example, chymotrypsin was shown to unfold on the surface of single-walled carbon nanotubes (SWNTs), whereas soybean peroxidase retained its three-dimensional conformation²⁵⁰. A further study revealed that SWNTs were able to stabilize soybean peroxidase at high temperature and in 100% methanol to a greater extent than flat graphite flakes. The different effects were explained by the curvature of SWNTs, which contributed to a reduction of detrimental interactions between protein molecules due to the longer

distance between enzyme molecules, thereby leading to increased protein stability on SWNTs compared to that on flat graphite²⁵¹.

A study that investigated the behavior of ribonuclease A on silica nanoparticles revealed the importance of nanoparticle size and surface curvature for the stability of adsorbed enzymes. The enzyme was less stable on the nanoparticle surface than in solution. It could be demonstrated that ribonuclease A unfolded and inactivated upon adsorption to the silica nanoparticles owing to the electrostatic interactions between the enzyme and the negatively charged nanoparticles. Moreover, the enzyme stability decreased on larger nanoparticles with smaller surface curvature owing to the increased interaction surface between enzymes and nanoparticles²⁵². A destabilizing effect of negative charges was also observed for chymotrypsin, which was inhibited by anionic functionalized gold nanoparticle clusters²⁵³. Enzymes covalently attached onto SWNTs showed increased stability over enzymes in solution because their covalent linkages incurred significant resistance against denaturation²⁵¹. The particular stability of covalently attached enzymes in nanoporous silica could also be explained by the internal curvature of this media, which allows an increased number of covalent linkages between the enzyme molecules and the inner surface of nanopores.

2.5.2.6. Application Potential of Nanobiocatalysis: Antifouling

Biofouling, which is known to start with the adsorption of proteins and other biomolecules on surfaces, represents a significant problem for medical implants, biosensors and membranes, amongst others. A lot of effort has been put into developing antifouling paints and membranes to effectively prevent or reduce associated biofouling problems. One environmentally friendly

approach is to incorporate enzymes into antifouling paints. For example, proteases have been added into antifouling paints to reduce protein binding on surfaces and to prevent the formation of protein-based ‘glues’ that organisms use to attach onto surfaces. Various proteases have been tested as active antifouling agents, including subtilisin, chymotrypsin, pronase, trypsin, pepsin and papain. The addition of enzymes into antifouling paints was effective in reducing the attachment of barnacles and algae on the surface of panels in a field test.

Nanobiocatalytic systems, with their increased enzyme stability, have been proven to be highly effective in reducing protein binding onto a surface. For example, biocatalytic films based on protease-SWNT conjugates within a polymer matrix showed higher enzyme stability than free enzymes in solution²⁵⁴ and proved to be effective as self cleaning nanobiocomposite films, thus preventing protein binding²⁵⁵. Nanobiocatalytic systems, being operationally stable with regard to their antifouling or self-cleaning properties, are anticipated to contribute to the development of long-lasting antifouling coatings, which can prevent or delay the attachment of barnacles and microorganisms on the surface of ship hulls, medical implants, biosensors and membranes.

CHAPTER 3

Quorum Sensing as a New Biofouling Control Paradigm in Membrane Bioreactor

3.1. Introduction

As was clearly shown in the literature review section, QS is closely involved in the biofilm formation on the solids surface in water environment and QS control using either chemical inhibitor (e.g., halogenated furanones) or biomaterial with autoinducer degrading activity (e.g., acylase and lactonase) can alleviate the biofilm formation efficiently, which implies its potential as a new biofouling control approach.

However, all of these previous researches adopted single culture system using model microorganism such as *Pseudomonas aeruginosa*. Microbial world in MBR is the basically undefined mixed culture system of which microbial community consists of various bacterial species. Therefore, no information is available about the application of QS in the MBR.

Therefore, the overall experiments in this chapter were conducted in the following three phases to introduce the concept of bacterial QS to mixed culture MBR system.

- (1) Demonstrating the presence of an autoinducer in the MBR
- (2) Showing a correlation between QS activity and membrane biofouling
- (3) Control of membrane biofouling by quorum quenching

3.2. Experimental Section

3.2.1. Reporter Strain for the Autoinducer Detection

Several strains have been developed for detecting autoinducers based on fusing a QS-controlled promoter to reporter gene (Table 3.1). Considering the microbial diversity in MBR system, an AHL biosensor having broader detection spectrum is required. In this study, *Agrobacterium tumefaciens* A136 (Ti)(pCF218)(pCF372) was used for the detection of N-acyl homoserine lactone (AHL) autoinducers of gram-negative bacteria²⁵⁶

Agrobacterium tumefaciens (Ti)(pCF218)(pCF372) is a genetically modified microorganism for the detection of exogenous AHL signal molecules. Its AHL detection mechanism is depicted in Figure 3.1. This microorganism has the three following genetic characteristics:

- (1) knockout of Ti plasmid (Ti)
- (2) pCF 218 which codes for *traR*
- (3) pCF 372 which contains *traI-lacZ* fusion, which is under *traR* regulation.

Agrobacterium tumefaciens A136 cannot produce the AHL autoinducers because the Ti plasmid on which regulatory components of the *Agrobacterium tumefaciens* QS system are located has been genetically removed. Instead, when exogenous AHL diffuses into *Agrobacterium tumefaciens* A136, it makes a complex with TraR protein from the pCF 218. TraR is an AHL-responsive transcription factor that recognizes 3-oxo-C8-HSL (AHL of *Agrobacterium tumefaciens*) as well as a wide range of related AHLs. This AHL-TraR complex activates *traI-lacZ* on pCF 372 and induces the production of beta-galactosidase, which degrades X-gal (5-bromo-4-chloro-3-

indolyl-beta-D-galactopyranoside) and develops a blue color. We can therefore detect AHL in a sample based on blue color development on an agar plate covered with X-gal. *Agrobacterium tumefaciens* A136 was cultured on Luria Bertani (LB) broth supplemented with spectinomycin and tetracycline to maintain two plasmids that provide the AHL response system²⁵⁷.

3.2.2. Bioassay for the in situ AHL Detection

AHL autoinducers were detected using an original bioassay which was designed in this study (Figure 3.2). This bioassay consisted of an indicating agar plate, a sterilized white filter and the sample to be tested. The indicating agar plate was made by mixing an overnight culture of *Agrobacterium tumefaciens* A136 and LB agar in the ratio of 1:9. The indicating agar was also supplemented by spectinomycin and tetracycline and covered with X-gal. The sterilized white filter was used to prevent the possible microbial pollution of the indicating agar. The sample, such as membrane-biocake, was placed upon the filter. If the sample produces or contains AHLs, they diffuse vertically into the indicating agar, developing the blue color as a result.

3.2.3. Thin Layer Chromatography (TLC) for the AHL Identification

AHLs were extracted from the biocake as follows: the membrane with the biocake was placed in ethyl acetate and biomass was detached from the membrane by means of sonication (150 W, 15 minutes). After the membrane was removed, the mixture of biomass and ethyl acetate was vortexed for 2 h. The cells were then removed by centrifugation at $9,000 \times g$ for 10 minutes.

The supernatant was dried in a rotary evaporator at 30 °C and was resuspended in 250 µL methanol. This crude AHL preparation was spotted on a C18 reverse-phase TLC plate and a chromatogram was developed in 70% methanol/30% water. After being completely dried at room temperature, the TLC plate was overlaid with 1.5% LB agar containing *Agrobacterium tumefaciens* A136, antibiotics and X-gal for the imaging of the AHLs. The TLC chromatogram and the R_f value, defined by the ratio of the distance moved by the spot to that moved by the solvent front, of each AHL standard are shown in the supporting information (Figure 3.3).

Table 3.1. List of the biosensor for the detection of AHL autoinducers.

Strain	Description
<i>Agrobacterium tumefaciens</i> A136(pCF218)(pcf732)	<i>traI-lacZ</i> fusion (pCF218)(pCF372)
<i>Chromobacterium violaceum</i> CV026	Mini <i>Tn5</i> mutant of 31532
<i>Agrobacterium tumefaciens</i> NTL4 (pZLR4)	NT1 derivative carrying a <i>traG:lacZ</i> reporter fusion

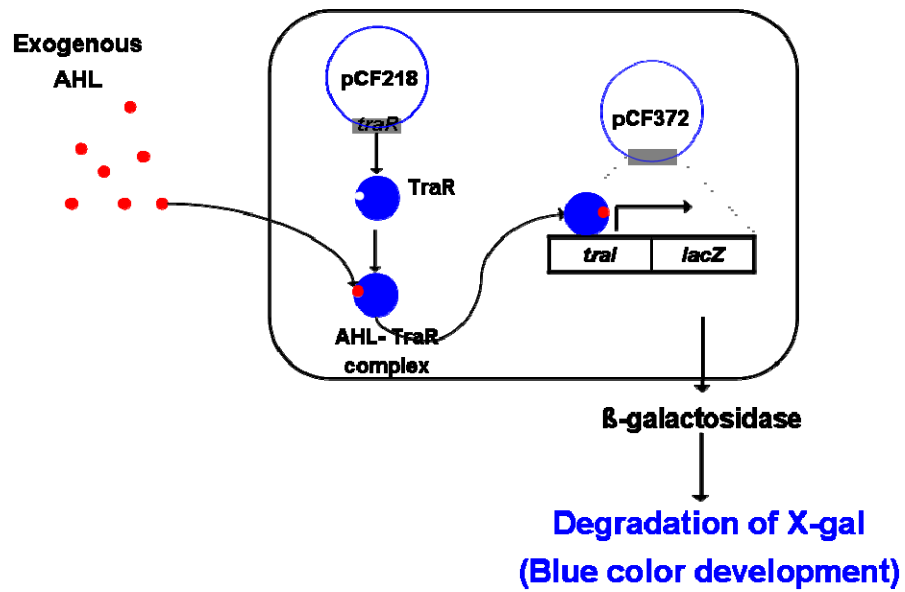


Figure 3.1. AHL detection mechanism of *Agrobacterium tumefaciens* A136 (Ti)(pCF218)(pCF372).

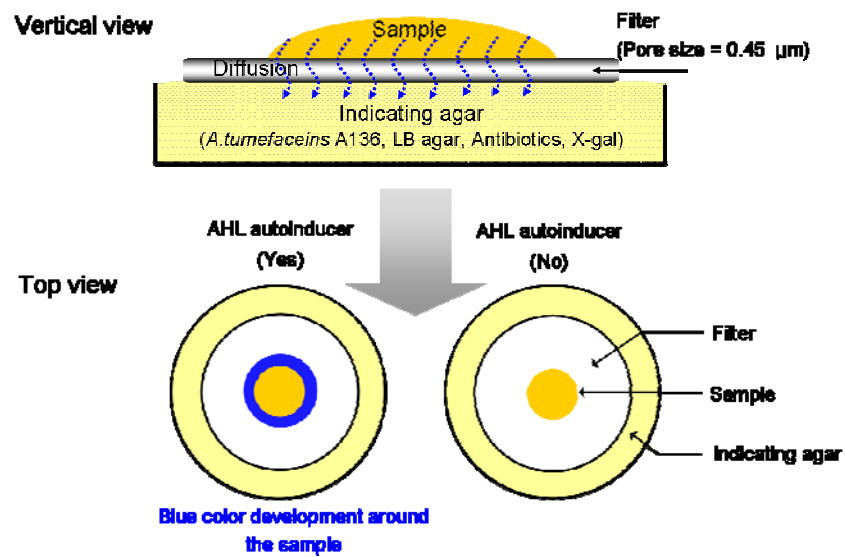


Figure 3.2. Schematic representation of *Agrobacterium tumefaciens* A136 bioassay for *in situ* detection of total AHL

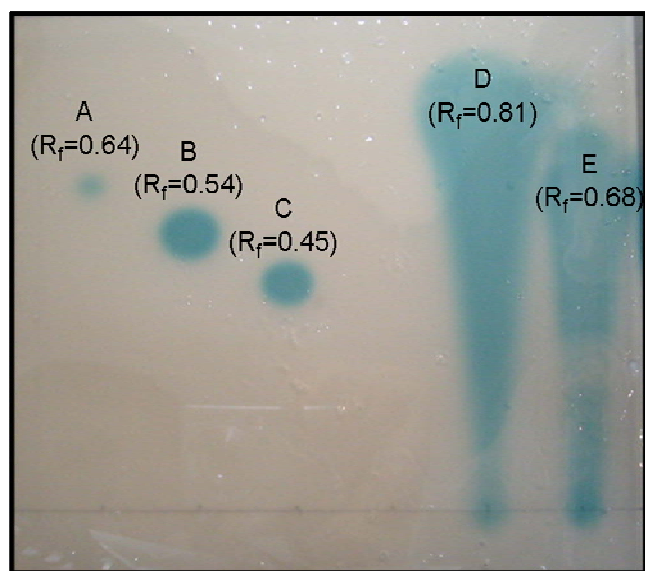


Figure 3.3. TLC chromatogram and R_f value of AHL standards:

A: *N*-hexanoyl-DL-homoserine lactone (C6-HSL).

B: *N*-heptanoyl-DL-homoserine lactone (C7-HSL).

C: *N*-octanoyl-DL-homoserine lactone (C8-HSL).

D: *N*-(3-oxo-hexanoyl)-DL-homoserine lactone (3-oxo-C6-HSL).

E: *N*-(3-oxo-octanoyl)-L homoserine lactone (3-oxo-C8-HSL).

3.2.4. DNA Extraction and PCR-DGGE Analysis

The bacterial community structure in the MBR was analyzed by polymerase chain reaction (PCR)-denaturing gradient gel electrophoresis (DGGE) targeting the 16S rRNA gene according to the procedure described by Park and Lee³⁸.

DNA was extracted from both mixed liquor and membrane-biocake respectively. The samples were harvested by centrifugation at 18,700g for 10 min. After discarding the supernatant, the pellets were used for the sample and the extraction procedure was conducted in accordance with the manufacturer's recommended protocol (Soil DNA extraction kit, Mobio, USA).

The total extracted DNA was used as the DNA template in the PCR reaction of 16S rDNA along with the primer set with GC clamp in Table 3.2. PCR was carried out in a total volume of 50 μ L and sterile water on a Thermo cycler (BioRad, USA). The PCR cycle was comprised as follows; initial denaturation at 94 °C for 5 minutes, 30 cycles of denaturation at 94 °C for 30 seconds, annealing at 56 °C for 30 seconds, elongation at 72 °C for 30 seconds, and a final elongation at 72 °C for 7 minutes. PCR products were purified using a DNA purification kit (Mobio, USA) in accordance with the manufacturer's recommendations prior to use in DGGE analysis.

The PCR purification products were resolved by DGGE for each sample using a universal Dcode system (BioRad, USA) in accordance with the manufacture's instructions. Polyacrylamide gels were poured using a gradient maker. The gels were run at 200 V for 6.0 h at 60. After electrophoresis, the polyacrylamide gel was stained with ethidium bromide for 30 minutes, and then visualized on a Gel Doc system (BioRad, USA).

Table 3.2. Primers used for the PCR amplification of 16S rDNA.

Primer	Sequence
Forward	5-CGC CCG CCG CGC GCG GCG GGC GGG GCG GGG GCA CGG GGG GTC CTACGGGAGGCAGCAG
Reverse	5-ATTACCGCGGCTGCTGG

3.2.5. Reactor Operation

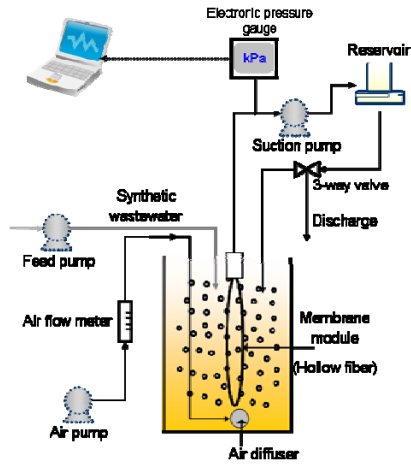
Activated sludge from Si-Hwa wastewater treatment plant (Korea) was inoculated into an MBR after being acclimated to synthetic wastewater by subculturing. The composition of the synthetic wastewater 1.0 g/L glucose, 0.05 g/L yeast extract, 0.05 g/L bactopeptone, 0.5 g/L (NH₄)₂SO₄, 0.3 g/L K₂H₂PO₄, 0.3 g/L KH₂PO₄, 0.009 g/L MgSO₄, 0.0002 g/L FeCl₃, 0.007 g/L NaCl, 0.0002 g/L CaCl₂, 0.0024 g/L CoCl₂ and 0.15 g/L NaHCO₃.

A laboratory-scale MBR with a working volume of 1L was constructed similar to those described by other MBR researchers and was in continuous operation (Figure 3.4a). The membrane was a hydrophilic polyvinylidene fluoride (PVDF) hollow fiber (GE-Zenon, US) with a pore size of 0.04 μm. The other operating parameters of this continuous MBR are summarized in Table 3.3.

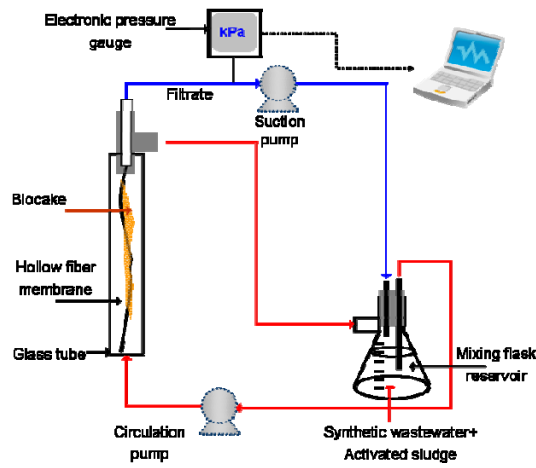
A batch type of MBR (Figure 3.4b) was also designed and operated under a total recycle mode to maintain the effective concentration of quorum quenching enzyme throughout the operation. It was constructed by combining the mixing reservoir flask (150 mL) and a vertical glass tube (3 cm in diameter and 35 cm in length) in which a PVDF hollow fiber membrane module with an effective area of 0.002 m² was inserted through a T-shaped fitting. An acylase or an autoinducer, if necessary, were added to the flask containing wastewater and activated sludge and then circulated within the system by the peristaltic pump. The cell concentration was around 2,500 mg MLSS/L. The membrane permeate was continuously suctioned by a peristaltic pump at a constant flux of 15 L/m²/h and then returned to the mixing reservoir (total recycle mode).

Table 3.3. Continuous MBR operating conditions.

Working volume	1 L
Mixed liquor suspended solids	12,000 (± 500) mg/L
Hydraulic retention time	10 h
Solids retention time	50 days
Membrane area	0.008 m ²
Flux	15 L/m ² /h
Chemical oxygen demand (COD) removal efficiency	98 %



(a)



(b)

Figure 3.4. Schematic diagram of (a) continuous MBR and (b) batch MBR.

3.2.6. Analytical Methods

Gram staining was carried out according to the procedure described by Holm and Jespersen²⁵⁸. Mixed-liquor suspended solids (MLSS) and chemical oxygen demand were determined according to the standard methods²⁵⁹. Glucose, the main carbon source in synthetic wastewater, was determined using the reflectometric method with a test strip (Merck test 1.16720). Extracellular polymeric substances (EPS) were extracted from the biocake using the cationic ion exchange resin method²⁶⁰. Protein and polysaccharides were measured using the modified Lowry method and phenol-sulfuric acid method, respectively.

3.3. Results and Discussion

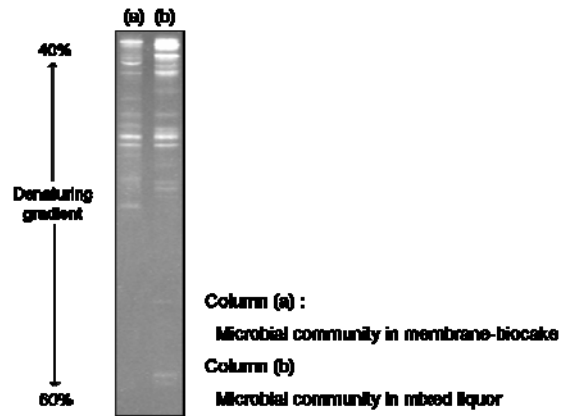
3.3.1. Evidence of the Autoinducer Signal in the MBR

PCR-DGGE analysis of the microbial community in the MBR (Figure 3.5a) shows that more than 10 different bacterial species were present in the biocake and the mixed liquor, respectively. Among various QS autoinducers, such as AHLs of gram-negative bacteria, modified oligopeptides of gram-positive bacteria and autoinducer-2 (AI-2) for interspecies communication, research focus was placed on the AHLs based on the Gram-staining results that Gram-negative bacteria were more dominant than Gram-positive bacteria in the biocake (Figure 3.5b).

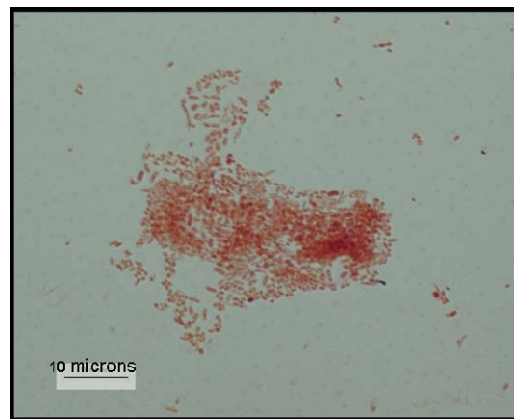
When the transmembrane pressure (TMP) reached 30 kPa, the submerged module was taken out of the bioreactor and disintegrated by aseptically cutting each fiber into lengths of 3–4 cm. Then, each fiber with biocake was bioassayed for the detection of AHLs. All the tested fibers showed blue color developments, proving the presence of AHL autoinducers in the biocake formed on each fiber (Figure 3.6a).

It has been reported that AHL autoinducers have a variety of acyl chains and each bacterium uses its own AHL to regulate QS mechanism. Therefore, it was anticipated that the mixed-cultured bacterial community in the MBR would produce various AHLs. In order to identify the various AHLs which might be involved in the MBR, 5, 10 and 15 μL of AHL extracts obtained from the biocake were developed by TLC and imaged by means of *Agrobacterium tumefaciens* A136 bioassay. The TLC chromatogram in Figure 3.6b indicates the presence of at least three different AHLs. Comparison of

their R_f values with those of the AHL standard showed that spots A and B were *N*-hexanoyl-DL-homoserine (C6-HSL) and *N*-octanoyl-DL-homoserine lactone (C8-HSL), respectively. The strongest blue color developed on spot B suggests that C8-HSL is the most abundant AHL in this biocake, whereas spot C has not yet been identified.

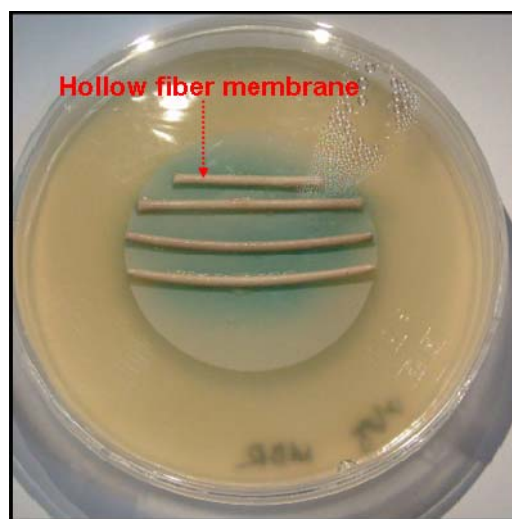


(a)

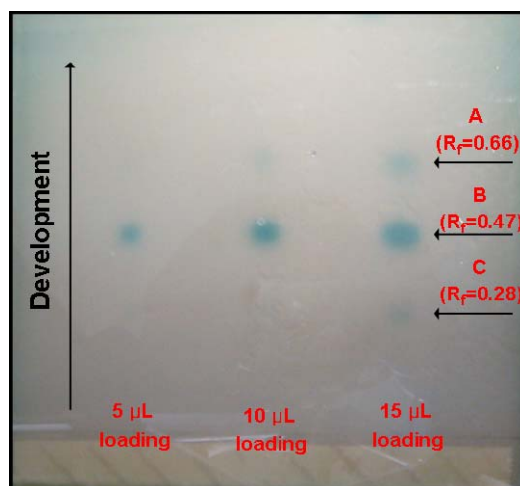


(b)

Figure 3.5. Characterization of bacterial community in MBR. (a) DGGE of bacteria 16S rDNA PCR products. (b) Gram-stained image of biocake detached from membrane module. Both 16S rDNA for PCR-DGGE and biocake for gram staining were obtained at the operation time of 72 h.



(a)



(b)

Figure 3.6. Characterization of the autoinducer signal in membrane-biocake.

(a) *Agrobacterium tumefaciens* A 136 bioassay result for the detection of total AHL. (b) TLC chromatogram of AHL extract from the membrane-biocake for identification

3.3.2. Correlation between QS Activity and Biofouling in MBR.

The AHL signal in biocake at various operating points was monitored using bioassay. As shown in Figure 3.7, the blue color indicating the presence of AHLs was not detected for the early stage (22 h) but started its partial development as the operation proceeded (46 h). It is worth noting that the blue color became intensified after a transition point (58 h, 72 h) simultaneously with the abrupt rise of TMP. In the operation of the MBR at constant flux, a two-stage TMP increase, i.e., an initial slow and gradual increase followed by an abrupt rise in the TMP, is often observed as shown in Figure 3.7d, but its mechanism remains to be clarified. In this context, this close correlation between TMP rise-up and the development of an AHL signal could provide a reasonable clue to such a TMP pattern because the correlation might imply a potential role of QS in the two-stage TMP increase. To investigate this correlation in more depth, the AHL activities in the biofilm and in the deposited microbial flocs (e.g., MLSS) were measured respectively. Different volumes of MBR mixed liquor were filtered on disc-type PVDF membranes to obtain three membranes with different MLSS depositions (0.1–0.5 mg MLSS). These three samples were directly bioassayed to measure AHL activity (Figure 3.8a). In parallel, five membranes with 0.1 mg MLSS were prepared by MLSS deposition and then they were incubated on a wastewater agar plate to let the biofilm grow on each membrane. However, the growth of biofilm reached the stationary phase after a certain incubation time due to the limit of the nutrient supply from the agar. At the incubation time of 0, 6, 9, 16 and 24 h, AHL activity in the biocake on each corresponding membrane was measured using bioassay (Figure 3.8a). Furthermore, the AHL level was

estimated quantitatively using the blue color length on the bioassay agar plate according to Yang et al²⁶¹ and Dong et al¹⁷⁹. Briefly, standard solution of C8-HSL, which was identified as a major autoinducer in this study, was prepared with concentration range of 0.5 ~ 20 mg/L. 2 µL of each standard solution was added to the bioassay agar and incubated overnight. After measuring the distance of blue color development at each AHL concentration, the following formula was obtained and used for the quantitative estimation of AHL level in sample to be tested (Figure 3.9).

$$\text{Amount of AHL (ng C8-HSL)} = 0.1204 e^{0.164X} \quad (r^2=0.9984)$$

X: distance of blue color on bioassay agar (mm)

As shown in Figure 3.8, the AHL signal in the deposited MLSS was negligible regardless of the mass of the deposited MLSS. This means that any microbial flocs deposited on the membrane surface from the mixed liquor during the filtration do not contribute substantially to the total AHL activity, but the microorganisms grown in the biocake do. On the contrary, all four samples except the incubation time of zero show strong AHL activities per unit mass of biocake (Figure 3.8b). Although the samples at the incubation time of 0–6 h hardly showed the AHL activity, the biofilm demonstrated sudden development and increase of AHL activity from 6 h of incubation. These results coincide with the previous one shown in Figure 3.7 and reasonably support that QS would take place in the biofilm grown on the membrane surface from a certain moment during the membrane filtration to give rise to maturations of biofilm, which might be the cause of the “two-stage TMP increase” mentioned above. To make a more quantitative correlation between AHL level and TMP variation, both the filtration resistance (i.e., TMP) and the AHL level of the biofilm were measured and

the correlation between these two parameters was investigated. As depicted in Figure 3.10a, 0.1 mg of MLSS from the mixed liquor in MBR was deposited on each of fourteen PVDF membranes using a filtration device and then they were incubated on wastewater agar plates to make biofilm grow on each membrane. Two membrane-biofilms were prepared at each incubation time of 0, 3, 6, 9, 12, 24, and 48 h. One was used to measure TMP when filtering distilled water at a constant flux of 45 L/m²/h. The other was bioassayed to determine the AHL level. As is shown in Figure 3.10b, the TMP and AHL levels of the biofilm increased under very similar tendencies, which makes us expect the potential of QS-based membrane biofouling control.

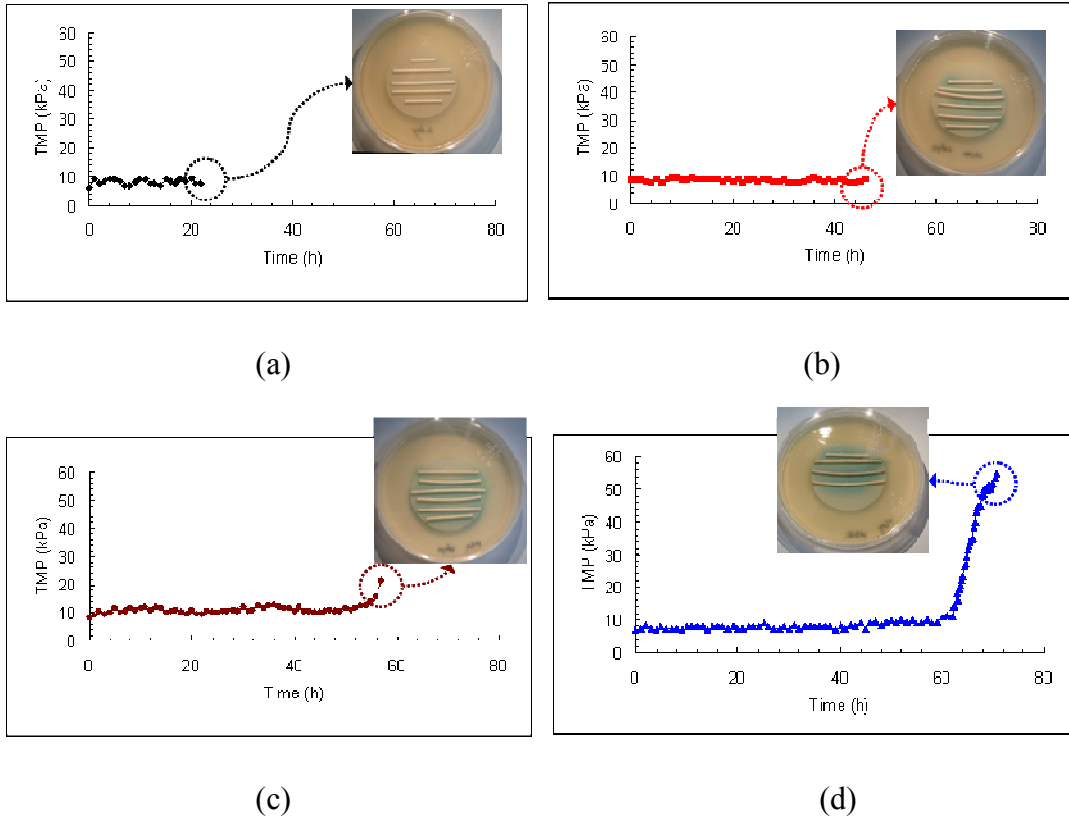


Figure 3.7. Occurrence of AHL signals in biocake during continuous MBR operation. (a) 22 h, (b) 46 h, (c) 58 h and (d) 72 h.

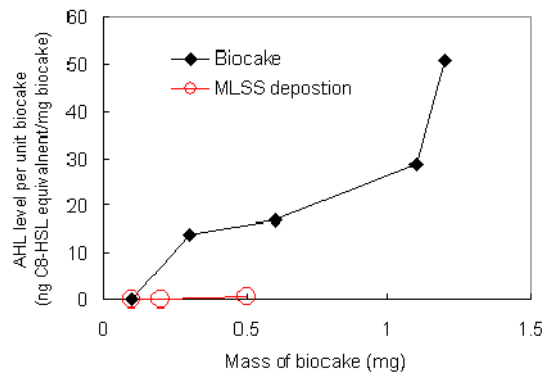
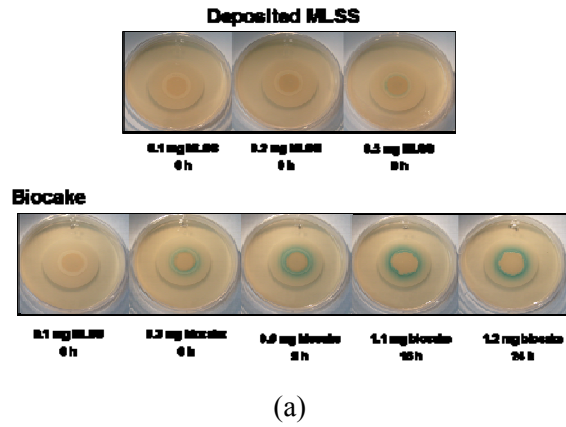


Figure 3.8. Comparison of the AHL level in deposited MLSS and biofilm on membrane. (a) *Agrobacterium tumefaciens* A136 bioassay, (b) AHL level per biomass.

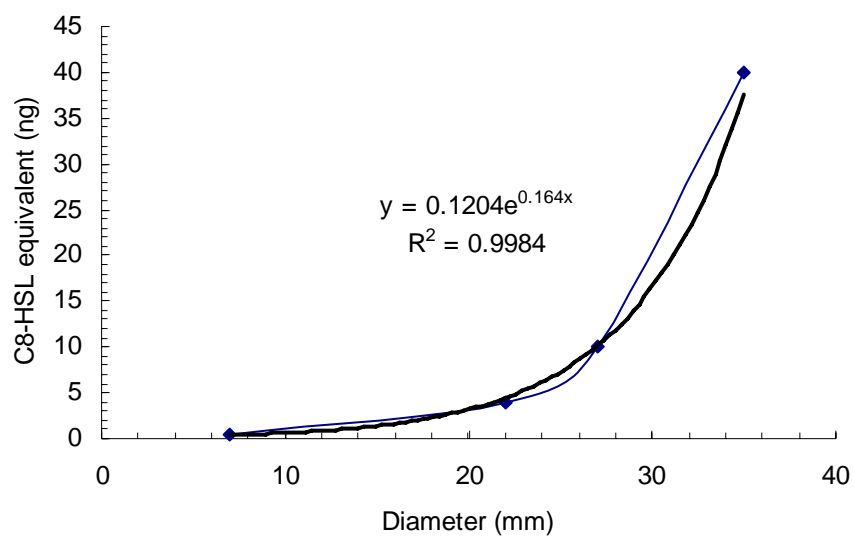
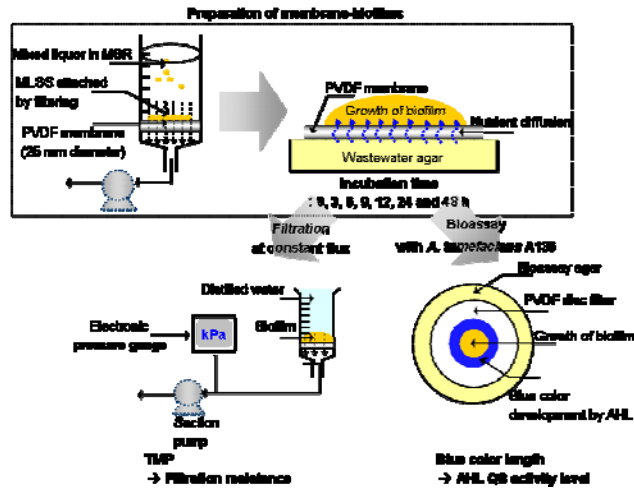
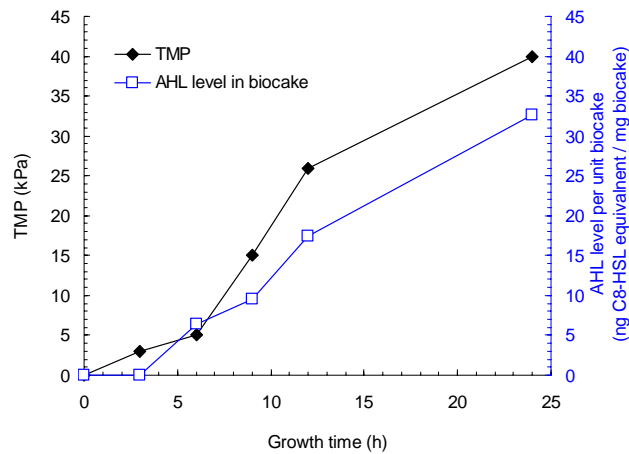


Figure 3.9. Calibration curve for the quantification of AHL level in membrane-biocake using C8-HSL as a standard.



(a)



(b)

Figure 3.10. Correlation between QS activity and filtration resistance of biofilm. (a) Experiment scheme. (b) Variation of TMP and AHL levels as a function of biofilm growth time.

3.3.3. Control of Membrane Biofouling Based on QS

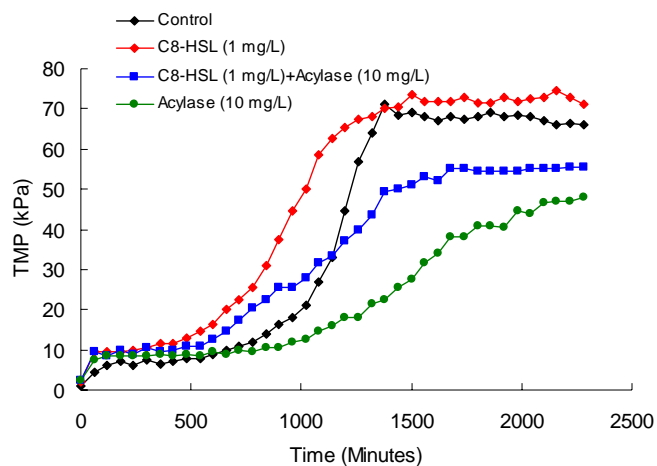
Three basic ways of controlling AHL quorum sensing have been reported:

- (1) blockage of AHL production
- (2) interference with the signal receptor
- (3) inactivation of AHL signal molecules.

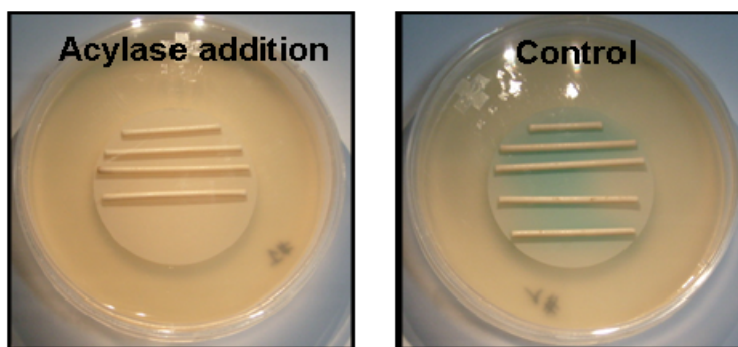
Of these three QS control strategies, a quorum quenching method in which AHLs are inactivated by hydrolysis either at the lactone ring with lactonase or at the acyl-amide linkage with acylase was adopted. Among various quorum quenching enzymes, we selected porcine kidney acylase I (EC-Number 3.5.1.14) in this study. An acylase stock solution of 1,000 mg/L was added exogenously to the batch reactor to make the final concentration of 10 mg/L. If the enzyme acylase is applied directly to the MBR under a continuous operation, enzyme loss could take place owing to passage through the membrane pore into the permeate and removal during the excess sludge disposal. Therefore, a batch type of MBR was designed and operated under a total recycle mode to maintain the effective enzyme concentration throughout the operation. As shown clearly in Figure 3.11a, the addition of acylase retarded the TMP rise-up compared with that of the control reactor, which implies that acylase can alleviate membrane biofouling. However, the biochemical reaction catalyzed with acylase is the general cleavage of amide bonds for any substrate. The reduction of biofouling by acylase would, therefore, result from either the interference of QS by the destruction of AHL autoinducers or the degradation of any organic foulants with amide bonds. Consequently, the following experiments were conducted to make clearer the role of acylase in the release of biofouling.

First, C8-HSL, which had been identified as a major autoinducer in this study, was deliberately and exogenously added to the batch reactor to a final concentration of 1 mg/L, a much higher concentration than that of the control. As shown in Figure 3.11a, with the addition of C8-HSL, the increase rate of TMP became more rapid than that of the control. However, when C8-HSL and acylase were added simultaneously to the reactor, the biofouling aggravated by AHL alone was counterbalanced by acylase, which proves the inactivation of AHL by acylase. This quorum quenching activity of acylase was also confirmed by *Agrobacterium tumefaciens* A136 bioassay of biocake. As shown in Figure 3.11b, biocake in the acylase-added reactor showed much weaker autoinducer activity than that in the control reactor. In view of these results, it has been concluded that acylase reduced the membrane biofouling by quenching AHL autoinducers. Considering that QS regulates gene transcription and determines microbial physiology, the wastewater treatment efficiency should be checked to see possible side effects of acylase or autoinducer. Consequently, the glucose concentrations were monitored during the batch reactor operations under the four different conditions, respectively. As shown in Figure 3.12, the differences in the glucose concentration profiles between the four cases are negligible, which indicates that the addition of acylase and/or AHL autoinducer did not affect the microbial activity. It has been concluded that quorum sensing control has nothing to do with the microbial activity required for the biodegradation of organics. In the final step, how quorum quenching prevents membrane biofouling was investigated. As it is known that EPS play a great role in the biofilm formation and are also key foulants in MBRs, the amount of EPS per unit mass of biocake under was measured the various operating conditions (Figure 3.13). The addition of

acylase reduced the EPS concentration per unit mass of biocake, whereas the addition of an autoinducer (C8-HSL) increased it. These results not only lead to the conclusion that quorum quenching can be a control method for membrane biofouling by regulating EPS concentration, but also that they provide additional evidence for the interrelation between QS activity and biofouling.



(a)



(b)

Figure 3.11. Evidence for membrane biofouling prevention by quorum quenching. (a) TMP profile, and (b) *Agrobacterium .tumefaciens* A136 bioassay results. Bioassay was carried out after 1 day of operation.

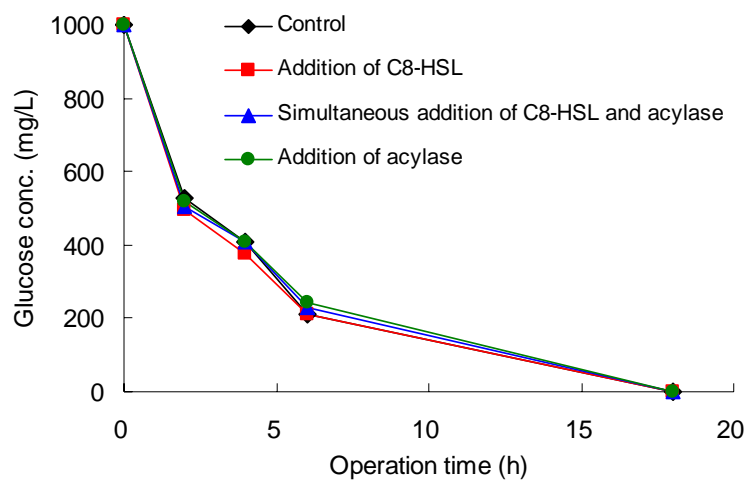


Figure 3.12. Change of glucose concentration during the batch reactor operation in a total recycle mode.

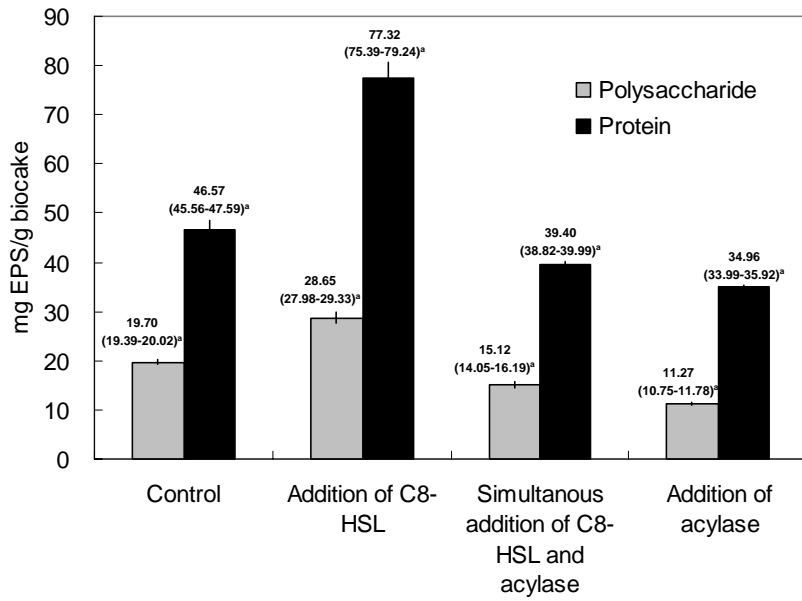


Figure 3.13. Quantitative analysis of EPS in biocakes in the MBR under various operating conditions (N=3).^a: 95% confidence interval.

3.4. Conclusions

The purpose of this chapter was to apply the concept of bacterial QS to MBR for advanced wastewater treatment as a new biofouling control paradigm. Based on the results of this study, the following conclusions were made:

- A bioassay with *Agrobacterium tumefaciens* A136 reporter strain proved that *N*-acyl homoserine lactone (AHL) autoinducers were produced in the MBR. Furthermore, thin-layer chromatographic analysis identified at least three different AHLs in the membrane-biocake, of which *N*-octanoyl-homoserine lactone was the most abundant.

- During continuous MBR operation, the membrane-biocake showed strong AHL activity simultaneously with the abrupt increase in the TMP. Furthermore, both autoinducer level per unit biomass and filtration resistance increased under very similar tendency, which implies that QS was closely associated with the membrane biofouling.

- Porcine kidney acylase I (EC-number 3.5.1.14), which can inactivate the AHL molecule by amide bond cleavage, was confirmed to prevent membrane biofouling by quenching AHL autoinducers, which implies that quorum quenching, enzymatic destruction of QS autoinducer could be a novel biofouling control approach in the MBR

CHAPTER 4

Magnetic Enzyme Carrier for the Biofouling Control in Membrane Bioreactor based on the Enzymatic Quorum Quenching

4.1 Introduction

In the previous chapter 3, it has been proved that quorum quenching can be a novel biofouling control approach in the MBR for advanced wastewater treatment. However, the application of this quorum quenching technique to MBR under a long-term continuous operation is hampered by a short catalytic life time and loss of free enzyme which could take place in the following three ways (Figure 4.1):

- (1) Enzyme lysis and denaturation by the various microorganisms and contamination material which coexist with high concentration in the bioreactor
- (2) Passage of free enzyme through the membrane pores into the permeate
- (3) Coming out of the bioreactor together with excess sludge withdrawing

In this chapter, a ‘magnetic enzyme carrier (MEC)’ was prepared by immobilizing the quorum quenching acylase on a magnetic carrier (Figure 4.2a) to overcome these technical limitations of free enzyme. The MEC will be retained within the bioreactor because of its larger size than the membrane pores, and can be easily recovered and reused via magnetic capture (Figure 4.2b). The MEC is also expected to be more stable than free enzymes in terms of its ability to degrade AHL autoinducers. To further improve the stability of MEC, we have employed the approach of enzyme coatings by cross-linking the adsorbed enzymes on the surface of the magnetic carrier¹⁹⁸. The overall research was carried out through the following phases:

- (1) Preparation of the MEC
- (2) Measurement of enzyme stability
- (3) Comparison of the MEC with free enzymes in a batch system

(4) Application of the MEC to the MBR under a continuous operation

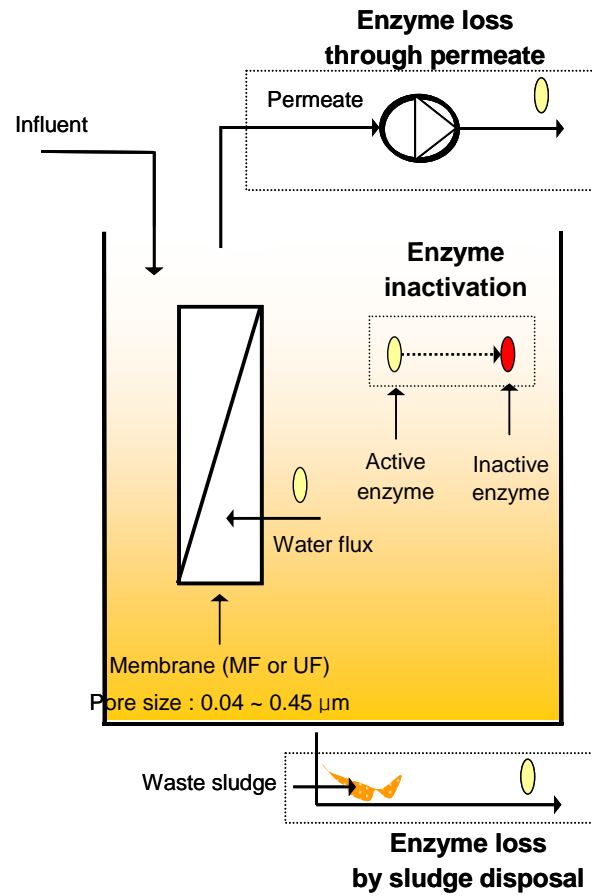
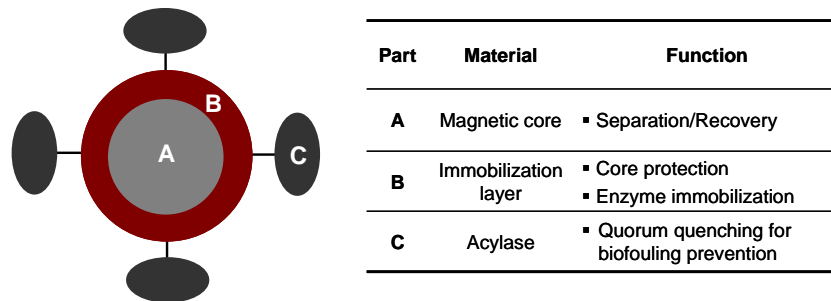
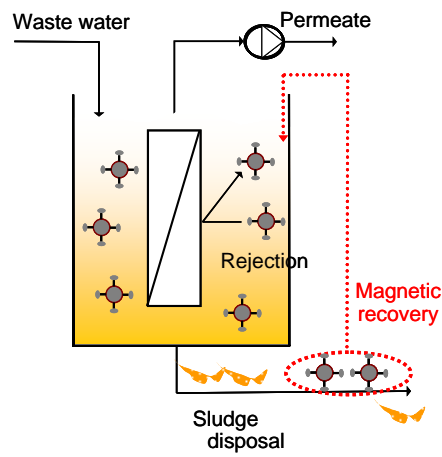


Figure 4.1. Technical problems of free enzyme in continuous MBR system.



(a)



(b)

Figure 4.2. (a) The magnetic enzyme carrier (MEC) concept, and (b) recovery and reuse of the MEC in MBR under continuous operation.

4.2 Experimental Section

4.2.1. Preparation of MEC

The overall preparation scheme of the MEC is depicted in Figure 4.3. Magnetic ion exchange resin (MIEX®, ORICA) has a net positive charge on the surface, and was adopted as a magnetic core for the follow-up enzyme immobilization. The functionalization of MIEX was performed by layer-by-layer (LBL) deposition of an anionic polyelectrolyte (Polystyrene sulfonate, PSS) and a cationic polyelectrolyte (chitosan). Each chemical structure of PSS and chitosan is shown in Figure 4.4. MIEX (1.0 g) was mixed with 50 mL of PSS solution (1 wt% in deionized water) at room temperature under the shaking condition (200 rpm) for 1 h to form MIEX-PSS. After washing with deionized water until no absorbance was read at 260 nm, MIEX-PSS was mixed with 50 mL of the chitosan solution (1 wt% in 1 wt% acetic acid) under the shaking condition (200 rpm) to form MIEX-PSS-chitosan. Then, porcine kidney acylase I (EC-Number 3.5.1.14, pI = 5.8) was covalently attached to the MIEX-PSS-chitosan using glutaraldehyde (GA) as a cross-linking agent. In detail, MIEX-PSS-chitosan was mixed with 20 mL of acylase solution (1000 mg/L in 100 mM phosphate buffer pH = 7.0) for one day at 10 °C under the shaking condition (200 rpm), and then the GA solution was added to make the final concentration of 0.05% v/v. The mixture was incubated at the same conditions without glutaraldehyde to prepare the control sample of enzyme adsorption. The MEC was washed with phosphate buffer until no enzymes were observed in the washing solution, and then stored at 4 °C before further experiments

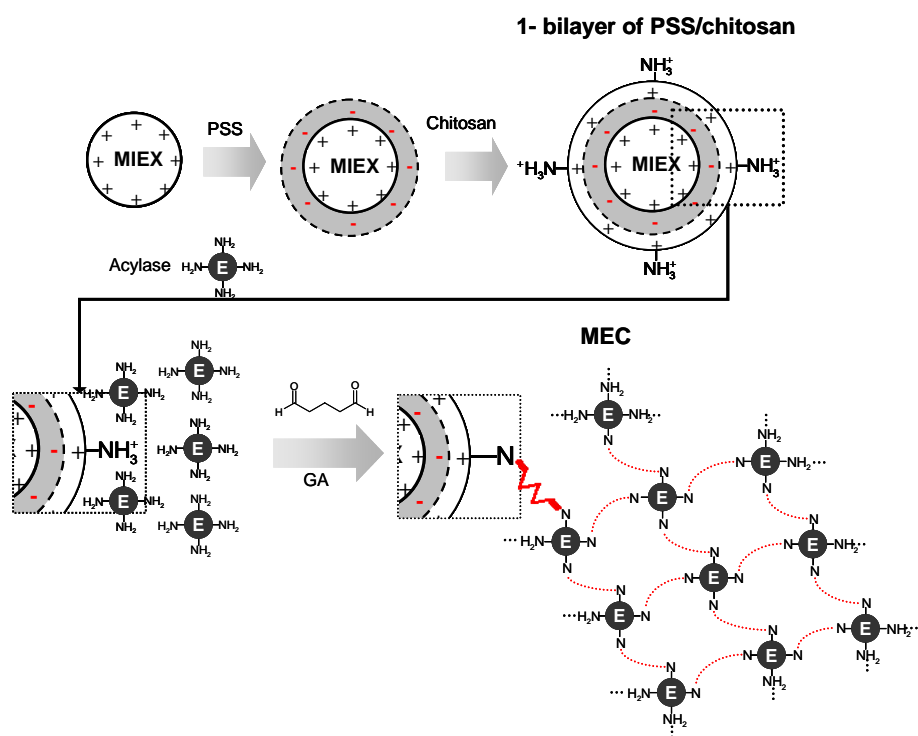
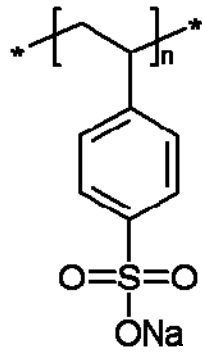
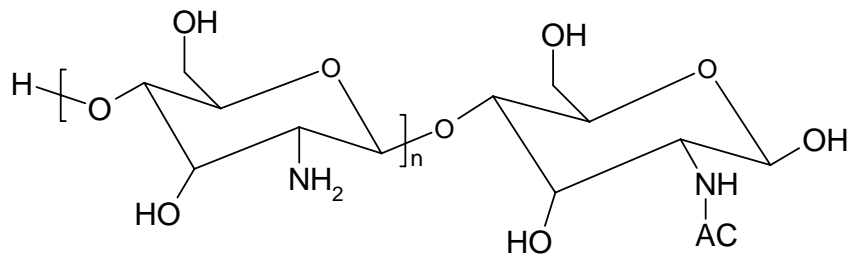


Figure 4.3. Schematic diagram showing the preparation of the MEC through LBL deposition of PSS/chitosan on MIEX resin and enzyme immobilization via glutaraldehyde treatment.



(a)



(b)

Figure 4.4. Chemical structure of (a) polystyrene sulfonate (PSS) and (b) chitosan.

4.2.2. Confocal Laser Scanning Microscopy (CLSM)

The deposition of chitosan on MIEX-PSS and the immobilization of acylase on the MEC was monitored using CLSM. For this purpose, chitosan was labeled with fluorescein isothiocyanate (FITC) based on the procedure described by Qaquish et al.²⁶² and was deposited on MIEX-PSS at the same experiment condition of non-labeled chitosan (Figure 4.5). SYPRO Orange (Molecular probe, US), a specific protein probe²⁶³, was used for fluorescent staining of acylase on the MEC according to the manufacturer's recommendation

Although SYPRO Orange has been used for the fluorescent staining of protein in various samples such as electrophoresis gel^{264,265}, microchip²⁶⁶, and biofilm²⁶⁷, the exact mechanism of the interaction between proteins and SYPRO Orange has not been fully characterized. Therefore, it should be confirmed that SYPRO Orange binds to only acylase in MEC not to other components such as MIEX resin, PSS, and chitosan. For this purpose, four samples of MIEX, MIEX-PSS, MIEX-PSS-chitosan and MEC were stained with SYPRO Orange and were observed with both optical and epifluorescence microscopy (Figure 4.6). Each microscopy image clearly shows that red fluorescence signal was detected only on MEC, which proves the binding specificity of SYPRO Orange to the acylase in MEC.

Both MIEX-PSS-(FITC labeled chitosan) and the MEC stained with SYPRO Orange were observed with CLSM (Nikon C1 plus), respectively. Images were recorded in green channel (excitation 488 nm and emission 515/30 nm) for FITC labeled chitosan and in red channel (excitation 543 nm and emission 600/50 nm) for acylase stained with SYPRO Orange. A Z-

section image stack of each green and red channel was constructed using IMARIS software (Bitplane AG, Zurich, Switzerland).

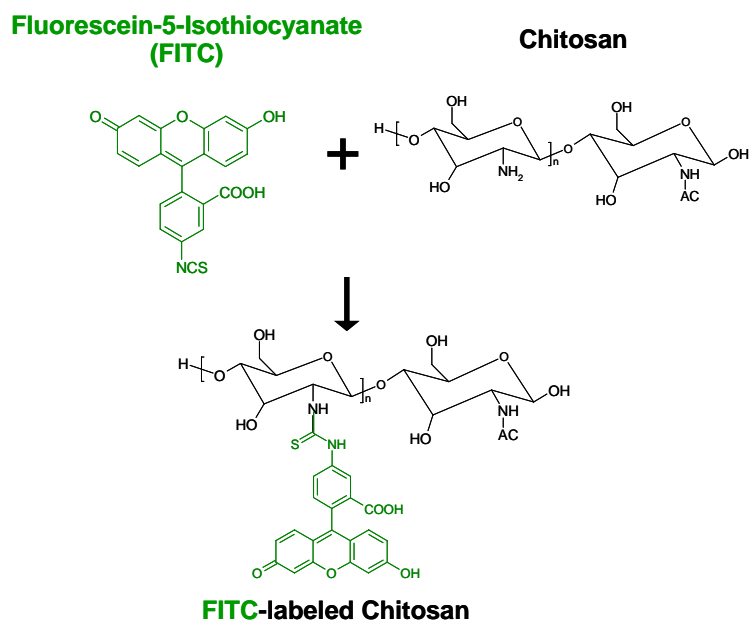


Figure 4.5. Preparation scheme of the FITC-labeled chitosan.

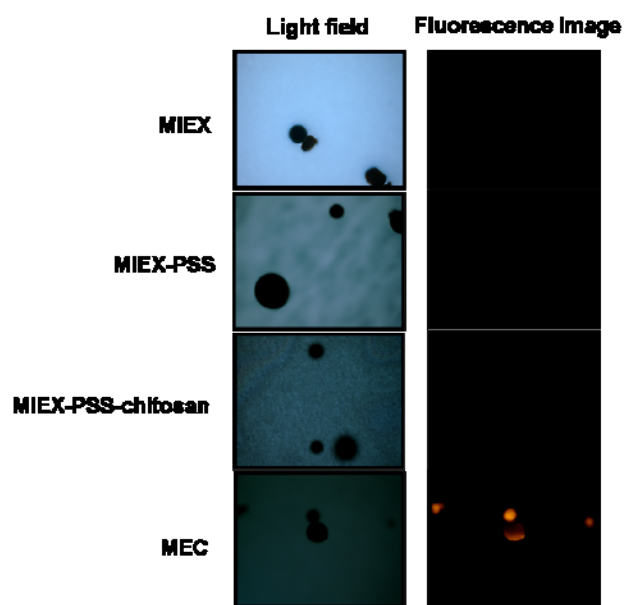


Figure 4.6. Specific binding of SYPRO Orange to acylase in the MEC.

4.2.3. Measurement of Enzyme Activity and Stability

The activity of acylase was measured by the hydrolysis of *N*-acetyl-L-methionine (Figure 4.7) in aqueous phosphate buffer (100 mM). The consumption of substrate was evaluated by measuring the decrease of absorbance at 238 nm (A238), and the activity was calculated from the slope of A238 with time²⁶⁸. Enzyme stability was determined under both iterative cycles and continuous shaking, as described by Kim²²⁶ and Lee²²⁵.

To check the stability under iterative uses, the sample of immobilized enzymes was added to the reaction buffer (10 mM substrate in phosphate buffer), and were shaken at 150 rpm for 50 minutes to measure the enzyme activity. The sample was recovered by using a magnet, excessively washed with fresh phosphate buffer, and the same amount of reaction buffer was added for the measurement of enzyme activity in the next cycle.

To check the enzyme stability in a continuous shaking condition, the samples in phosphate buffer without substrate were shaken at 150 rpm. At each time point, an aliquot was withdrawn for the measurement of residual activity as described above. The relative activity at each time point was calculated by the ratio of residual activity to initial activity.

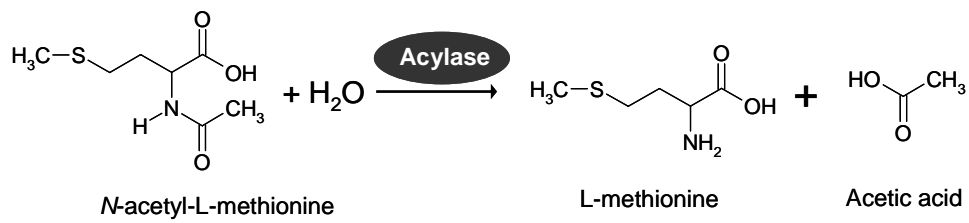


Figure 4.7. Enzyme reaction of acylase using *N*-acetyl-L-methionine as a substrate.

4.2.4. Reactor Operation

Activated sludge from the Si-Hwa wastewater treatment plant (Korea) was used after being acclimated to the synthetic wastewater by subculturing. The composition of synthetic wastewater was same as that used in chapter 3. Preliminary research has confirmed that this activated sludge consists of more than 10 different bacteria species and produces three different AHLs of which *N*-octanoyl-L-homoserine lactone (C8-HSL) was the most dominant. A batch type of the MBR (Figure 4.8a) was designed and operated under a total recycle mode to maintain the effective concentration of free acylase during the operation. It was constructed by combining the mixing reservoir flask and a vertical glass tube (3 cm in diameter and 35 cm in length) in which a polyvinylidene fluoride (PVDF) hollow fiber membrane (ZeeWeed 500, GE-Zeone, US) module with an effective area of 0.002 m² was inserted through a T-shaped fitting. Free acylase or the MEC, if necessary, were added to the flask containing wastewater and activated sludge. The total working volume was 150 mL, and the cell concentration was around 2,500 mg MLSS/L. The membrane permeate was continuously suctioned by a peristaltic pump at a constant flux of 15 L/m²/h and then returned to the mixing reservoir (total recycle mode).

In addition, two lab scale MBRs, a control MBR and the MEC MBR were constructed in a similar way to those described by other MBR researches^{12, 13} and were operated in parallel (Figure 4.8b). Operating parameters of each reactor are summarized in Table 4.1. 20 mL of sludge was withdrawn everyday from each MBR to adjust solids retention time (SRT) to 50 days. The MEC contained in the withdrawn sludge was recovered by the magnet and returned to the MEC MBR.

When the MEC was added to both the batch and continuous MBR, all reactors were placed on the magnetic stirrer to hold the MEC at the bottom of the reactor and, therefore, minimize possible biofouling by preventing the physical collision of the MEC on the membrane surface.

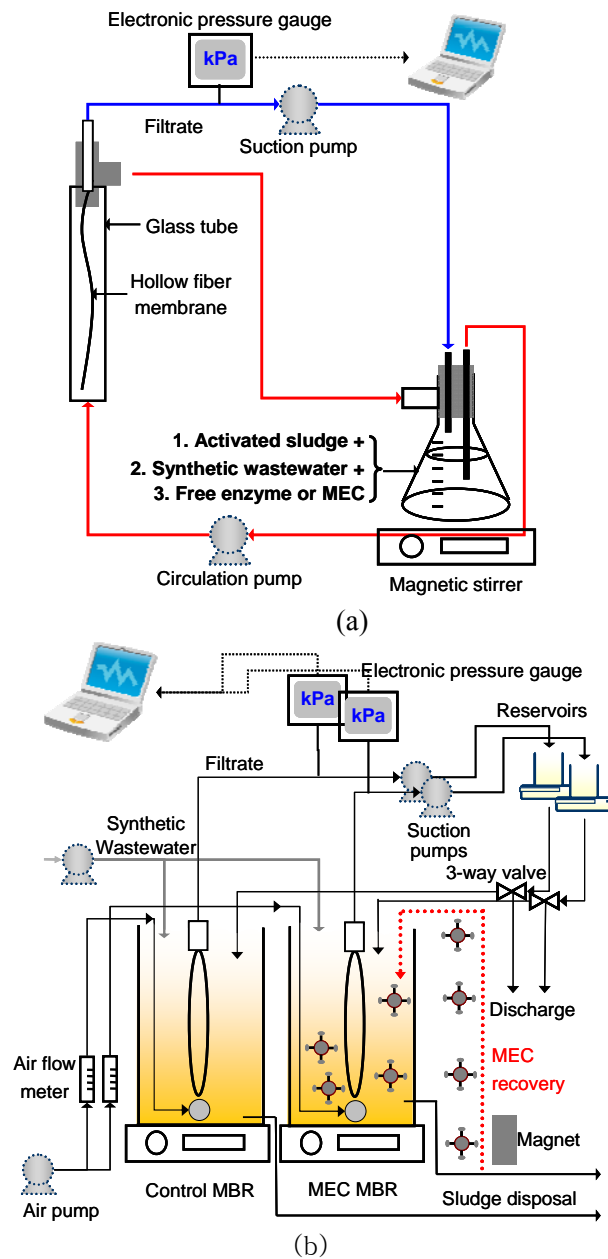


Figure 4.8. Schematic diagram of (a) batch type MBR in total recycle filtration mode and (b) MBR in continuous operation.

Table 4.1. Operating conditions of each control and MEC MBR.

	Control MBR	MEC MBR
Working volume (L)		1
Hydraulic retention time (HRT) (h)		10
Solids retention time (SRT) (days)		50
Membrane area (m ²)		0.008
Flux (L/m ² /h)		15
Mixed liquor suspended solids (mg/L)	24,000 (±3,500)	26,000 (±1,300)
Dosage of MEC (g)	0	0.5

4.2.5. Analytical Methods

Surface charge of MIEX at each polyelectrolyte deposition step was measured using a zetameter (Zetasizer Nano Z, Malvern). PSS concentration was determined by measuring the absorbance at 260 nm. Chitosan was quantitatively analyzed using the ninhydrin method. Mixed liquor suspended solids (MLSS) and chemical oxygen demand (COD) were determined according to the Standard methods. Glucose, the main carbon source in synthetic wastewater, was determined reflectrometrically (Merck, RQflex) after enzymatic conversion of glucose to gluconic acid-lactone (Merck test 1.16720). Soluble microbial products (SMP) were obtained by centrifuging the mixed liquor (12,000×g, 10 minutes) and then filtering the supernatant with membrane (pore size of 0.45 μm). Extracellular polymeric substances (EPS) were extracted from the membrane-biocake using cationic ion exchange resin method²⁶⁰. Protein and polysaccharides were measured using the modified Lowry method and phenol-sulfuric acid method, respectively¹². The molecular weight distribution of SMP and EPS was analyzed using gel filtration chromatography (GFC) with a Ultrahydrogel 250 column (Waters, US). The mobile phase was the NaNO₃ (0.01 M) solution and flow rate was 0.6 mL/min. Polyethylene glycol was used as a standard and the calibration curve was obtained by analyzing the retention times of standards with various molecular weight. The eluted SMP and EPS were detected using both refractive index (RI) and UV detector (280 nm).

4.3. Results and Discussion

4.3.1. Preparation of the MEC

The layer-by-layer (LBL) deposition of PSS and chitosan on MIEX was monitored by measuring the zeta potentials of MIEX, MIEX-PSS and MIEX-PSS-chitosan (Figure 4.9). MIEX contains quaternary ammonium functional groups on the surface and, therefore, the net surface charge was positive (16.3 mV). This was inverted to negative charge by the deposition of anionic polyelectrolyte PSS (-10.0 mV). Finally, the cationic polyelectrolyte chitosan was deposited onto the MIEX-PSS, resulting in positive surface charge (24.4 mV). The disappearance of PSS and chitosan from the solution was measured during the LBL deposition process (Figure 4.10), and the amounts of polyelectrolytes deposited on MIEX support were calculated to be 107.4 mg PSS/g MIEX and 17.5 mg chitosan/g MIEX-PSS respectively. Then, acylase was immobilized onto the MIEX-PSS-chitosan via a simple enzyme adsorption or chemical cross-linking of adsorbed enzymes using glutaraldehyde. The final enzyme loadings were calculated from the disappeared amount of protein from the solution during immobilization, and were 13.6 and 18.1 mg enzyme/g MIEX-PSS-chitosan for adsorbed enzyme and the MEC respectively.

Each projection CLSM image of MIEX-PSS-(FITC labeled chitosan) (Figure 4.11a) and the MEC stained with SYPRO Orange (Figure 4.11b) visually confirmed the deposition of the chitosan layer on the MIEX-PSS and immobilization of acylase on the MIEX-PSS-chitosan respectively. Furthermore, a cross-sectioned CLSM image of the MEC showed a layer of

acylase aggregates on the outer surface of the magnetic support, suggesting that the MEC was successfully constructed by the combination of MIEX, 1-bilayer LBL film of PSS/chitosan and immobilization of acylase via GA treatment. Considering that MIEX has a macroporous structure, we should check the possibility that acylase could be entrapped in the pore of the MIEX by 'ship-in-a-bottle' way when GA was added in the final preparation step. To make this point more clearly, acylase was immobilized on the support of MIEX-PSS-(FITC-labeled chitosan) using GA. Then, this MIEX-PSS-(FITC-labeled chitosan)-acylase was stained again with SYPRO Orange and was observed using CLSM with both green and red channel simultaneously (Figure 4. 12). The cross section image of each laser channel shows that chitosan and acylase was placed on the same location on the magnetic support, which means that immobilization mechanism of acylase in this study was not a 'ship-in-a-bottle' but 'enzyme aggregation'.

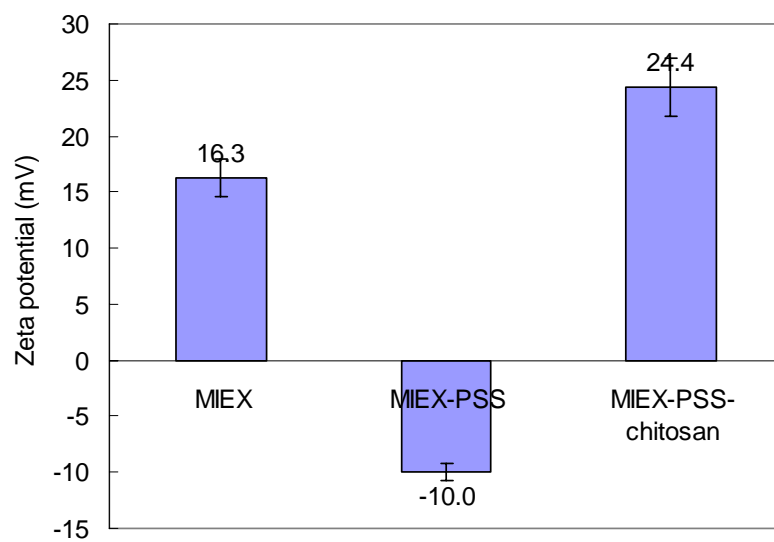
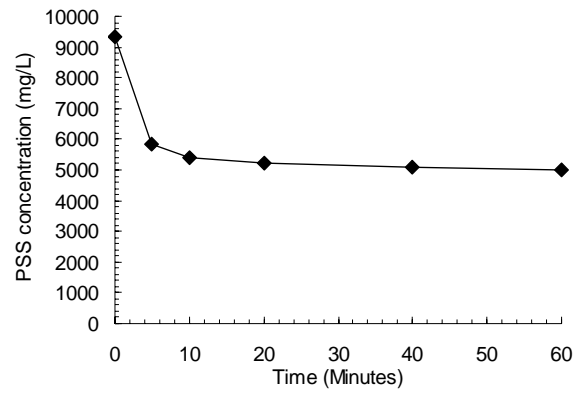
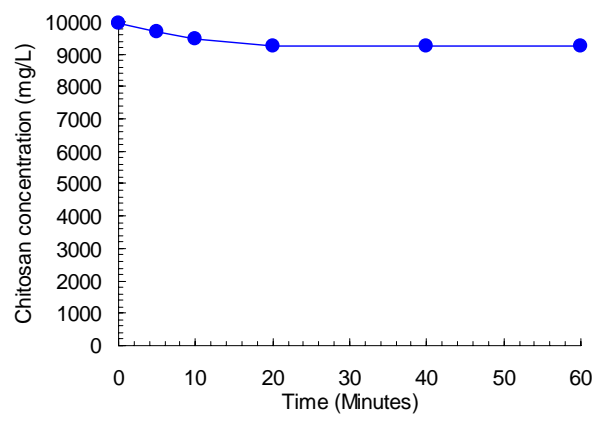


Figure 4.9. Change of zeta potential on MIEX support during LBL process.

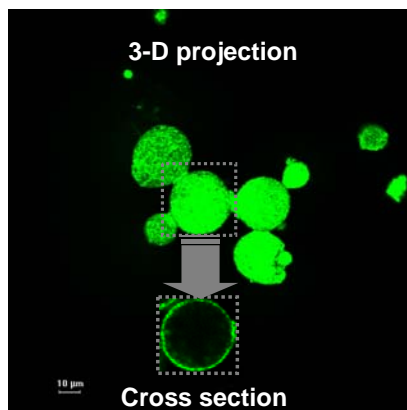


(a)

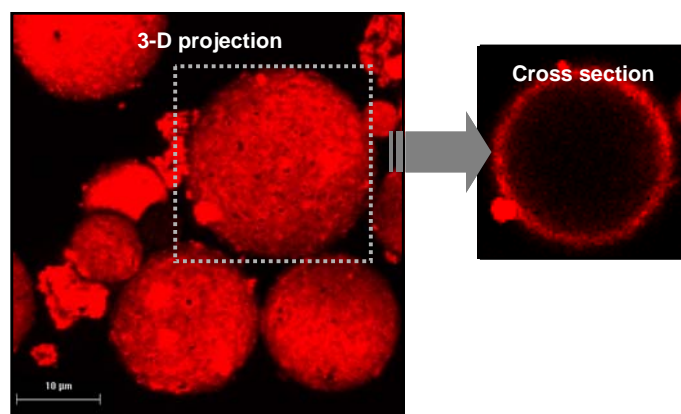


(b)

Figure 4.10. Concentration profile of (a) PSS and (b) chitosan in solution during LBL process.



(a)



(b)

Figure 4.11. CLSM image of (a) MIEX-PSS-(FITC labeled chitosan) and (b) MEC stained with SYPRO Orange.

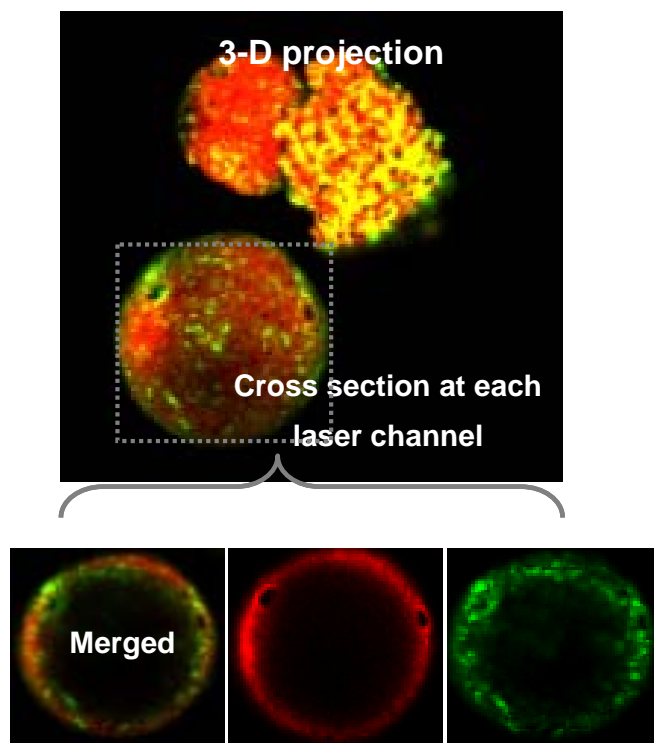


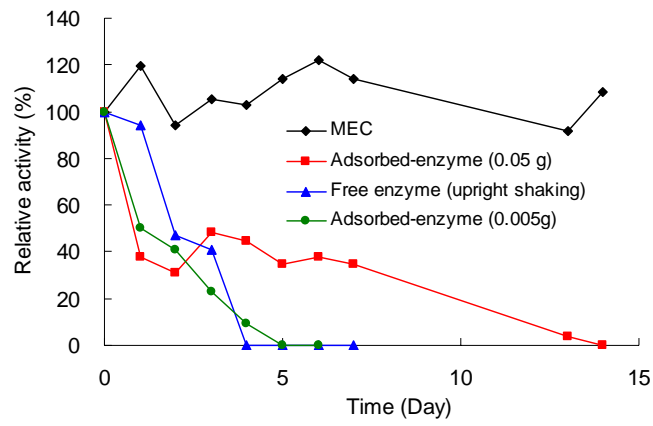
Figure 4.12. CLSM image of MIEX-PSS-(FITC labeled chitosan)-acylase stained with SYPRO Orange.

4.3.2. Stabilities of free enzyme, adsorbed enzyme and the MEC

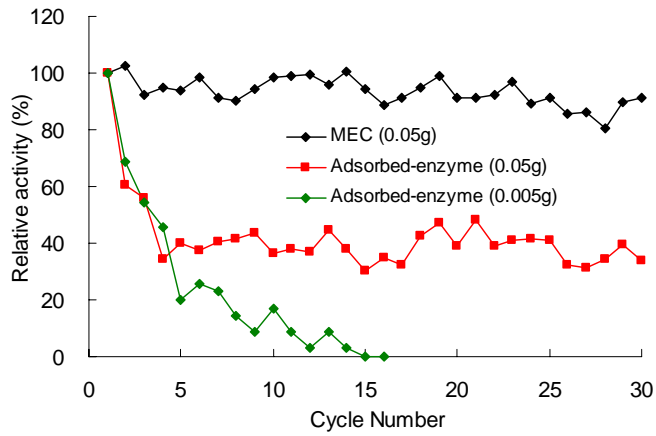
The enzymatic stability was determined by the relative activity of each sample under both continuous shaking at 150 rpm for 14 days and 29 iterative cycles of enzyme reuse. Acylase adsorbed on MIEX-PSS-chitosan without GA treatment (adsorbed enzyme) was used as a control sample. The initial activities of the MEC and adsorbed enzyme were measured to be 15.6 and 13.0 $\mu\text{M}\cdot\text{min}^{-1}$ per mg acylase, respectively. Figure 4.13a shows the stability of free enzyme, adsorbed enzyme and the MEC under continuous shaking (150 rpm). Free enzyme was completely inactivated after four days. Adsorbed enzyme (0.05g total weight) was also completely inactivated after 14 days, however, maintained about 40% of initial activity during the early phase of the experiment. The inactivation of adsorbed enzyme can be explained by the leaching of physically adsorbed acylase under shaking, followed by the inactivation of free enzyme in the same mechanism. To check the effect of enzyme leaching, 0.005 g of adsorbed enzyme was continuously shaken under the same condition, resulting in complete inactivation after five days. This implies that enzyme leaching plays a role in the inactivation of adsorbed enzyme. On the other hand, the MEC (0.05 g) maintained its initial activity for 14 days. This good stability of the MEC can be explained by the prevention of enzyme leaching and enzyme denaturation because of multi-point linkages on the surface of enzyme molecules.

The enzyme stabilities of adsorbed enzyme and the MEC showed similar trends under iterative cycles of enzyme reuse (Figure 4.13b). For example, 86% of initial activity was preserved in the MEC after 29 iterative cycles of enzyme reaction and separation. However, adsorbed enzyme (0.05 g) lost

60% of initial activity after four iterative cycles and 40% of initial activity was maintained thereafter. If enzyme loading was lowered by ten times, adsorbed enzyme showed complete inactivation after 15 cycles, suggesting that enzyme leaching is an inactivation mechanism of adsorbed enzyme. To prove that there was no enzyme leaching in MEC experimentally, the enzyme stability of 0.005 g MEC was measured under iterative cycle during continuous shaking. In detail, MEC was continuously shaken in the phosphate buffer. At each day, 6 cycles of enzyme reaction and magnetic recovery were conducted measuring relative activity. Figure 4.14 clearly shows that the initial activity of MEC was maintained during 5 days under 30 cycles, which means that there was little enzyme leaching in MEC.



(a)



(b)

Figure 4.13. (a) Stability of free enzyme, adsorbed-enzyme and the MEC under continuous shaking conditions. (b) stability of adsorbed-enzyme and the MEC under iterative cycles of enzyme reaction and magnetic separation.

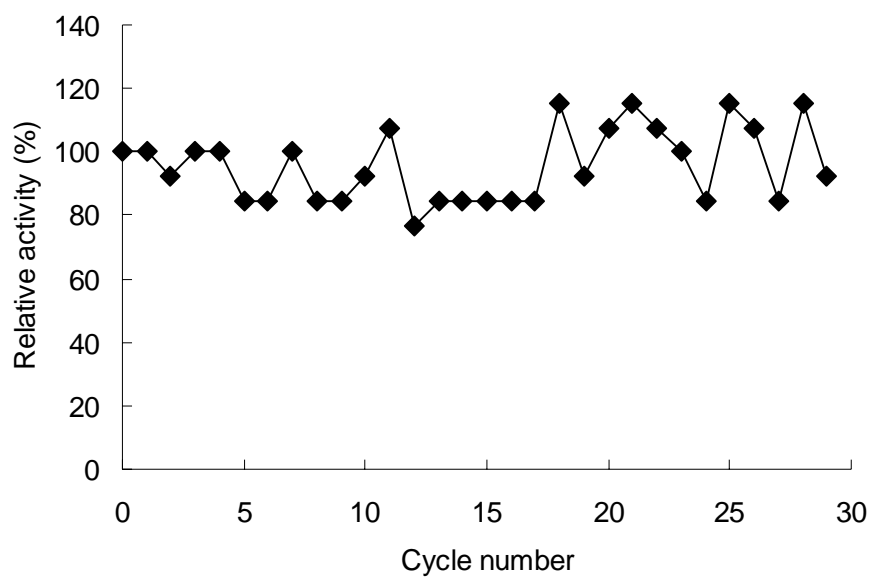


Figure 4.14. Stability of MEC during 6 days under 29 cycles of enzyme reaction and reuse.

4.3.3. Comparison of the MEC with Free Enzyme in Batch Type MBR

The next research phase was to compare the performance of the MEC with that of free acylase in iterative batch reactor operation. Three reactors – a control without enzyme, one with free acylase and one with the MEC – were operated in parallel. To set the final enzyme concentration to 15 mg/L, 1.5 mL of enzyme stock solution (1,000 mg/L) and 0.08 g of the MEC were added to the reactors of free acylase and the MEC respectively at the start of the first batch operation. When the first batch operation ended, 25mL of mixed liquor was discharged from each reactor, and the same volume of fresh synthetic wastewater was added to each reactor. One of the key advantages with the MEC is that all MEC samples could be retained in the reactor by using a magnet during the discharge procedure. After the membrane module was replaced with a new one, the next batch operation started. The rise-up pattern of transmembrane pressure (TMP) in the batch reactors during three operation cycles was compared (Figure 4.15).

In the first operation, free acylase and the MEC both reduced membrane biofouling to a large extent compared with the control reactor. It is worth noting that free enzyme (final TMP: 32 kPa) alleviated membrane biofouling a little more efficiently than the MEC (final TMP: 37 kPa). However, in the second operation, TMP in the free acylase reactor increased much more rapidly than that in the MEC reactor and showed little difference to that in the control reactor, although about 80 % of free enzyme remained in the reactor. This implies that the MEC was much more stable than free enzyme in MBR mixed liquor, which contains microorganism and organic contaminants in high concentration. This operation stability of the MEC was confirmed by the

third operation in which the MEC reactor showed much slower TMP rise than the other two reactors. Figure 4.15 clearly shows that MEC alleviated membrane biofouling. The possible biofouling prevention mechanisms of MEC were thought to be i) inhibition of biofilm growth on the membrane surface and ii) detachment of biofilm from the membrane surface. To distinguish which mechanism was responsible for the fouling prevention mechanism of MEC, the following experiments were conducted. At first, control batch MBR without MEC and MEC batch MBR with 0.125g MEC were operated in parallel. After 1 day filtration, same amount of MEC was added to the control reactor and change of TMP was monitored thereafter. Figure 4.16 clearly shows that MEC could successfully reduced biofouling only at the initial stage, which implies that MEC alleviated biofouling by the inhibition of biofilm growth on the membrane surface.

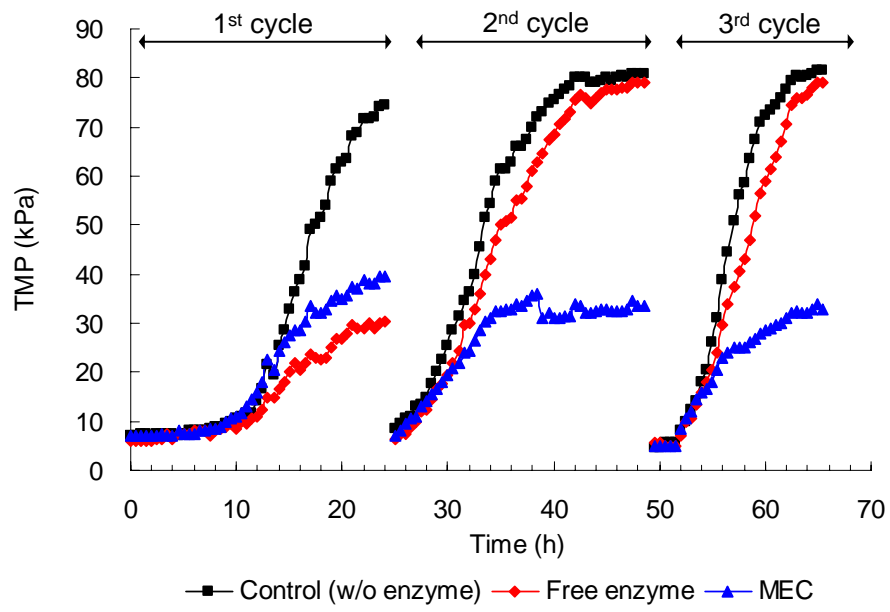


Figure 4.15. Comparison of TMP profile among each batch MBR during the three operation cycles.

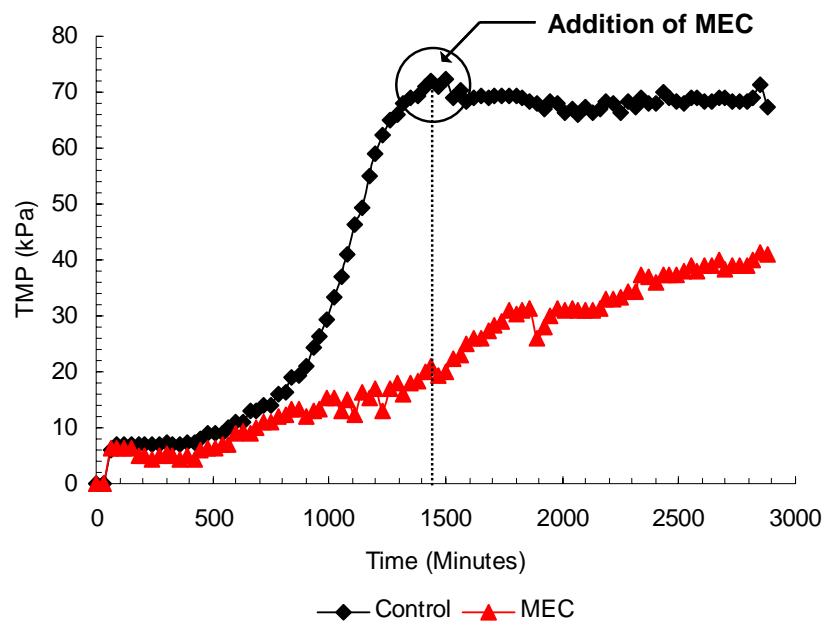


Figure 4.16. Effect of MEC on the biofilm detachment in batch type MBR.

4.4.4. Application of the MEC to the MBR in Continuous Operation

The MEC was also tested to confirm its ability to improve membrane biofouling in the continuous MBR. Two lab scale MBRs in the continuous modes were operated in parallel under identical operation conditions except for the dosage of MEC to one MBR at the start of the operation (Figure 4.8b). First, the TMP rise-up profile of both the control and the MEC MBRs was compared to evaluate the biofouling prevention by the MEC (Figure 4.17).

In the control MBR, for both first and second operations TMP exceeded 30 kPa after 48 h of operation at which the membrane module was to be replaced with a new one. However, TMP in the MEC MBR maintained almost its initial value of around 10 kPa for the entire of both first and second operations, which means that the MEC prevented membrane biofouling efficiently in the continuous MBR operation. In addition to the TMP change, a water quality of the membrane permeate, e.g. the effluent of the MEC MBR is another important factor to be considered regarding MBR performance. The effluent COD of each control and the MEC MBR was 16.9 (± 5.7) mg/L and 13.2 (± 4.5) mg/L respectively, which revealed that the MEC alleviated membrane biofouling but did not deteriorate the microbial activity for the degradation of organics in the bioreactor.

As a final phase we investigated the reason why the addition of the MEC could reduce membrane biofouling. Basically, QS systems regulate the target gene transcription and determine the physiology of the microbial community. Therefore, it was anticipated that the addition of the MEC, which was expected to disrupt the QS signal molecules, might change the microbial physiology in the bioreactor, which is now generally accepted to be closely

associated with membrane biofouling^{31, 39}. In this context we investigated the difference in the microbial physiological characteristics between the control and the MEC MBRs in terms of soluble microbial products (SMP) in mixed liquor and extracellular polymeric substances (EPS) in membrane-biocide respectively.

When the first operation of control MBR ended after 48 h, both SMP in mixed liquor and EPS in membrane-biocide were analyzed not only qualitatively by gel filtration chromatography (GFC) (Figure 4.18), but also quantitatively by spectrophotometry (Figure 4.19). SMP are defined as the metabolites excreted by the cells using substrate in the influents²⁶⁹ and, therefore, should be distinguished from the residual organic materials in the effluent such as glucose in synthetic wastewater. As the glucose concentration in the SMP sample was negligible, the fraction of residual substrates in the SMP sample could be ignored.

Looking at GFC spectrums of SMP and EPS (Figure 4.18), the intensities of peaks which appeared mainly at the elution time of 8~10 min were found to be reduced by adding the MEC. The molecular weight of these peaks was calculated to be about 11,000 Da. This means that microbial metabolites corresponding to this elution time were under the control of the MEC, e.g. quorum quenching. The reductions of SMP and EPS generation were determined quantitatively. As shown in Figure 4.16, SMP were reduced by the addition of the MEC (polysaccharide from 66.0 to 55.0 mg/L, protein from 141.2 to 55.0 mg/L). EPS in membrane-biocide extracted after 48 hours of operation from both MBRs showed the same tendency as SMP. The production of EPS in the biocide layer was retarded approximately nine times

by the addition of the MEC (polysaccharide from 370.2 to 39.0 mg/m² membrane, protein from 503.4 to 56.9 mg/m² membrane).

It has been reported that SMP play an important role in membrane fouling and flux decline in the MBR²⁷⁰. A gel-like matrix of EPS is a main biofilm constituent²⁷¹ and, therefore, also closely associated with membrane biofouling^{12, 31, 39}. As results from both qualitative and quantitative analyses coincided well, it could be concluded that the reduction of SMP in mixed liquor and EPS in membrane-biocake is one of main reasons why the addition of the MEC alleviates membrane biofouling.

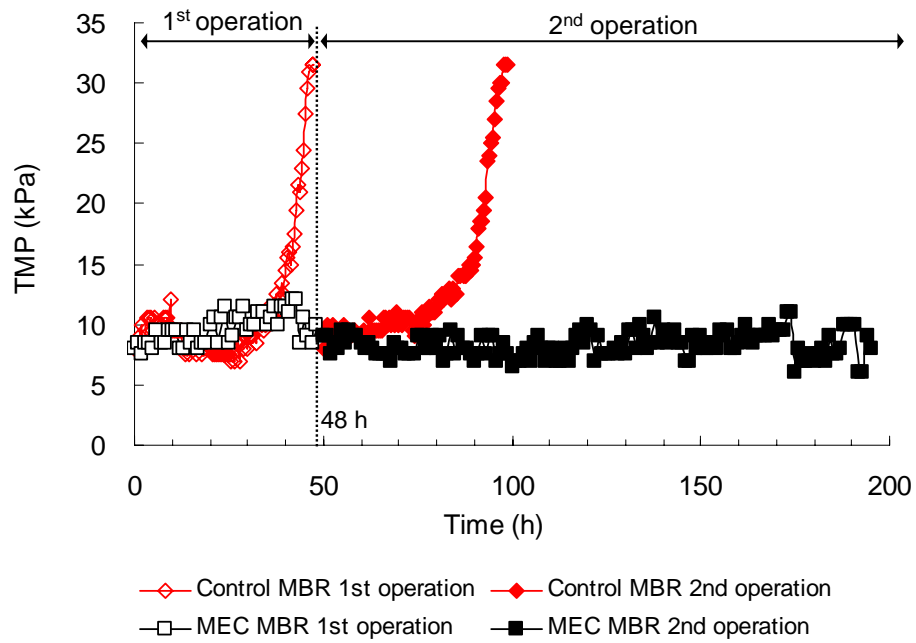
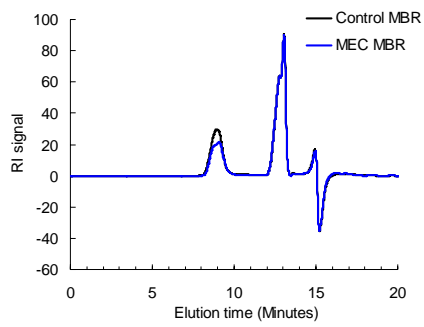
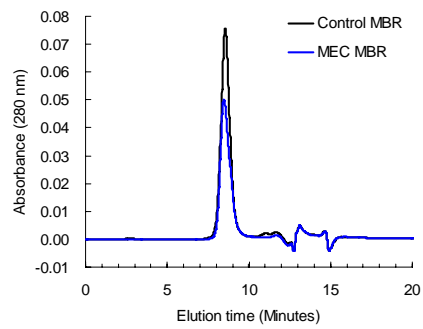


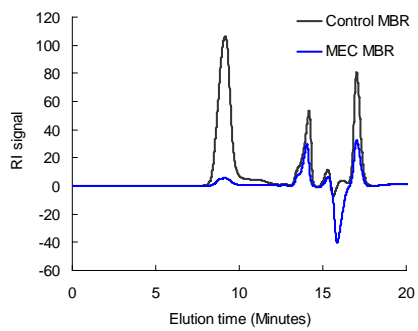
Figure 4.17. Comparison of TMP build-up between the control and the MEC MBR under continuous mode.



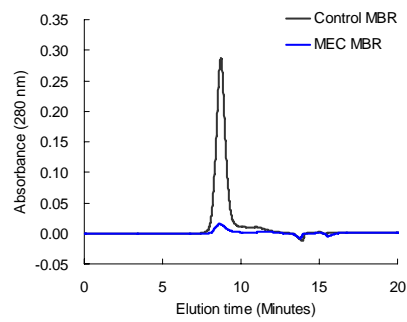
(a)



(b)

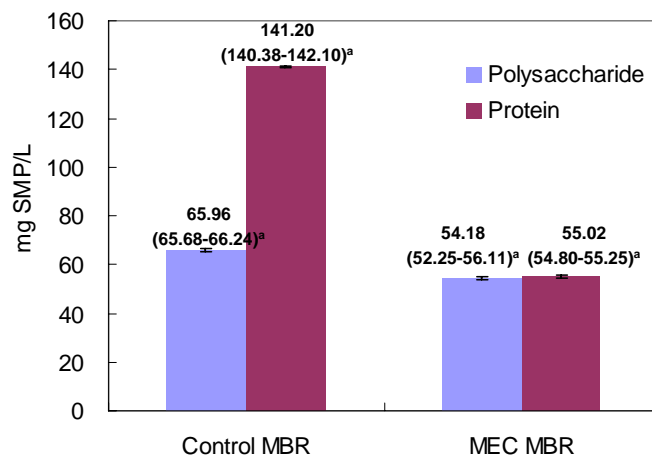


(c)

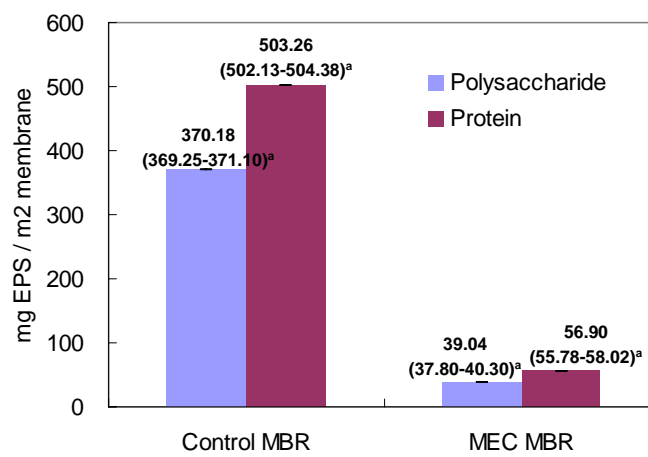


(d)

Figure 4.18. GFC spectrum of (a) SMP (RI), (b) SMP (280 nm), (c) EPS (RI) and (d) EPS (280 nm).



(a)



(b)

Figure 4.19. Quantitative analysis of (a) SMP in mixed liquor and (b) EPS in membrane-biocake (N=3).^a: 95% confidence interval.

4.4. Conclusions

The purpose of this chapter was to overcome the technical limitations of free enzyme such as short catalytic life time and difficulties in recovery by the magnetic enzyme carrier. Based on the results of this study, the following conclusions were made:

- MEC was constructed by the combination of MIEX resin, 1-bilayer LBL film of PSS/chitosan, and immobilization of acylase via GA treatment.
- The MEC showed no activity decrease under both continuous shaking for 14 days and 29 iterative cycles of reuse. Furthermore, the comparison of the MEC with free enzyme in a batch-type MBR showed that the MEC efficiently alleviated the membrane biofouling and showed a great advantage over free enzyme in terms of recycled use and stability in mixed liquor.
- When the MEC was applied to the lab scale MBR in a continuous operation, it also enhanced the membrane permeability to a large extent compared with a conventional MBR with no enzyme.

초 록

세균은 신호분자의 일종인 자기유도물질을 이용하여 주변 세포의 밀도를 인식하고 이를 바탕으로 특정 유전자를 발현하여 고체 표면에서의 생물막 형성과 같은 군집특성을 조절하는데 이를 정족수 감지라고 한다. 본 연구에서는 생물학적 고도 수처리 시스템인 막결합형 생물반응기에 상기의 정족수 감지 개념을 도입한 새로운 막오염 제어 기술을 개발하고자 하였다. 이를 위한 연구는 다음의 순서로 진행되었다.

- (1) 막결합형 생물반응기내에서 정족수 감지 활성 여부
- (2) 생물막오염과 정족수 감지 기작간의 관계
- (3) 자기유도물질 분해효소를 이용한 생물막오염 제어
- (4) 자기유도물질 분해효소가 고정화된 자성담체의 개발
- (5) 자기유도물질 분해효소가 고정화된 자성담체의 적용

Agrobacterium tumefaciens A136 bioassay 결과 그람 음성균의 자기유도물질인 아실화 호모세린 락톤 (*N*-acyl homoserine lactone)의 강한 활성이 분리막 표면에 형성된 biocake에서 검출되었다. 또한 박막크로마토그래피 분석을 통하여 biocake내에 최소 3종류의 아실화 호모세린 락톤이 존재하고, 그 중에 *N*-octanoyl-L-homoserine lactone이 가장 많음을 확인하였다.

막결합형 생물반응기의 각 운전지점에서 분리막 표면에 형성된 biocake 내에서 아실화 호모세린 락톤 계열의 자기유도물질을 검출한 결과 막간차압이 급격히 증가하기 시작하는 전이점을 전후로 정족수 감지 활성이 강하게 나타남을 확인하였다. 또한 분리막 표면에서 biocake의 성장에 따른 단위 미생물 질량당 자기유도물질의 농도 및 투과저항의 관계를 분석한 결과 biocake내에서 정족수 감지 활성의 유도와 분리막의 생물막오염 간에 밀접한 관계가 있음을 확인하였다.

세균의 정족수 감지는 자기유도물질을 분해하는 효소를 이용하여 제어할 수 있다. 자기유도물질 분해 활성을 가지는 다양한 효소들 중에서 아실화 호모세린 락톤의 acyl-amide 결합을 절단하는 효소인

acylase를 회분식 막결합형 생물반응기에 적용한 결과 acylase를 통한 세균의 정족수 인식 차단 및 이로 인한 분리막의 생물막오염 현상의 억제를 확인할 수 있었다.

최종적으로, 상기의 acylase를 연속운전식 막결합형 생물반응기에 적용하기 위하여 효소 고정화 자성담체를 개발하였다. 14일 간의 연속교반 및 29회의 반복사용 조건에서 효소 고정화 자성담체의 효소활성의 저하는 일어나지 않았다. 상기의 효소 고정화 담체와 용존 효소를 각각 회분식 막결합형 생물반응기에 적용한 결과 효소 고정화 담체는 용존 효소에 비해 자성 회수 및 재이용이 가능하고 미생물과 오염물질이 높은 농도로 존재하는 막결합형 생물반응기에서 보다 안정적으로 사용할 수 있음을 확인하였다. 최종적으로 효소 고정화 담체는 연속 운전식 막결합형 생물반응기에 성공적으로 적용되어 기존의 막결합형 생물반응기에 비하여 월등히 높은 성능 향상을 이끌어 내었다.

주요어: 막결합형 생물반응기, 막오염 제어, 정족수 감지,
효소 고정화 자성담체

학 번: 2003-30957

References

1. Hanft, S. *Membrane Bioreactors: Global Markets*; Business Communications Company, Inc.: 2008.
2. Hanft, S. *Membrane Bioreactors in the Changing World Water Market*; Business Communications Company, Inc. : 2006.
3. Phattaranawik, J.; Fane, A. G.; Pasquier, A. C. S.; Bing, W., Membrane bioreactor with bubble-size transformer: Design and fouling control. *AICHE Journal* **2007**, *53* (1), 243-248.
4. Hai, F. I.; Yamamoto, K.; Fukushi, K.; Nakajima, F., Fouling resistant compact hollow-fiber module with spacer for submerged membrane bioreactor treating high strength industrial wastewater. *Journal of Membrane Science* **2008**, *317* (1-2), 34-42.
5. Yeon, K. M.; Park, J. S.; Lee, C. H.; Kim, S. M., Membrane coupled high-performance compact reactor: A new MBR system for advanced wastewater treatment. *Water Research* **2005**, *39* (10), 1954-1961.
6. Tan, K. T.; Obendorf, S. K., Development of an antimicrobial microporous polyurethane membrane. *Journal of Membrane Science* **2007**, *289* (1-2), 199-209.
7. Yu, H. Y.; Xu, Z. K.; Lei, H.; Hu, M. X.; Yang, Q., Photoinduced graft polymerization of acrylamide on polypropylene microporous membranes for the improvement of antifouling characteristics in a submerged membrane-bioreactor. *Separation and Purification Technology* **2007**, *53* (1), 119-125.
8. Yoon, S. H.; Collins, J. H.; Musale, D.; Sundararajan, S.; Tsai, S. P.; Hallsby, G. A.; Kong, J. F.; Koppes, J.; Cachia, P., Effects of flux enhancing polymer on the characteristics of sludge in membrane bioreactor process. *Water*

- Science and Technology* **2005**, *51*, 151-157.
9. Lee, J. C.; Kim, J. S.; Kang, I. J.; Cho, M. H.; Park, P. K.; Lee, C. H., Potential and limitations of alum or zeolite addition to improve the performance of a submerged membrane bioreactor. *Water Science and Technology* **2001**, *43*, 59-66.
 10. Kim, J. S.; Lee, C. H., Effect of powdered activated carbon on the performance of an aerobic membrane bioreactor: Comparison between cross-flow and submerged membrane systems. *Water Environment Research* **2003**, *75* (4), 300-307.
 11. Lee, C. H.; Park, P. K.; Lee, W. N.; Hwang, B. K.; Hong, S. H.; Yeon, K. M.; Oh, H. S.; Chang, I. S., Correlation of biofouling with the bio-cake architecture in an MBR. *Desalination* **2008**, *231*, 115-123.
 12. Yun, M. A.; Yeon, K. M.; Park, J. S.; Lee, C. H.; Chun, J.; Lim, D. J., Characterization of biofilm structure and its effect on membrane permeability in MBR for dye wastewater treatment. *Water Research* **2006**, *40* (1), 45-52.
 13. Hong, S. H.; Lee, W. N.; Oh, H. S.; Yeon, K. M.; Hwang, B. K.; Lee, C. H.; Chang, I. S.; Lee, S., The effects of intermittent aeration on the characteristics of bio-cake layers in a membrane bioreactor. *Environmental Science & Technology* **2007**, *41* (17), 6270-6276.
 14. Eberhard, A.; Burlingame, A. L.; Eberhard, C.; Kenyon, G. L.; Neilson, K. H.; Oppenheimer, N. J., Structural identification of autoinducer of *Photobacterium fischeri* luciferase. *Biochemistry* **1981**, *20* (9), 2444-2449.
 15. Pierson, L. S.; Keppenne, V. D.; Wood, D. W., Phenazine antibiotic biosynthesis in *Pseudomonas aureofaciens* 30-84 is regulated by PhzR in response to cell density. *Journal of Bacteriology* **1994**, *176* (13), 3966-3974.

16. Vonbodman, S. B.; Farrand, S. K., Capsular polysaccharide biosynthesis and pathogenicity in *Erwinia stewartii* require induction by an N-acylhomoserine lactone autoinducer. *Journal of Bacteriology* **1995**, *177* (17), 5000-5008.
17. Davies, D. G.; Parsek, M. R.; Pearson, J. P.; Iglewski, B. H.; Costerton, J. W.; Greenberg, E. P., The involvement of cell-to-cell signals in the development of a bacterial biofilm. *Science* **1998**, *280* (5361), 295-298.
18. Hoch, J. A., Regulation of the phosphorelay and the initiation of sporulation in *Bacillus subtilis*. *Annual Review of Microbiology* **1993**, *47*, 441-465.
19. Baveja, J. K.; Wilcox, M. D. P.; Hume, E. B. H.; Kumar, N.; Odell, R.; Poole-Warren, L. A., Furanones as potential anti-bacterial coatings on biomaterials. *Biomaterials* **2004**, *25* (20), 5003-5012.
20. Dong, Y. H.; Wang, L. H.; Xu, J. L.; Zhang, H. B.; Zhang, X. F.; Zhang, L. H., Quenching quorum-sensing-dependent bacterial infection by an N-acyl homoserine lactonase. *Nature* **2001**, *411* (6839), 813-817.
21. Judd, S., The status of membrane bioreactor technology. *Trends in Biotechnology* **2008**, *26* (2), 109-116.
22. Meng, F. G.; Yang, F. L.; Shi, B. Q.; Zhang, H. M., A comprehensive study on membrane fouling in submerged membrane bioreactors operated under different aeration intensities. *Separation and Purification Technology* **2008**, *59* (1), 91-100.
23. Smith, B. M.; Deutschmann, A. A.; Goodboy, K. P. In situ cleaning system for fouled membranes US 005403479A, 1993.
24. Kim, J. Y.; Chang, I. S.; Shin, D. H.; Park, H. H., Membrane fouling control through the change of the depth of a membrane module in a

- submerged membrane bioreactor for advanced wastewater treatment. *Desalination* **2008**, *231*, 35-43.
25. Li, X. F.; Gao, F. S.; Hua, Z. Z.; Du, G. C.; Chen, J., Treatment of synthetic wastewater by a novel MBR with granular sludge developed for controlling membrane fouling. *Separation and Purification Technology* **2005**, *46* (1-2), 19-25.
26. Futamura, O.; Katoh, M.; Takeuchi, K., Organic waste water treatment by activated sludge process using integrated type membrane separation *Desalination* **1994**, *98*, 17-25.
27. Sainbayar, A.; Kim, J. S.; Jung, W. J.; Lee, Y. S.; Lee, C. H., Application of surface modified polypropylene membranes to an anaerobic membrane bioreactor. *Environmental Technology* **2001**, *22* (9), 1035-1042.
28. Asymmetric ultrafiltration and microfiltration membranes containing chitosan molecules and the method for preparation thereof 2006.
29. Wu, J. L.; Chen, F. T.; Huang, X.; Geng, W. Y.; Wen, X. H., Using inorganic coagulants to control membrane fouling in a submerged membrane bioreactor. *Desalination* **2006**, *197* (1-3), 124-136.
30. Akram, A.; Stuckey, D. C., Flux and performance improvement in a submerged anaerobic membrane bioreactor (SAMBR) using powdered activated carbon (PAC). *Process Biochemistry* **2008**, *43* (1), 93-102.
31. Chang, I. S.; Lee, C. H., Membrane filtration characteristics in membrane-coupled activated sludge system - the effect of physiological states of activated sludge on membrane fouling. *Desalination* **1998**, *120* (3), 221-233.
32. Nagaoka, H.; Yamanishi, S.; Miya, A., Modeling of biofouling by extracellular polymers in a membrane separation activated sludge system.

- Water Science and Technology* **1998**, 63 (7), 497-504.
33. Collins, J. H.; Yoon, S. H.; Musale, D.; Kong, J. F.; Koppes, J.; Sundararajan, S.; Tsai, S. P.; Hallsby, G. A.; Cachia, P.; Kronoveter, K., Membrane performance enhancer evaluations on pilot- and full-scale membrane bioreactors. *Water and Environment Journal* **2006**, 20 (1), 43-47.
 34. Koseoglu, H.; Yigit, N. O.; Iversen, V.; Drews, A.; Kitis, M.; Lesjean, B.; Kraume, M., Effects of several different flux enhancing chemicals on filterability and fouling reduction of membrane bioreactor (MBR) mixed liquors. *Journal of Membrane Science* **2008**, 320 (1-2), 57-64.
 35. Ying, Z.; Ping, G., Effect of powdered activated carbon dosage on retarding membrane fouling in MBR. *Separation and Purification Technology* **2006**, 52 (1), 154-160.
 36. Costerton, J. W.; Lewandowski, Z.; Caldwell, D. E.; Korber, D. R.; Lappinscott, H. M., Microbial biofilms. *Annual Review of Microbiology* **1995**, 49, 711-745.
 37. Stewart, P. S.; Franklin, M. J., Physiological heterogeneity in biofilms. *Nature Reviews Microbiology* **2008**, 6 (3), 199-210.
 38. Park, J. S.; Lee, C. H., Removal of soluble COD by a biofilm formed on a membrane in a jet loop type membrane bioreactor. *Water Research* **2005**, 39 (19), 4609-4622.
 39. Kim, H. Y.; Yeon, K. M.; Lee, C. H.; Lee, S.; Swaminathan, T., Biofilm structure and extracellular polymeric substances in low and high dissolved oxygen membrane bioreactors. *Separation Science and Technology* **2006**, 41 (7), 1213-1230.
 40. Hwang, B. K.; Lee, W. N.; Park, P. K.; Lee, C. H.; Chang, I. S., Effect of membrane fouling reducer on cake structure and membrane permeability in

- membrane bioreactor. *Journal of Membrane Science* **2007**, 288 (1-2), 149-156.
41. Lee, W.-N.; Cheong, W.-S.; Yeon, K.-M.; Hwang, B.-K.; Lee, C.-H., Correlation between local TMP distribution and bio-cake porosity on the membrane in a submerged MBR. *Journal of Membrane Science* **2009**, 332 (1-2), 50-55.
42. Fuqua, C.; Greenberg, E. P., Listening in on bacteria: Acyl-homoserine lactone signalling. *Nature Reviews Molecular Cell Biology* **2002**, 3 (9), 685-695.
43. Miller, M. B.; Bassler, B. L., Quorum sensing in bacteria. *Annual Review of Microbiology* **2001**, 55, 165-199.
44. Swift, S.; Karlyshev, A. V.; Fish, L.; Durant, E. L.; Winson, M. K.; Chhabra, S. R.; Williams, P.; MacIntyre, S.; Stewart, G., Quorum sensing in *Aeromonas hydrophila* and *Aeromonas salmonicida*: Identification of the LuxRI homologs AhyRI and AsaRI and their cognate *N*-acylhomoserine lactone signal molecules. *Journal of Bacteriology* **1997**, 179 (17), 5271-5281.
45. Swift, S.; Lynch, M. J.; Fish, L.; Kirke, D. F.; Tomas, J. M.; Stewart, G.; Williams, P., Quorum sensing-dependent regulation and blockade of exoprotease production in *Aeromonas hydrophila*. *Infection and Immunity* **1999**, 67 (10), 5192-5199.
46. Piper, K. R.; Vonbodman, S. B.; Farrand, S. K., Conjugation factor of *Agrobacterium tumefaciens* regulates Ti plasmid transfer by autoinduction. *Nature* **1993**, 362 (6419), 448-450.
47. Lewenza, S.; Conway, B.; Greenberg, E. P.; Sokol, P. A., Quorum sensing in *Burkholderia cepacia*: Identification of the LuxRI homologs CepRI.

- Journal of Bacteriology* **1999**, *181* (3), 748-756.
48. McClean, K. H.; Winson, M. K.; Fish, L.; Taylor, A.; Chhabra, S. R.; Camara, M.; Daykin, M.; Lamb, J. H.; Swift, S.; Bycroft, B. W.; Stewart, G.; Williams, P., Quorum sensing and *Chromobacterium violaceum*: exploitation of violacein production and inhibition for the detection of *N*-acylhomoserine lactones. *Microbiology-Sgm* **1997**, *143*, 3703-3711.
49. Swift, S.; Winson, M. K.; Chan, P. F.; Bainton, N. J.; Birdsall, M.; Reeves, P. J.; Rees, C. E. D.; Chhabra, S. R.; Hill, P. J.; Throup, J. P.; Bycroft, B. W.; Salmond, G. P. C.; Williams, P.; Stewart, G., A novel strategy for the isolation of luxI homologues: evidence for the widespread distribution of a LuxR:LuxI superfamily in enteric bacteria. *Molecular Microbiology* **1993**, *10* (3), 511-520.
50. Pirhonen, M.; Flego, D.; Heikinheimo, R.; Palva, E. T., A small diffusible signal molecule is responsible for the global control of virulence and exoenzyme production in the plant pathogen *Erwinia carotovora*. *EMBO Journal* **1993**, *12* (6), 2467-2476.
51. Bainton, N. J.; Stead, P.; Chhabra, S. R.; Bycroft, B. W.; Salmond, G. P. C.; Stewart, G.; Williams, P., *N*-(3-oxohexanoyl)-L-homoserine lactone regulates carbapenem antibiotic production in *Erwinia carotovora*. *Biochemical Journal* **1992**, *288*, 997-1004.
52. Reverchon, S.; Bouillant, M. L.; Salmond, G.; Nasser, W., Integration of the quorum-sensing system in the regulatory networks controlling virulence factor synthesis in *Erwinia chrysanthemi*. *Molecular Microbiology* **1998**, *29* (6), 1407-1418.
53. Wood, D. W.; Gong, F. C.; Daykin, M. M.; Williams, P.; Pierson, L. S., *N*-acyl-homoserine lactone-mediated regulation of phenazine gene expression

- by *Pseudomonas aureofaciens* 30-84 in the wheat rhizosphere. *Journal of Bacteriology* **1997**, *179* (24), 7663-7670.
54. Pearson, J. P.; Gray, K. M.; Passador, L.; Tucker, K. D.; Eberhard, A.; Iglewski, B. H.; Greenberg, E. P., Structure of the autoinducer required for expression of *Pseudomonas aeruginosa* virulence genes. *Proceedings of the National Academy of Sciences of the United States of America* **1994**, *91* (1), 197-201.
55. Pearson, J. P.; Passador, L.; Iglewski, B. H.; Greenberg, E. P., A second *N*-acylhomoserine lactone signal produced by *Pseudomonas aeruginosa*. *Proceedings of the National Academy of Sciences of the United States of America* **1995**, *92* (5), 1490-1494.
56. Flavier, A. B.; GanovaRaeva, L. M.; Schell, M. A.; Denny, T. P., Hierarchical autoinduction in *Ralstonia solanacearum*: Control of acyl-homoserine lactone production by a novel autoregulatory system responsive to 3-hydroxypalmitic acid methyl ester. *Journal of Bacteriology* **1997**, *179* (22), 7089-7097.
57. Rosemeyer, V.; Michiels, J.; Verreth, C.; Vanderleyden, J., luxI- and luxR-homologous genes of *Rhizobium etli* CNPAF512 contribute to synthesis of autoinducer molecules and nodulation of *Phaseolus vulgaris*. *Journal of Bacteriology* **1998**, *180* (4), 815-821.
58. Rodelas, B.; Lithgow, J. K.; Wisniewski-Dye, F.; Hardman, A.; Wilkinson, A.; Economou, A.; Williams, P.; Downie, J. A., Analysis of quorum-sensing-dependent control of rhizosphere-expressed (*rhi*) genes in *Rhizobium leguminosarum* *bv. viciae*. *Journal of Bacteriology* **1999**, *181* (12), 3816-3823.
59. Lithgow, J. K.; Wilkinson, A.; Hardman, A.; Rodelas, B.; Wisniewski-Dye,

- F.; Williams, P.; Downie, J. A., The regulatory locus *cinRI* in *Rhizobium leguminosarum* controls a network of quorum-sensing loci. *Molecular Microbiology* **2000**, *37* (1), 81-97.
60. Puskas, A.; Greenberg, E. P.; Kaplan, S.; Schaeffer, A. L., A quorum-sensing system in the free-living photosynthetic bacterium *Rhodobacter sphaeroides*. *Journal of Bacteriology* **1997**, *179* (23), 7530-7537.
61. Givskov, M.; Eberl, L.; Molin, S., Control of exoenzyme production, motility and cell differentiation in *Serratia liquefaciens*. *FEMS Microbiology Letters* **1997**, *148* (2), 115-122.
62. Milton, D. L.; Hardman, A.; Camara, M.; Chhabra, S. R.; Bycroft, B. W.; Stewart, G.; Williams, P., Quorum sensing in *Vibrio anguillarum*: Characterization of the *vanI/vanR* locus and identification of the autoinducer N-(3-oxodecanoyl)-L-homoserine lactone. *Journal of Bacteriology* **1997**, *179* (9), 3004-3012.
63. Throup, J. P.; Camara, M.; Briggs, G. S.; Winson, M. K.; Chhabra, S. R.; Bycroft, B. W.; Williams, P.; Stewart, G., Characterisation of the *yenI/yenR* locus from *Yersinia enterocolitica* mediating the synthesis of two N-acylhomoserine lactone signal molecules. *Molecular Microbiology* **1995**, *17* (2), 345-356.
64. Atkinson, S.; Throup, J. P.; Stewart, G.; Williams, P., A hierarchical quorum-sensing system in *Yersinia pseudotuberculosis* is involved in the regulation of motility and clumping. *Molecular Microbiology* **1999**, *33* (6), 1267-1277.
65. Nealson, K. H.; Hastings, J. W., Bacterial bioluminescence: its control and ecological significance. *Microbiological Reviews* **1979**, *43* (4), 496-518.
66. Engebrecht, J.; Nealson, K.; Silverman, M., Bacterial bioluminescence:

- Isolation and genetic analysis of functions from *Vibrio fischeri*. *Cell* **1983**, 32 (3), 773-781.
67. Passador, L.; Cook, J. M.; Gambello, M. J.; Rust, L.; Iglewski, B. H., Expression of *Pseudomonas aeruginosa* virulence genes requires cell-to-cell communication. *Science* **1993**, 260 (5111), 1127-1130.
68. Brint, J. M.; Ohman, D. E., Synthesis of multiple exoproducts in *Pseudomonas aeruginosa* is under the control of RhlR-RhII, another set of regulators in strain PAO1 with homology to the autoinducer-responsive LuxR-LuxI family. *Journal of Bacteriology* **1995**, 177 (24), 7155-7163.
69. de Kievit, T. R.; Iglewski, B. H., Bacterial quorum sensing in pathogenic relationships. *Infection and Immunity* **2000**, 68 (9), 4839-4849.
70. Jones, S.; Yu, B.; Bainton, N. J.; Birdsall, M.; Bycroft, B. W.; Chhabra, S. R.; Cox, A. J. R.; Golby, P.; Reeves, P. J.; Stephens, S.; Winson, M. K.; Salmond, G. P. C.; Stewart, G.; Williams, P., The lux autoinducer regulates the production of exoenzyme virulence determinants in *Erwinia carotovora* and *Pseudomonas aeruginosa*. *EMBO Journal* **1993**, 12 (6), 2477-2482.
71. Seed, P. C.; Passador, L.; Iglewski, B. H., Activation of the *Pseudomonas aeruginosa lasI* gene by LasR and the *Pseudomonas autoinducer* PAI: an autoinduction regulatory hierarchy. *Journal of Bacteriology* **1995**, 177 (3), 654-659.
72. Pesci, E. C.; Pearson, J. P.; Seed, P. C.; Iglewski, B. H., Regulation of *las* and *rhl* quorum sensing in *Pseudomonas aeruginosa*. *Journal of Bacteriology* **1997**, 179 (10), 3127-3132.
73. Parsek, M. R.; Greenberg, E. P., Acyl-homoserine lactone quorum sensing in Gram-negative bacteria: A signaling mechanism involved in associations with higher organisms. *Proceedings of the National Academy of Sciences of*

- the United States of America* **2000**, 97 (16), 8789-8793.
74. Christie, P. J., *Agrobacterium tumefaciens* T-complex transport apparatus: A paradigm for a new family of multifunctional transporters in eubacteria. *Journal of Bacteriology* **1997**, 179 (10), 3085-3094.
75. Sheng, J. S.; Citovsky, V., *Agrobacterium* plant cell DNA transport: Have virulence proteins, will travel. *Plant Cell* **1996**, 8 (10), 1699-1710.
76. Fuqua, W. C.; Winans, S. C., A LuxR-LuxI type regulatory system activates *Agrobacterium* Ti plasmid conjugal transfer in the presence of a plant tumor metabolite. *Journal of Bacteriology* **1994**, 176 (10), 2796-2806.
77. Zhang, L. H.; Murphy, P. J.; Kerr, A.; Tate, M. E., *Agrobacterium* conjugation and gene-regulation by *N*-acyl-L-homoserine lactones. *Nature* **1993**, 362 (6419), 446-448.
78. Magnuson, R.; Solomon, J.; Grossman, A. D., Biochemical and genetic characterization of a competence pheromone from *Bacillus subtilis*. *Cell* **1994**, 77 (2), 207-216.
79. Solomon, J. M.; Magnuson, R.; Srivastava, A.; Grossman, A. D., Convergent sensing pathways mediate response to two extracellular competence factors in *Bacillus subtilis*. *Genes & Development* **1995**, 9 (5), 547-558.
80. Solomon, J. M.; Lazazzera, B. A.; Grossman, A. D., Purification and characterization of an extracellular peptide factor that affects two different developmental pathways in *Bacillus subtilis*. *Genes & Development* **1996**, 10 (16), 2014-2024.
81. Janson, L.; Arvidson, S., The role of the delta-lysin gene (*hld*) in the regulation of virulence genes by the accessory gene regulator (*agr*) in *Staphylococcus aureus*. *EMBO Journal* **1990**, 9 (5), 1391-1399.

82. Morfeldt, E.; Taylor, D.; Vongabain, A.; Arvidson, S., Activation of alpha-toxin translation in *Staphylococcus aureus* by the trans-encoded antisense RNA, RNAIII. *EMBO Journal* **1995**, *14* (18), 4569-4577.
83. Ji, G. Y.; Beavis, R. C.; Novick, R. P., Cell density control of staphylococcal virulence mediated by an octapeptide pheromone. *Proceedings of the National Academy of Sciences of the United States of America* **1995**, *92* (26), 12055-12059.
84. Ji, G. Y.; Beavis, R.; Novick, R. P., Bacterial interference caused by autoinducing peptide variants. *Science* **1997**, *276* (5321), 2027-2030.
85. Mayville, P.; Ji, G. Y.; Beavis, R.; Yang, H. M.; Goger, M.; Novick, R. P.; Muir, T. W., Structure-activity analysis of synthetic autoinducing thiolactone peptides from *Staphylococcus aureus* responsible for virulence. *Proceedings of the National Academy of Sciences of the United States of America* **1999**, *96* (4), 1218-1223.
86. Otto, M.; Sussmuth, R.; Vuong, C.; Jung, G.; Gotz, F., Inhibition of virulence factor expression in *Staphylococcus aureus* by the *Staphylococcus epidermidis agr* pheromone and derivatives. *FEBS Letters* **1999**, *450* (3), 257-262.
87. Schauder, S.; Shokat, K.; Surette, M. G.; Bassler, B. L., The LuxS family of bacterial autoinducers: biosynthesis of a novel quorum-sensing signal molecule. *Molecular Microbiology* **2001**, *41* (2), 463-476.
88. Schauder, S.; Bassler, B. L., The languages of bacteria. *Genes & Development* **2001**, *15* (12), 1468-1480.
89. Chen, X.; Schauder, S.; Potier, N.; Van Dorsselaer, A.; Pelczer, I.; Bassler, B. L.; Hughson, F. M., Structural identification of a bacterial quorum-sensing signal containing boron. *Nature* **2002**, *415* (6871), 545-549.

90. Winzer, K.; Hardie, K. R.; Burgess, N.; Doherty, N.; Kirke, D.; Holden, M. T. G.; Linforth, R.; Cornell, K. A.; Taylor, A. J.; Hill, P. J.; Williams, P., LuxS: its role in central metabolism and the in vitro synthesis of 4-hydroxy-5-methyl-3(2H)-furanone. *Microbiology-Sgm* **2002**, *148*, 909-922.
91. Bassler, B. L.; Wright, M.; Showalter, R. E.; Silverman, M. R., Intercellular signalling in *Vibrio harveyi*: sequence and function of genes regulating expression of luminescence. *Molecular Microbiology* **1993**, *9* (4), 773-786.
92. Bassler, B. L.; Wright, M.; Silverman, M. R., Multiple signalling systems controlling expression of luminescence in *Vibrio harveyi*: sequence and function of genes encoding a second sensory pathway. *Molecular Microbiology* **1994**, *13* (2), 273-286.
93. Miller, M. B.; Skorupski, K.; Lenz, D. H.; Taylor, R. K.; Bassler, B. L., Parallel quorum sensing systems converge to regulate virulence in *Vibrio cholerae*. *Cell* **2002**, *110* (3), 303-314.
94. Ohtani, K.; Hayashi, H.; Shimizu, T., The *luxS* gene is involved in cell-cell signalling for toxin production in *Clostridium perfringens*. *Molecular Microbiology* **2002**, *44* (1), 171-179.
95. Stevenson, B.; Babb, K., LuxS-mediated quorum sensing in *Borrelia burgdorferi*, the Lyme disease spirochete. *Infection and Immunity* **2002**, *70* (8), 4099-4105.
96. Derzelle, S.; Duchaud, E.; Kunst, F.; Danchin, A.; Bertin, P., Identification, characterization, and regulation of a cluster of genes involved in carbapenem biosynthesis in *Photobacterium luminescens*. *Applied and Environmental Microbiology* **2002**, *68* (8), 3780-3789.
97. Surette, M. G.; Bassler, B. L., Regulation of autoinducer production in

- Salmonella typhimurium*. *Molecular Microbiology* **1999**, 31 (2), 585-595.
98. DeLisa, M. P.; Valdes, J. J.; Bentley, W. E., Mapping stress-induced changes in autoinducer AI-2 production in chemostat-cultivated *Escherichia coli* K-12. *Journal of Bacteriology* **2001**, 183 (9), 2918-2928.
99. Beeston, A. L.; Surette, M. G., pfs-dependent regulation of autoinducer 2 production in *Salmonella enterica* serovar *Typhimurium*. *Journal of Bacteriology* **2002**, 184 (13), 3450-3456.
100. Taga, M. E.; Semmelhack, J. L.; Bassler, B. L., The LuxS-dependent autoinducer AI-2 controls the expression of an ABC transporter that functions in AI-2 uptake in *Salmonella typhimurium*. *Molecular Microbiology* **2001**, 42 (3), 777-793.
101. Vendeville, A.; Winzer, K.; Heurlier, K.; Tang, C. M.; Hardie, K. R., Making 'sense' of metabolism: Autoinducer-2, LuxS and pathogenic bacteria. *Nature Reviews Microbiology* **2005**, 3 (5), 383-396.
102. Fong, K. P.; Chung, W. S. O.; Lamont, R. J.; Demuth, D. R., Intra- and interspecies regulation of gene expression by *Actinobacillus actinomycetemcomitans* LuxS. *Infection and Immunity* **2001**, 69 (12), 7625-7634.
103. DeLisa, M. P.; Wu, C. F.; Wang, L.; Valdes, J. J.; Bentley, W. E., DNA microarray-based identification of genes controlled by autoinducer 2-stimulated quorum sensing in *Escherichia coli*. *Journal of Bacteriology* **2001**, 183 (18), 5239-5247.
104. Sperandio, V.; Mellies, J. L.; Nguyen, W.; Shin, S.; Kaper, J. B., Quorum sensing controls expression of the type III secretion gene transcription and protein secretion in enterohemorrhagic and enteropathogenic *Escherichia coli*. *Proceedings of the National Academy of Sciences of the United States*

- of America* **1999**, 96 (26), 15196-15201.
105. Sperandio, V.; Torres, A. G.; Kaper, J. B., Quorum sensing *Escherichia coli* regulators B and C (QseBC): a novel two-component regulatory system involved in the regulation of flagella and motility by quorum sensing in *E.coli*. *Molecular Microbiology* **2002**, 43 (3), 809-821.
106. Sperandio, V.; Li, C. Y. C.; Kaper, J. B., Quorum-sensing *Escherichia coli* regulator A: A regulator of the LysR family involved in the regulation of the locus of enterocyte effacement pathogenicity island in enterohemorrhagic *E.coli*. *Infection and Immunity* **2002**, 70 (6), 3085-3093.
107. Giron, J. A.; Torres, A. G.; Freer, E.; Kaper, J. B., The flagella of enteropathogenic *Escherichia coli* mediate adherence to epithelial cells. *Molecular Microbiology* **2002**, 44 (2), 361-379.
108. Winzer, K.; Sun, Y. H.; Green, A.; Delory, M.; Blackley, D.; Hardie, K. R.; Baldwin, T. J.; Tang, C. M., Role of *Neisseria meningitidis* luxS in cell-to-cell signaling and bacteremic infection. *Infection and Immunity* **2002**, 70 (4), 2245-2248.
109. Chung, W. S. O.; Park, Y.; Lamont, R. J.; McNab, R.; Barbieri, B.; Demuth, D. R., Signaling system in *Porphyromonas gingivalis* based on a LuxS protein. *Journal of Bacteriology* **2001**, 183 (13), 3903-3909.
110. Burgess, N. A.; Kirke, D. F.; Williams, P.; Winzer, K.; Hardie, K. R.; Meyers, N. L.; Aduse-Opoku, J.; Curtis, M. A.; Camara, M., LuxS-dependent quorum sensing in *Porphyromonas gingivalis* modulates protease and haemagglutinin activities but is not essential for virulence. *Microbiology-Sgm* **2002**, 148, 763-772.
111. Prouty, A. M.; Schwesinger, W. H.; Gunn, J. S., Biofilm formation and interaction with the surfaces of gallstones by *Salmonella spp.* *Infection and*

- Immunity* **2002**, 70 (5), 2640-2649.
112. Day, W. A.; Maurelli, A. T., *Shigella flexneri* LuxS quorum-sensing system modulates *virB* expression but is not essential for virulence. *Infection and Immunity* **2001**, 69 (1), 15-23.
113. Lyon, W. R.; Madden, J. C.; Levin, J. C.; Stein, J. L.; Caparon, M. G., Mutation of *luxS* affects growth and virulence factor expression in *Streptococcus pyogenes*. *Molecular Microbiology* **2001**, 42 (1), 145-157.
114. Zhu, J.; Miller, M. B.; Vance, R. E.; Dziejman, M.; Bassler, B. L.; Mekalanos, J. J., Quorum-sensing regulators control virulence gene expression in *Vibrio cholerae*. *Proceedings of the National Academy of Sciences of the United States of America* **2002**, 99 (5), 3129-3134.
115. Lilley, B. N.; Bassler, B. L., Regulation of quorum sensing in *Vibrio harveyi* by LuxO and Sigma-54. *Molecular Microbiology* **2000**, 36 (4), 940-954.
116. Mashburn, L. M.; Whiteley, M., Membrane vesicles traffic signals and facilitate group activities in a prokaryote. *Nature* **2005**, 437 (7057), 422-425.
117. Walters, M.; Sperandio, V., Autoinducer 3 and epinephrine signaling in the kinetics of locus of enterocyte effacement gene expression in enterohemorrhagic *Escherichia coli*. *Infection and Immunity* **2006**, 74 (10), 5445-5455.
118. Pesci, E. C.; Milbank, J. B. J.; Pearson, J. P.; McKnight, S.; Kende, A. S.; Greenberg, E. P.; Iglewski, B. H., Quinolone signaling in the cell-to-cell communication system of *Pseudomonas aeruginosa*. *Proceedings of the National Academy of Sciences of the United States of America* **1999**, 96 (20), 11229-11234.

119. Bakker, D. P.; Postmus, B. R.; Busscher, H. J.; van der Mei, H. C., Bacterial strains isolated from different niches can exhibit different patterns of adhesion to substrata. *Applied and Environmental Microbiology* **2004**, *70* (6), 3758-3760.
120. Yarwood, J. M.; Schlievert, P. M., Quorum sensing in *Staphylococcus* infections. *Journal of Clinical Investigation* **2003**, *112* (11), 1620-1625.
121. Beenken, K. E.; Blevins, J. S.; Smeltzer, M. S., Mutation of *sarA* in *Staphylococcus aureus* limits biofilm formation. *Infection and Immunity* **2003**, *71* (7), 4206-4211.
122. Vuong, C.; Saenz, H. L.; Gotz, F.; Otto, M., Impact of the *agr* quorum-sensing system on adherence to polystyrene in *Staphylococcus aureus*. *Journal of Infectious Diseases* **2000**, *182* (6), 1688-1693.
123. Pratten, J.; Foster, S. J.; Chan, P. F.; Wilson, M.; Nair, S. P., *Staphylococcus aureus* accessory regulators: expression within biofilms and effect on adhesion. *Microbes and Infection* **2001**, *3* (8), 633-637.
124. Cole, S. P.; Harwood, J.; Lee, R.; She, R.; Guiney, D. G., Characterization of monospecies biofilm formation by *Helicobacter pylori*. *Journal of Bacteriology* **2004**, *186* (10), 3124-3132.
125. Klausen, M.; Aaes-Jorgensen, A.; Molin, S.; Tolker-Nielsen, T., Involvement of bacterial migration in the development of complex multicellular structures in *Pseudomonas aeruginosa* biofilms. *Molecular Microbiology* **2003**, *50* (1), 61-68.
126. Hentzer, M.; Teitzel, G. M.; Balzer, G. J.; Heydorn, A.; Molin, S.; Givskov, M.; Parsek, M. R., Alginate overproduction affects *Pseudomonas aeruginosa* biofilm structure and function. *Journal of Bacteriology* **2001**, *183* (18), 5395-5401.

127. Davey, M. E.; Caiazza, N. C.; O'Toole, G. A., Rhamnolipid surfactant production affects biofilm architecture in *Pseudomonas aeruginosa* PAO1. *Journal of Bacteriology* **2003**, *185* (3), 1027-1036.
128. Labbate, M.; Queek, S. Y.; Koh, K. S.; Rice, S. A.; Givskov, M.; Kjelleberg, S., Quorum sensing-controlled biofilm development in *Serratia liquefaciens* MG1. *Journal of Bacteriology* **2004**, *186* (3), 692-698.
129. Eberl, L.; Winson, M. K.; Sternberg, C.; Stewart, G.; Christiansen, G.; Chhabra, S. R.; Bycroft, B.; Williams, P.; Molin, S.; Givskov, M., Involvement of *N*-acyl-L-homoserine lactone autoinducers in controlling the multicellular behaviour of *Serratia liquefaciens*. *Molecular Microbiology* **1996**, *20* (1), 127-136.
130. Huber, B.; Riedel, K.; Hentzer, M.; Heydorn, A.; Gotschlich, A.; Givskov, M.; Molin, S.; Eberl, L., The *cep* quorum-sensing system of *Burkholderia cepacia* H111 controls biofilm formation and swarming motility. *Microbiology-Sgm* **2001**, *147*, 2517-2528.
131. Lynch, M. J.; Swift, S.; Kirke, D. F.; Keevil, C. W.; Dodd, C. E. R.; Williams, P., The regulation of biofilm development by quorum sensing in *Aeromonas hydrophila*. *Environmental Microbiology* **2002**, *4* (1), 18-28.
132. Wen, Z. T.; Burne, R. A., LuxS-mediated signaling in *Streptococcus mutans* is involved in regulation of acid and oxidative stress tolerance and biofilm formation. *Journal of Bacteriology* **2004**, *186* (9), 2682-2691.
133. Hall-Stoodley, L.; Costerton, J. W.; Stoodley, P., Bacterial biofilms: From the natural environment to infectious diseases. *Nature Reviews Microbiology* **2004**, *2* (2), 95-108.
134. Parsek, M. R.; Fuqua, C., Biofilms 2003: Emerging themes and challenges in studies of surface-associated microbial life. *Journal of*

- Bacteriology* **2004**, *186* (14), 4427-4440.
135. Dow, J. M.; Crossman, L.; Findlay, K.; He, Y. Q.; Feng, J. X.; Tang, J. L., Biofilm dispersal in *Xanthomonas campestris* is controlled by cell-cell signaling and is required for full virulence to plants. *Proceedings of the National Academy of Sciences of the United States of America* **2003**, *100* (19), 10995-11000.
136. Barber, C. E.; Tang, J. L.; Feng, J. X.; Pan, M. Q.; Wilson, T. J. G.; Slater, H.; Dow, J. M.; Williams, P.; Daniels, M. J., A novel regulatory system required for pathogenicity of *Xanthomonas campestris* is mediated by a small diffusible signal molecule. *Molecular Microbiology* **1997**, *24* (3), 555-566.
137. Crossman, L.; Dow, J. M., Biofilm formation and dispersal in *Xanthomonas campestris*. *Microbes and Infection* **2004**, *6* (6), 623-629.
138. Vance, R. E.; Zhu, J.; Mekalanos, J. J., A constitutively active variant of the quorum-sensing regulator LuxO affects protease production and biofilm formation in *Vibrio cholerae*. *Infection and Immunity* **2003**, *71* (5), 2571-2576.
139. Zhu, J.; Mekalanos, J. J., Quorum sensing-dependent biofilms enhance colonization in *Vibrio cholerae*. *Developmental Cell* **2003**, *5* (4), 647-656.
140. Yildiz, F. H.; Liu, X. S.; Heydorn, A.; Schoolnik, G. K., Molecular analysis of rugosity in a *Vibrio cholerae* O1 El Tor phase variant. *Molecular Microbiology* **2004**, *53* (2), 497-515.
141. Heydorn, A.; Ersboll, B.; Kato, J.; Hentzer, M.; Parsek, M. R.; Tolker-Nielsen, T.; Givskov, M.; Molin, S., Statistical analysis of *Pseudomonas aeruginosa* biofilm development: Impact of mutations in genes involved in twitching motility, cell-to-cell signaling, and stationary-phase sigma factor

- expression. *Applied and Environmental Microbiology* **2002**, 68 (4), 2008-2017.
142. Parsek, M. R.; Val, D. L.; Hanzelka, B. L.; Cronan, J. E.; Greenberg, E. P., Acyl homoserine-lactone quorum-sensing signal generation. *Proceedings of the National Academy of Sciences of the United States of America* **1999**, 96 (8), 4360-4365.
143. Rudrappa, T.; Bais, H. P., Curcumin, a known phenolic from curcuma longa, attenuates the virulence of *Pseudomonas aeruginosa* PAO1 in whole plant and animal pathogenicity models. *Journal of Agricultural and Food Chemistry* **2008**, 56 (6), 1955-1962.
144. Rasmussen, T. B.; Bjarnsholt, T.; Skindersoe, M. E.; Hentzer, M.; Kristoffersen, P.; Kote, M.; Nielsen, J.; Eberl, L.; Givskov, M., Screening for quorum-sensing inhibitors (QSI) by use of a novel genetic system, the QSI selector. *Journal of Bacteriology* **2005**, 187 (5), 1799-1814.
145. Holden, M. T. G.; Chhabra, S. R.; de Nys, R.; Stead, P.; Bainton, N. J.; Hill, P. J.; Manefield, M.; Kumar, N.; Labatte, M.; England, D.; Rice, S.; Givskov, M.; Salmond, G. P. C.; Stewart, G.; Bycroft, B. W.; Kjelleberg, S. A.; Williams, P., Quorum-sensing cross talk: isolation and chemical characterization of cyclic dipeptides from *Pseudomonas aeruginosa* and other Gram-negative bacteria. *Molecular Microbiology* **1999**, 33 (6), 1254-1266.
146. Prasad, C., Bioactive cyclic dipeptides. *Peptides* **1995**, 16 (1), 151-164.
147. Teplitski, M.; Robinson, J. B.; Bauer, W. D., Plants secrete substances that mimic bacterial *N*-acyl homoserine lactone signal activities and affect population density-dependent behaviors in associated bacteria. *Molecular Plant-Microbe Interactions* **2000**, 13 (6), 637-648.

148. Mathesius, U.; Mulders, S.; Gao, M. S.; Teplitski, M.; Caetano-Anolles, G.; Rolfe, B. G.; Bauer, W. D., Extensive and specific responses of a eukaryote to bacterial quorum-sensing signals. *Proceedings of the National Academy of Sciences of the United States of America* **2003**, *100* (3), 1444-1449.
149. Teplitski, M.; Chen, H. C.; Rajamani, S.; Gao, M. S.; Merighi, M.; Sayre, R. T.; Robinson, J. B.; Rolfe, B. G.; Bauer, W. D., *Chlamydomonas reinhardtii* secretes compounds that mimic bacterial signals and interfere with quorum sensing regulation in bacteria. *Plant Physiology* **2004**, *134* (1), 137-146.
150. Gao, M. S.; Teplitski, M.; Robinson, J. B.; Bauer, W. D., Production of substances by *Medicago truncatula* that affect bacterial quorum sensing. *Molecular Plant-Microbe Interactions* **2003**, *16* (9), 827-834.
151. Schaefer, A. L.; Hanzelka, B. L.; Eberhard, A.; Greenberg, E. P., Quorum sensing in *Vibrio fischeri*: Probing autoinducer-LuxR interactions with autoinducer analogs. *Journal of Bacteriology* **1996**, *178* (10), 2897-2901.
152. Persson, T.; Hansen, T. H.; Rasmussen, T. B.; Skinderso, M. E.; Givskov, M.; Nielsen, J., Rational design and synthesis of new quorum-sensing inhibitors derived from acylated homoserine lactones and natural products from garlic. *Organic & Biomolecular Chemistry* **2005**, *3* (2), 253-262.
153. Castang, S.; Chantegrel, B.; Deshayes, C.; Dolmazon, R.; Gouet, P.; Haser, R.; Reverchon, S.; Nasser, W.; Hugouvieux-Cotte-Pattat, N.; Doutheau, A., *N*-sulfonyl homoserine lactones as antagonists of bacterial quorum sensing. *Bioorganic & Medicinal Chemistry Letters* **2004**, *14* (20), 5145-5149.
154. Reverchon, S.; Chantegrel, B.; Deshayes, C.; Doutheau, A.; Cotte-Pattat,

- N., New synthetic analogues of *N*-acyl homoserine lactones as agonists or antagonists of transcriptional regulators involved in bacterial quorum sensing. *Bioorganic & Medicinal Chemistry Letters* **2002**, *12* (8), 1153-1157.
155. Ishida, T.; Ikeda, T.; Takiguchi, N.; Kuroda, A.; Ohtake, H.; Kato, J., Inhibition of quorum sensing in *Pseudomonas aeruginosa* by *N*-acyl cyclopentylamides. *Applied and Environmental Microbiology* **2007**, *73* (10), 3183-3188.
156. de Nys, R.; Wright, A. D.; Konig, G. M.; Sticher, O., New halogenated furanones from the marine alga *Delisea pulchra* (cf. *fimbriata*). *Tetrahedron* **1993**, *49* (48), 11213-11220.
157. Manny, A. J.; Kjelleberg, S.; Kumar, N.; deNys, R.; Read, R. W.; Steinberg, P., Reinvestigation of the sulfuric acid-catalysed cyclisation of brominated 2-alkyllevulinic acids to 3-alkyl-5-methylene-2(5H)-furanones. *Tetrahedron* **1997**, *53* (46), 15813-15826.
158. Ren, D. C.; Sims, J. J.; Wood, T. K., Inhibition of biofilm formation and swarming of *Escherichia coli* by (5*Z*)-4-bromo-5(bromomethylene)-3-butyl-2(5H)-furanone. *Environmental Microbiology* **2001**, *3* (11), 731-736.
159. Ren, D. C.; Bedzyk, L. A.; Ye, R. W.; Thomas, S. M.; Wood, T. K., Stationary-phase quorum-sensing signals affect autoinducer-2 and gene expression in *Escherichia coli*. *Applied and Environmental Microbiology* **2004**, *70* (4), 2038-2043.
160. Hentzer, M.; Wu, H.; Andersen, J. B.; Riedel, K.; Rasmussen, T. B.; Bagge, N.; Kumar, N.; Schembri, M. A.; Song, Z. J.; Kristoffersen, P.; Manefield, M.; Costerton, J. W.; Molin, S.; Eberl, L.; Steinberg, P.; Kjelleberg, S.; Hoiby, N.; Givskov, M., Attenuation of *Pseudomonas*

- aeruginosa* virulence by quorum sensing inhibitors. *EMBO Journal* **2003**, 22 (15), 3803-3815.
161. Ren, D.; Sims, J. J.; Wood, T. K., Inhibition of biofilm formation and swarming of *Bacillus subtilis* by (5Z)-4-bromo-5-(bromomethylene)-3-butyl-2(5H)-furanone. *Letters in Applied Microbiology* **2002**, 34 (4), 293-299.
162. Ren, D.; Wood, T. K., (5Z)-4-bromo-5-(bromomethylene)-3-butyl-2(5H)-furanone reduces corrosion from *Desulfotomaculum orientis*. *Environmental Microbiology* **2004**, 6 (5), 535-540.
163. Hume, E. B. H.; Baveja, J.; Muir, B.; Schubert, T. L.; Kumar, N.; Kjelleberg, S.; Griesser, H. J.; Thissen, H.; Read, R.; Poole-Warren, L. A.; Schindhelm, K.; Willcox, M. D. P., The control of *Staphylococcus epidermidis* biofilm formation and in vivo infection rates by covalently bound furanones. *Biomaterials* **2004**, 25 (20), 5023-5030.
164. Jones, M. B.; Jani, R.; Ren, D. C.; Wood, T. K.; Blaser, M. J., Inhibition of *Bacillus anthracis* growth and virulence-gene expression by inhibitors of quorum-sensing. *The Journal of Infectious Disease* **2005**, 191 (11), 1881-1888.
165. Jones, M. B.; Blaser, M. J., Detection of a *luxS*-signaling molecule in *Bacillus anthracis*. *Infection and Immunity* **2003**, 71 (7), 3914-3919.
166. Ren, D. C.; Bedzyk, L. A.; Setlow, P.; England, D. F.; Kjelleberg, S.; Thomas, S. M.; Ye, R. W.; Wood, T. K., Differential gene expression to investigate the effect of (5Z)-4-bromo-5-(bromomethylene)-3-butyl-2(5H)-furanone on *Bacillus subtilis*. *Applied and Environmental Microbiology* **2004**, 70 (8), 4941-4949.
167. Manefield, M.; de Nys, R.; Kumar, N.; Read, R.; Givskov, M.; Steinberg,

- P.; Kjelleberg, S. A., Evidence that halogenated furanones from *Delisea pulchra* inhibit acylated homoserine lactone (AHL)-mediated gene expression by displacing the AHL signal from its receptor protein. *Microbiology-Uk* **1999**, *145*, 283-291.
168. Manefield, M.; Rasmussen, T. B.; Hentzer, M.; Andersen, J. B.; Steinberg, P.; Kjelleberg, S.; Givskov, M., Halogenated furanones inhibit quorum sensing through accelerated LuxR turnover. *Microbiology-Sgm* **2002**, *148*, 1119-1127.
169. Hentzer, M.; Riedel, K.; Rasmussen, T. B.; Heydorn, A.; Andersen, J. B.; Parsek, M. R.; Rice, S. A.; Eberl, L.; Molin, S.; Hoiby, N.; Kjelleberg, S.; Givskov, M., Inhibition of quorum sensing in *Pseudomonas aeruginosa* biofilm bacteria by a halogenated furanone compound. *Microbiology-Sgm* **2002**, *148*, 87-102.
170. Wu, H.; Song, Z.; Hentzer, M.; Andersen, J. B.; Molin, S.; Givskov, M.; Hoiby, N., Synthetic furanones inhibit quorum-sensing and enhance bacterial clearance in *Pseudomonas aeruginosa* lung infection in mice. *Journal of Antimicrobial Chemotherapy* **2004**, *53* (6), 1054-1061.
171. Koch, B.; Lijefors, T.; Persson, T.; Nielsen, J.; Kjelleberg, S.; Givskov, M., The LuxR receptor: the sites of interaction with quorum-sensing signals and inhibitors. *Microbiology-Sgm* **2005**, *151*, 3589-3602.
172. Givskov, M.; DeNys, R.; Manefield, M.; Gram, L.; Maximilien, R.; Eberl, L.; Molin, S.; Steinberg, P. D.; Kjelleberg, S., Eukaryotic interference with homoserine lactone-mediated prokaryotic signaling. *Journal of Bacteriology* **1996**, *178* (22), 6618-6622.
173. Manefield, M.; Harris, L.; Rice, S. A.; De Nys, R.; Kjelleberg, S., Inhibition of luminescence and virulence in the black tiger prawn (*Penaeus*

- monodon) pathogen *Vibrio harveyi* by intercellular signal antagonists. *Applied and Environmental Microbiology* **2000**, *66* (5), 2079-2084.
174. Ren, D. C.; Zuo, R. J.; Wood, T. K., Quorum-sensing antagonist (5Z)-4-bromo-5-(bromomethylene)-3-butyl-2(5H)-furanone influences siderophore biosynthesis in *Pseudomonas putida* and *Pseudomonas aeruginosa*. *Applied Microbiology and Biotechnology* **2005**, *66* (6), 689-695.
175. Gram, L.; deNys, R.; Maximilien, R.; Givskov, M.; Steinberg, P.; Kjelleberg, S., Inhibitory effects of secondary metabolites from the red alga *Delisea pulchra* on swarming motility of *Proteus mirabilis*. *Applied and Environmental Microbiology* **1996**, *62* (11), 4284-4287.
176. Kato, N.; Morohoshi, T.; Nozawa, T.; Matsumoto, H.; Ikeda, T., Control of gram-negative bacterial quorum sensing with cyclodextrin immobilized cellulose ether gel. *Journal of Inclusion Phenomena and Macrocyclic Chemistry* **2006**, *56*, 55-59.
177. Kato, N.; Tanaka, T.; Nakagawa, S.; Morohoshi, T.; Hiratani, K.; Ikeda, T., Control of virulence factor expression in opportunistic pathogens using cyclodextrin immobilized gel. *Journal of Inclusion Phenomena and Macrocyclic Chemistry* **2007**, 419-423.
178. Yates, E. A.; Philipp, B.; Buckley, C.; Atkinson, S.; Chhabra, S. R.; Sockett, R. E.; Goldner, M.; Dessaux, Y.; Camara, M.; Smith, H.; Williams, P., *N*-acylhomoserine Lactones undergo lactonolysis in a pH-, temperature-, and acyl chain length-dependent manner during growth of *Yersinia pseudotuberculosis* and *Pseudomonas aeruginosa*. *Infection and Immunity* **2002**, *70* (10), 5635-5646.
179. Dong, Y. H.; Xu, J. L.; Li, X. Z.; Zhang, L. H., AiiA, an enzyme that inactivates the acylhomoserine lactone quorum-sensing signal and

- attenuates the virulence of *Erwinia carotovora*. *Proceedings of the National Academy of Sciences of the United States of America* **2000**, 97 (7), 3526-3531.
180. Dong, Y. H.; Gusti, A. R.; Zhang, Q.; Xu, J. L.; Zhang, L. H., Identification of quorum-quenching *N*-acyl homoserine lactonases from *Bacillus* species. *Applied and Environmental Microbiology* **2002**, 68 (4), 1754-1759.
181. Lee, S. J.; Park, S. Y.; Lee, J. J.; Yum, D. Y.; Koo, B. T.; Lee, J. K., Genes encoding the *N*-acyl homoserine lactone-degrading enzyme are widespread in many subspecies of *Bacillus thuringiensis*. *Applied and Environmental Microbiology* **2002**, 68 (8), 3919-3924.
182. Uroz, S.; D'Angelo-Picard, C.; Carlier, A.; Elasri, M.; Sicot, C.; Petit, A.; Oger, P.; Faure, D.; Dessaux, Y., Novel bacteria degrading *N*-acylhomoserine lactones and their use as quenchers of quorum-sensing-regulated functions of plant-pathogenic bacteria. *Microbiology-Sgm* **2003**, 149, 1981-1989.
183. Park, S. Y.; Lee, S. J.; Oh, T. K.; Oh, J. W.; Koo, B. T.; Yum, D. Y.; Lee, J. K., AhlD, an *N*-acylhomoserine lactonase in *Arthrobacter sp.*, and predicted homologues in other bacteria. *Microbiology-Sgm* **2003**, 149, 1541-1550.
184. Carlier, A.; Uroz, S.; Smadja, B.; Fray, R.; Latour, X.; Dessaux, Y.; Faure, D., The Ti plasmid of *Agrobacterium tumefaciens* harbors an *attM*-paralogous gene, *aiiB*, also encoding *N*-acyl homoserine lactonase activity. *Applied and Environmental Microbiology* **2003**, 69 (8), 4989-4993.
185. Park, S. Y.; Hwang, B. J.; Shin, M. H.; Kim, J. A.; Kim, H. K.; Lee, J. K., *N*-acylhomoserine lactonase producing *Rhodococcus spp.* with different AHL-degrading activities. *FEMS Microbiology Letters* **2006**, 261 (1), 102-

108.

186. Camara, M.; Williams, P.; Hardman, A., Controlling infection by tuning in and turning down the volume of bacterial small-talk. *Lancet Infectious Diseases* **2002**, *2* (11), 667-676.
187. Molina, L.; Constantinescu, F.; Michel, L.; Reimann, C.; Duffy, B.; Defago, G., Degradation of pathogen quorum-sensing molecules by soil bacteria: a preventive and curative biological control mechanism. *Fems Microbiology Ecology* **2003**, *45* (1), 71-81.
188. Lin, Y. H.; Xu, J. L.; Hu, J. Y.; Wang, L. H.; Ong, S. L.; Leadbetter, J. R.; Zhang, L. H., Acyl-homoserine lactone acylase from *Ralstonia* strain XJ12B represents a novel and potent class of quorum-quenching enzymes. *Molecular Microbiology* **2003**, *47* (3), 849-860.
189. Leadbetter, J. R.; Greenberg, E. P., Metabolism of acyl-homoserine lactone quorum-sensing signals by *Variovorax paradoxus*. *Journal of Bacteriology* **2000**, *182* (24), 6921-6926.
190. Park, S. Y.; Kang, H. O.; Jang, H. S.; Lee, J. K.; Koo, B. T.; Yum, D. Y., Identification of extracellular *N*-acylhomoserine lactone acylase from a *Streptomyces* sp and its application to quorum quenching. *Applied and Environmental Microbiology* **2005**, *71* (5), 2632-2641.
191. Xu, F.; Byun, T.; Dussen, H. J.; Duke, K. R., Degradation of *N*-acylhomoserine lactones, the bacterial quorum-sensing molecules, by acylase. *Journal of Biotechnology* **2003**, *101* (1), 89-96.
192. Huang, J. J.; Han, J. I.; Zhang, L. H.; Leadbetter, J. R., Utilization of acyl-homoserine lactone quorum signals for growth by a soil *pseudomonad* and *Pseudomonas aeruginosa* PAO1. *Applied and Environmental Microbiology* **2003**, *69* (10), 5941-5949.

193. Chowdhary, P. K.; Keshavan, N.; Nguyen, H. Q.; Peterson, J. A.; Gonzalez, J. E.; Haines, D. C., *Bacillus megaterium* CYP102A1 oxidation of acyl homoserine lactones and acyl homoserines. *Biochemistry* **2007**, *46* (50), 14429-14437.
194. Marin, S. D.; Xu, Y.; Meijler, M. M.; Janda, K. D., Antibody catalyzed hydrolysis of a quorum sensing signal found in Gram-negative bacteria. *Bioorganic & Medicinal Chemistry Letters* **2007**, *17* (6), 1549-1552.
195. Uroz, S.; Oger, P.; Chhabra, S. R.; Camara, M.; Williams, P.; Dessaux, Y., *N*-acyl homoserine lactones are degraded via an amidolytic activity in *Comamonas* sp strain D1. *Archives of Microbiology* **2007**, *187* (3), 249-256.
196. Sio, C. F.; Otten, L. G.; Cool, R. H.; Diggle, S. P.; Braun, P. G.; Bos, R.; Daykin, M.; Camara, M.; Williams, P.; Quax, W. J., Quorum quenching by an *N*-acyl-homoserine lactone acylase from *Pseudomonas aeruginosa* PAO1. *Infection and Immunity* **2006**, *74* (3), 1673-1682.
197. You, J. L.; Xue, X. L.; Cao, L. X.; Lu, X.; Wang, J.; Zhang, L. X.; Zhou, S. N., Inhibition of *Vibrio* biofilm formation by a marine actinomycete strain A66. *Applied Microbiology and Biotechnology* **2007**, *76* (5), 1137-1144.
198. Kim, J. B.; Grate, J. W.; Wang, P., Nanobiocatalysis and its potential applications. *Trends in Biotechnology* **2008**, *26* (11), 639-646.
199. Kim, J.; Grate, J. W.; Wang, P., Nanostructures for enzyme stabilization. *Chemical Engineering Science* **2006**, *61* (3), 1017-1026.
200. Willner, B.; Katz, E.; Willner, I., Electrical contacting of redox proteins by nanotechnological means. *Current Opinion in Biotechnology* **2006**, *17* (6), 589-596.
201. Wang, J.; Liu, G. D.; Jan, M. R., Ultrasensitive electrical biosensing of

- proteins and DNA: Carbon-nanotube derived amplification of the recognition and transduction events. *Journal of the American Chemical Society* **2004**, *126* (10), 3010-3011.
202. Wang, Q. G.; Yang, Z. M.; Ma, M. L.; Chang, C. K.; Xu, B., High catalytic activities of artificial peroxidases based on supramolecular hydrogels that contain heme models. *Chemistry-a European Journal* **2008**, *14* (16), 5073-5078.
203. Jang, C. H.; Stevens, B. D.; Phillips, R.; Calter, M. A.; Ducker, W. A., A strategy for the sequential patterning of proteins: Catalytically active multiprotein nanofabrication. *Nano Letters* **2003**, *3* (6), 691-694.
204. Willner, I.; Basnar, B.; Willner, B., Nanoparticle-enzyme hybrid systems for nanobiotechnology. *Febs Journal* **2007**, *274* (2), 302-309.
205. Daubresse, C.; Grandfils, C.; Jerome, R.; Teyssie, P., Enzyme immobilization in reactive nanoparticles produced by inverse microemulsion polymerization *Journal of Colloid and Interface Science* **1994**, *168* (1), 222-229.
206. Jain, T. K.; Roy, I.; De, T. K.; Maitra, A., Nanometer silica particles encapsulating active compounds: A novel ceramic drug carrier. *Journal of the American Chemical Society* **1998**, *120* (43), 11092-11095.
207. Ma, D.; Li, M.; Patil, A. J.; Mann, S., Fabrication of protein/silica core-shell nanoparticles by microemulsion-based molecular wrapping. *Advanced Materials* **2004**, *16* (20), 1838-1841.
208. Munshi, N.; De, T. K.; Maitra, A., Size modulation of polymeric nanoparticles under controlled dynamics of microemulsion droplets. *Journal of Colloid and Interface Science* **1997**, *190* (2), 387-391.
209. Yang, H. H.; Zhang, S. Q.; Chen, X. L.; Zhuang, Z. X.; Xu, J. G.; Wang,

- X. R., Magnetite-containing spherical silica nanoparticles for biocatalysis and bioseparations. *Analytical Chemistry* **2004**, 76 (5), 1316-1321.
210. Kim, J.; Grate, J. W., Single-enzyme nanoparticles armored by a nanometer-scale organic/inorganic network. *Nano Letters* **2003**, 3 (9), 1219-1222.
211. Paradkar, V. M.; Dordick, J. S., Aqueous-like activity of α -chymotrypsin dissolved in nearly anhydrous organic solvents. *Journal of the American Chemical Society* **1994**, 116 (11), 5009-5010.
212. Wangikar, P. P.; Michels, P. C.; Clark, D. S.; Dordick, J. S., Structure and function of subtilisin BPN' solubilized in organic solvents. *Journal of the American Chemical Society* **1997**, 119 (1), 70-76.
213. Kim, J.; Jia, H. F.; Lee, C. W.; Chung, S. W.; Kwak, J. H.; Shin, Y.; Dohnalkova, A.; Kim, B. G.; Wang, P.; Grate, J. W., Single enzyme nanoparticles in nanoporous silica: A hierarchical approach to enzyme stabilization and immobilization. *Enzyme and Microbial Technology* **2006**, 39, 474-480.
214. Wang, P.; Dai, S.; Waezsada, S. D.; Tsao, A. Y.; Davison, B. H., Enzyme stabilization by covalent binding in nanoporous sol-gel glass for nonaqueous biocatalysis. *Biotechnology and Bioengineering* **2001**, 74 (3), 249-255.
215. Yan, M.; Ge, J.; Liu, Z.; Ouyang, P. K., Encapsulation of single enzyme in nanogel with enhanced biocatalytic activity and stability. *Journal of the American Chemical Society* **2006**, 128 (34), 11008-11009.
216. Patil, A. J.; Muthusamy, E.; Mann, S., Synthesis and self-assembly of organoclay-wrapped biomolecules. *Angewandte Chemie-International Edition* **2004**, 43 (37), 4928-4933.

217. Diaz, J. F.; Balkus, K. J., Enzyme immobilization in MCM-41 molecular sieve. *Journal of Molecular Catalysis B-Enzymatic* **1996**, *2* (2-3), 115-126.
218. Fan, J.; Lei, J.; Wang, L. M.; Yu, C. Z.; Tu, B.; Zhao, D. Y., Rapid and high-capacity immobilization of enzymes based on mesoporous silicas with controlled morphologies. *Chemical Communications* **2003**, (17), 2140-2141.
219. Fan, J.; Yu, C. Z.; Gao, T.; Lei, J.; Tian, B. Z.; Wang, L. M.; Luo, Q.; Tu, B.; Zhou, W. Z.; Zhao, D. Y., Cubic mesoporous silica with large controllable entrance sizes and advanced adsorption properties. *Angewandte Chemie-International Edition* **2003**, *42* (27), 3146-3150.
220. Han, Y. J.; Watson, J. T.; Stucky, G. D.; Butler, A., Catalytic activity of mesoporous silicate-immobilized chloroperoxidase. *Journal of Molecular Catalysis B-Enzymatic* **2002**, *17* (1), 1-8.
221. Lei, C. H.; Shin, Y.; Liu, J.; Ackerman, E. J., Synergetic effects of nanoporous support and urea on enzyme activity. *Nano Letters* **2007**, *7* (4), 1050-1053.
222. Lei, C. H.; Shin, Y. S.; Liu, J.; Ackerman, E. J., Entrapping enzyme in a functionalized nanoporous support. *Journal of the American Chemical Society* **2002**, *124* (38), 11242-11243.
223. Takahashi, H.; Li, B.; Sasaki, T.; Miyazaki, C.; Kajino, T.; Inagaki, S., Catalytic activity in organic solvents and stability of immobilized enzymes depend on the pore size and surface characteristics of mesoporous silica. *Chemistry of Materials* **2000**, *12* (11), 3301-3305.
224. Wang, L. F.; Zhu, G. Y.; Wang, P.; Newby, B. M. Z., Self-assembling of polymer-enzyme conjugates at oil/water interfaces. *Biotechnology Progress* **2005**, *21* (4), 1321-1328.

225. Lee, J.; Kim, J.; Jia, H. F.; Kim, M. I.; Kwak, J. H.; Jin, S. M.; Dohnalkova, A.; Park, H. G.; Chang, H. N.; Wang, P.; Grate, J. W.; Hyeon, T., Simple synthesis of hierarchically ordered mesocellular mesoporous silica materials hosting crosslinked enzyme aggregates. *Small* **2005**, *1* (7), 744-753.
226. Kim, J.; Lee, J.; Na, H. B.; Kim, B. C.; Youn, J. K.; Kwak, J. H.; Moon, K.; Lee, E.; Park, J.; Dohnalkova, A.; Park, H. G.; Gu, M. B.; Chang, H. N.; Grate, J. W.; Hyeon, T., A magnetically separable, highly stable enzyme system based on nanocomposites of enzymes and magnetic nanoparticles shipped in hierarchically ordered, mesocellular, mesoporous silica. *Small* **2005**, *1* (12), 1203-1207.
227. Kim, M. I.; Kim, J.; Lee, J.; Jia, H.; Bin Na, H.; Youn, J. K.; Kwak, J. H.; Dohnalkova, A.; Grate, J. W.; Wang, P.; Hyeon, T.; Park, H. G.; Chang, H. N., Crosslinked enzyme aggregates in hierarchically-ordered mesoporous silica: A simple and effective method for enzyme stabilization. *Biotechnology and Bioengineering* **2007**, *96* (2), 210-218.
228. Heilmann, A.; Teuscher, N.; Kiesow, A.; Janasek, D.; Spohn, U., Nanoporous aluminum oxide as a novel support material for enzyme biosensors. *Journal of Nanoscience and Nanotechnology* **2003**, *3* (5), 375-379.
229. Lee, D.; Lee, J.; Kim, J.; Na, H. B.; Kim, B.; Shin, C. H.; Kwak, J. H.; Dohnalkova, A.; Grate, J. W.; Hyeon, T.; Kim, H. S., Simple fabrication of a highly sensitive and fast glucose biosensor using enzymes immobilized in mesocellular carbon foam. *Advanced Materials* **2005**, *17* (23), 2828-+.
230. Xing, G. W.; Li, X. W.; Tian, G. L.; Ye, Y. H., Enzymatic peptide synthesis in organic solvent with different zeolites as immobilization

- matrixes. *Tetrahedron* **2000**, *56* (22), 3517-3522.
231. Han, Y.; Lee, S. S.; Ying, J. Y., Pressure-driven enzyme entrapment in siliceous mesocellular foam. *Chemistry of Materials* **2006**, *18* (3), 643-649.
232. Sasaki, T.; Kajino, T.; Li, B.; Sugiyama, H.; Takahashi, H., New pulp biobleaching system involving manganese peroxidase immobilized in a silica support with controlled pore sizes. *Applied and Environmental Microbiology* **2001**, *67* (5), 2208-2212.
233. Lee, J.; Lee, D.; Oh, E.; Kim, J.; Kim, Y. P.; Jin, S.; Kim, H. S.; Hwang, Y.; Kwak, J. H.; Park, J. G.; Shin, C. H.; Hyeon, T., Preparation of a magnetically switchable bioelectrocatalytic system employing cross-linked enzyme aggregates in magnetic mesocellular carbon foam. *Angewandte Chemie-International Edition* **2005**, *44* (45), 7427-7432.
234. Fan, J.; Shui, W. Q.; Yang, P. Y.; Wang, X. Y.; Xu, Y. M.; Wang, H. H.; Chen, X.; Zhao, D. Y., Mesoporous silica nanoreactors for highly efficient proteolysis. *Chemistry-a European Journal* **2005**, *11* (18), 5391-5396.
235. Shui, W. Q.; Fan, J.; Yang, P. Y.; Liu, C. L.; Zhai, J. J.; Lei, J.; Yan, Y.; Zhao, D. Y.; Chen, X., Nanopore-based proteolytic reactor for sensitive and comprehensive proteomic analyses. *Analytical Chemistry* **2006**, *78* (14), 4811-4819.
236. Zuo, C.; Yu, W. J.; Zhou, X. F.; Zhao, D. Y.; Yang, P. Y., Highly efficient enrichment and subsequent digestion of proteins in the mesoporous molecular sieve silicate SBA-15 for matrix-assisted laser desorption/ionization mass spectrometry with time-of-flight/time-of-flight analyzer peptide mapping. *Rapid Communications in Mass Spectrometry* **2006**, *20* (20), 3139-3144.
237. Kim, B. C.; Nair, S.; Kim, J.; Kwak, J. H.; Grate, J. W.; Kim, S. H.; Gu,

- M. B. In *Preparation of biocatalytic nanofibres with high activity and stability via enzyme aggregate coating on polymer nanofibres*, 2005; pp S382-S388.
238. Lee, J. H.; Hwang, E. T.; Kim, B. C.; Lee, S. M.; Sang, B. I.; Choi, Y. S.; Kim, J.; Gu, M. B., Stable and continuous long-term enzymatic reaction using an enzyme-nanofiber composite. *Applied Microbiology and Biotechnology* **2007**, *75* (6), 1301-1307.
239. Nair, S.; Kim, J.; Crawford, B.; Kim, S. H., Improving biocatalytic activity of enzyme-loaded nanofibers by dispersing entangled nanofiber structure. *Biomacromolecules* **2007**, *8* (4), 1266-1270.
240. Fischback, M. B.; Youn, J. K.; Zhao, X. Y.; Wang, P.; Park, H. G.; Chang, H. N.; Kim, J.; Ha, S., Miniature biofuel cells with improved stability under continuous operation. *Electroanalysis* **2006**, *18* (19-20), 2016-2022.
241. Lee, J.; Lee, Y.; Youn, J. K.; Bin Na, H.; Yu, T.; Kim, H.; Lee, S. M.; Koo, Y. M.; Kwak, J. H.; Park, H. G.; Chang, H. N.; Hwang, M.; Park, J. G.; Kim, J.; Hyeon, T., Simple synthesis of functionalized superparamagnetic magnetite/silica core/shell nanoparticles and their application as magnetically separable high-performance biocatalysts. *Small* **2008**, *4* (1), 143-152.
242. Govardhan, C. P., Crosslinking of enzymes for improved stability and performance. *Current Opinion in Biotechnology* **1999**, *10* (4), 331-335.
243. Sheldon, R. A., Enzyme immobilization: The quest for optimum performance. *Advanced Synthesis & Catalysis* **2007**, *349* (8-9), 1289-1307.
244. Zhu, G. Y.; Wang, P., Polymer-enzyme conjugates can self-assemble at oil/water interfaces and effect interfacial biotransformations. *Journal of the American Chemical Society* **2004**, *126* (36), 11132-11133.

245. Zhu, G. Y.; Wang, P., Novel interface-binding chloroperoxidase for interfacial epoxidation of styrene. *Journal of Biotechnology* **2005**, *117* (2), 195-202.
246. Asuri, P.; Karajanagi, S. S.; Dordick, J. S.; Kane, R. S., Directed assembly of carbon nanotubes at liquid-liquid interfaces: Nanoscale conveyors for interfacial biocatalysis. *Journal of the American Chemical Society* **2006**, *128* (4), 1046-1047.
247. Narayanan, R.; Zhu, G. Y.; Wang, P., Stabilization of interface-binding chloroperoxidase for interfacial biotransformation. *Journal of Biotechnology* **2007**, *128* (1), 86-92.
248. Qhobosheane, M.; Zhang, P.; Tan, W. H., Assembly of silica nanoparticles for two-dimensional nanomaterials. *Journal of Nanoscience and Nanotechnology* **2004**, *4* (6), 635-640.
249. Shipway, A. N.; Katz, E.; Willner, I., Nanoparticle arrays on surfaces for electronic, optical, and sensor applications. *Chemphyschem* **2000**, *1* (1), 18-52.
250. Karajanagi, S. S.; Yang, H. C.; Asuri, P.; Sellitto, E.; Dordick, J. S.; Kane, R. S., Protein-assisted solubilization of single-walled carbon nanotubes. *Langmuir* **2006**, *22* (4), 1392-1395.
251. Asuri, P.; Bale, S. S.; Pangule, R. C.; Shah, D. A.; Kane, R. S.; Dordick, J. S., Structure, function, and stability of enzymes covalently attached to single-walled carbon nanotubes. *Langmuir* **2007**, *23* (24), 12318-12321.
252. Shang, W.; Nuffer, J. H.; Dordick, J. S.; Siegel, R. W., Unfolding of ribonuclease A on silica nanoparticle surfaces. *Nano Letters* **2007**, *7* (7), 1991-1995.
253. Fischer, N. O.; McIntosh, C. M.; Simard, J. M.; Rotello, V. M., Inhibition

- of chymotrypsin through surface binding using nanoparticle-based receptors. *Proceedings of the National Academy of Sciences of the United States of America* **2002**, 99 (8), 5018-5023.
254. Rege, K.; Ravivkar, N. R.; Kim, D. Y.; Schadler, L. S.; Ajayan, P. M.; Dordick, J. S., Enzyme-polymer-single walled carbon nanotube composites as biocatalytic films. *Nano Letters* **2003**, 3 (6), 829-832.
255. Asuri, P.; Karajanagi, S. S.; Kane, R. S.; Dordick, J. S., Polymer-nanotube-enzyme composites as active antifouling films. *Small* **2007**, 3 (1), 50-53.
256. Fuqua, C.; Winans, S. C., Conserved *cis*-acting promoter elements are required for density-dependent transcription of *Agrobacterium tumefaciens* conjugal transfer genes. *Journal of Bacteriology* **1996**, 178 (2), 435-440.
257. McLean, R. J. C.; Pierson, L. S.; Fuqua, C., A simple screening protocol for the identification of quorum signal antagonists. *Journal of Microbiological Methods* **2004**, 58 (3), 351-360.
258. Holm, C.; Jespersen, L., A flow-cytometric gram-staining technique for milk-associated bacteria. *Applied and Environmental Microbiology* **2003**, 69 (5), 2857-2863.
259. APHA, *Standard Methods for the Examination of Water and Wastewater*. 20 ed.; American Public Health Association: Washington, DC, 1998.
260. Jahn, A.; Nielsen, P. H., Extraction of extracellular polymeric substances (EPS) from biofilms using a cation exchange resin. *Water Science and Technology* **1995**, 157-164.
261. Yang, F.; Wang, L. H.; Wang, J.; Dong, Y. H.; Hu, J. Y.; Zhang, L. H., Quorum quenching enzyme activity is widely conserved in the sera of mammalian species. *FEBS Letters* **2005**, 579 (17), 3713-3717.

262. Qaqish, R. B.; Amiji, M. M., Synthesis of a fluorescent chitosan derivative and its application for the study of chitosan-mucin interactions. *Carbohydrate Polymers* **1999**, *38* (2), 99-107.
263. Neu, T. R.; Kuhlicke, U.; Lawrence, J. R., Assessment of fluorochromes for two-photon laser scanning microscopy of biofilms. *Applied and Environmental Microbiology* **2002**, *68* (2), 901-909.
264. Steinberg, T. H.; Jones, L. J.; Haugland, R. P.; Singer, V. L., SYPRO Orange and SYPRO Red protein gel stains: One-step fluorescent staining of denaturing gels for detection of nanogram levels of protein. *Analytical Biochemistry* **1996**, *239* (2), 223-237.
265. Steinberg, T. H.; Haugland, R. P.; Singer, V. L., Applications of SYPRO Orange and SYPRO Red protein gel stains. *Analytical Biochemistry* **1996**, *239* (2), 238-245.
266. Bousse, L.; Mouradian, S.; Minalla, A.; Yee, H.; Williams, K.; Dubrow, R., Protein sizing on a microchip. *Analytical Chemistry* **2001**, *73* (6), 1207-1212.
267. Ivleva, N. P.; Wagner, M.; Horn, H.; Niessner, R.; Haisch, C., Towards a nondestructive chemical characterization of biofilm matrix by Raman microscopy. *Analytical and Bioanalytical Chemistry* **2009**, *393* (1), 197-206.
268. Mitz, M. A.; Schlueter, R. J., Direct spectrophotometric measurement of the peptide bond; application to the determination of acylase I. *Biochim. Biophys. Acta.* **1958** *27* (1), 168-172.
269. Barker, D. J.; Salvi, S. M. L.; Langenhoff, A. A. M.; Stuckey, D. C., Soluble microbial products in ABR treating low-strength wastewater. *Journal of Environmental Engineering-Asce* **2000**, *126* (3), 239-249.

270. Jarusutthirak, C.; Amy, G., Role of soluble microbial products (SMP) in membrane fouling and flux decline. *Environmental Science & Technology* **2006**, *40* (3), 969-974.
271. Wingender, J.; Neu, T. R.; Flemming, H. C., What are bacterial extracellular polymeric substnaces? . In *Microbial Extracellular Polymeric Substacnes*, Springer-Verlag: Berlin, 1999; pp 1-19.